In presenting the dissertation as a partial fulfillment of the requirements for an advanced degree from the Georgia Institute of Technology, I agree that the Library of the Institute shall make it available for inspection and circulation in accordance with its regulations governing materials of this type. I agree that permission to copy from, or to publish from, this dissertation may be granted by the professor under whose direction it was written, or, in his absence, by the Dean of the Graduate Division when such copying or publication is solely for scholarly purposes and does not involve potential financial gain. It is understood that any copying from, or publication of, this dissertation which involves potential financial gain will not be allowed without written permission.

7/25/68

AN INVESTIGATION OF A TURBULENT BOUNDARY LAYER WITH HOMOGENEOUS POLYMER INJECTION

A THESIS

Presented to

The Faculty of the Graduate Division

by

Jan Hulsebos

In Partial Fulfillment

of the Requirements for the Degree

Doctor of Philosophy in the School of Chemical Engineering

Georgia Institute of Technology

December, 1968

AN INVESTIGATION OF A TURBULENT BOUNDARY LAYER

WITH HOMOGENEOUS POLYMER INJECTION

Approved:

Chairman

Date approved by Chairman: 11/12/68

ACKNOWLEDGMENTS

The author wishes to express his sincere appreciation to the many persons who have had a part in the completion of this work. Special thanks are due to Dr. Wm. Meese Newton, who gave much advice and made suggestions concerning experimental technique in the early phase of this investigation. The author is also very much indebted to Dr. C. W. Gorton, who served as thesis advisor when illness forced Dr. Newton to take a temporary leave of absence; his many constructive suggestions and criticisms helped immeasurably in this investigation. Regents Professor W. T. Ziegler and Dr. Wm. Meese Newton served on the thesis reading committee. Their constructive criticism, advice, and cooperation are greatly appreciated.

The writer expresses his appreciation to the Lockheed-Georgia Company and, in particular, to Dr. J. J. Cornish III, Dr. W. F. Jacobs, and Dr. J. F. Sutton for making this course of study possible. Mr. G. H. Hunnicutt deserves recognition for his help in erecting the experimental apparatus and Mlles. Ginga Jacobson and Rita Kinney for their conscientious and efficient clerical services during the preparation of this manuscript.

TABLE OF CONTENTS

TABLE OF CONTENTS (Continued)

LIST OF TABLES

LIST OF TABLES (Continued)

LIST OF TABLES (Continued)

LIST OF TABLES (Continued)

LIST OF ILLUSTRATIONS

LIST OF ILLUSTRATIONS (Continued)

NOMENCLATURE

In this tabulation, dimensions are given in terms of mass (M), length (L), time (t), and temperature (T). Equations referred to are defining relations in the body of the text. Symbols that appear infrequently are not listed.

Symbol	Quantity	Dimensions
A	Area of the porous plate	L^2
A_i	Coefficient in a polynomial	Dimensionless
c	Concentration	M/L^3
C	Concentration in ppm	Dimensionless
C_{Cr}	Critical concentration, defined on page 23	Dimensionless
c_f	Local skin-friction coefficient	Dimensionless
D	Pipe diameter	L
D_H	Hydraulic diameter	L
D_m	Effective diameter of a random-coiling macromolecule in dilute solution	L
e_v	Friction loss factor associated with viscous dissipation	Dimensionless
g	Gravitational acceleration	L/t^2
g_c	Dimensional constant	ML/Ft^2
h	Elevation	L
k	Prandtl's constant	Dimensionless
ℓ	Prandtl mixing length	L
M	Momentum flux with respect to stationary coordinates	ML/t^2

Symbol	Quantity	Dimensions
M_i	Molecular weight of species i	M/mole
n	Mass flux with respect to stationary coordinates	M/L^2t
N	Molar flux with respect to stationary coordinates	$moles/L^2t$
p	Pressure	M/Lt^2
Q	Volumetric flow rate	L^3/t
R	Radius	L
R_G	Root-mean-square radius of gyration of a random-coiling macromolecule in dilute solution	L
R_H	Hydraulic radius	L
Re	Reynolds number based on diameter	Dimensionless
Re_x	Reynolds number based on length	Dimensionless
t	Time	t
T	Temperature	T
u	Velocity in the x direction	L/t
u^*	Friction velocity, $u^* = \sqrt{\frac{\tau_w}{\rho}}$	L/t
v	Velocity in the y direction	L/t
W	Rate of doing work on surroundings	ML^2/t^3
x	Coordinate parallel to the porous surface	L
x_o	Value of x at the test-section inlet	L
y	Coordinate normal to the porous wall	L
y^+	$y^+ = yu^*/\nu$	Dimensionless
α	Fluid property parameter related to the concentration and dimensional characteristics of the polymer, Equation (12) page 23	Dimensionless

Symbol	Quantity	Dimensions
δ	Boundary-layer thickness	L
$[\eta]$	Intrinsic viscosity defined by Equation (17), page 34	L^3/M
λ	Relaxation time of the polymer molecule in solution	t
μ	Viscosity	M/Lt
μ'	Limiting value of the viscosity at high rates of shear	M/Lt
ν	Kinematic viscosity	L^2/t
Π	Profile parameter in Equation (.5), page 7	Dimensionless
ρ	Density	M/L^3
τ	Shear stress	M/Lt^2
ω	Parameter in Equation (.6), page 7	Dimensionless

Subscripts

A	Component A
B	Component B
Cr	Critical
o	In the pure solvent, or at zero mass transfer
w	At the wall
x	In the x direction
y	In the y direction
∞	Free stream

Symbol	
	Superscripts
$'$	Turbulent fluctuating quantity
$\overline{\quad}$	Time-averaged quantity
$\square$	At the onset of drag reduction
	Brackets
$\langle a \rangle$	Average value of "a" over the flow cross section

SUMMARY

Various studies have been conducted in the past few years dealing with drag reductions in water caused by the addition of certain chemicals. These studies indicate that certain long-chain organic molecules are extremely efficient in reducing drag, even in quantities as low as a few parts per million. An investigation conducted by the U. S. Naval Ordnance Test Station[21] in Pasadena has shown that the polymer polyethylene oxide WSR-301, manufactured by Union Carbide Chemicals Company, is one of the most effective materials presently known to reduce friction in water.

A careful study of the pertinent literature indicates that most investigations have dealt with the flow of pre-mixed solutions. The possibilities of using drag-reducing additives in this type of application are intriguing. Some of these are the pumping of crude oil over long distances and the drilling of oil wells. However, additional applications could be developed based on injection of dilute polymer solutions along solid-liquid interfaces with the object of reducing skin-friction drag. This type of application could be utilized on:

(1) Surface and underwater vessels.

(2) Hydrofoils.

(3) Skis of amphibian aircraft.

(4) Torpedoes.

(5) Deep-sea, submersible research vehicles.

The application to underwater research vehicles seems particularly attractive. These vehicles are usually battery powered and will permit

continuous operations of only a few days at the most, due to limitations in power supply. A reduction in drag would directly increase the deep-sea operating time and, therefore would be of extreme importance.

One method of introducing dilute polymer solutions in the turbulent boundary layer is by ejection through slots. Love[8] has investigated this type of mass addition on a flat plate and achieved drag reductions of up to 50 percent when ejecting solutions of polyethylene oxide WSR-301 through slots at the leading edge of a flat plate. Another technique is to eject the solutions through a porous surface. In view of the results of Wells and Spangler[10] who found that the presence of the polymer in the neighborhood of the viscous sub-layer alone is sufficient to cause the reduction in drag, distributed surface injection of polymeric additives seemed to be an approach that would make the most efficient use of drag-reducing additives. In this technique, the material is introduced into the boundary layer through a porous surface in a direction normal to the direction of the main stream. This method of ejection was examined in this investigation. For ease of analysis, injection of dilute solutions into a two-dimensional, turbulent boundary layer was selected. The specific objectives were:

(a) To determine how the additives affect the velocity profiles in the turbulent boundary layer.

(b) To evaluate the effect of injections on the boundary-layer thickness.

(c) To determine the magnitude of the drag reductions by measuring velocity profiles at several stations along the flat plate and using these in a momentum-deficit, integral analysis.

(d) To calculate the shear-stress distributions in the boundary layer and to investigate how they are influenced by the presence of the injected fluids.

(e) To determine the distribution of the additive in the boundary layer.

In order to conduct the investigation, a single-pass, continuous-flow, low-speed water tunnel was built in the School of Chemical Engineering, Georgia Institute of Technology. The test section of this tunnel was 96.0 inches long and had a rectangular cross-sectional area of 12.0 by 6.0 inches. This area was reduced to 12.0 by 2.8 inches in the present investigation to obtain accurate velocity measurements with a water supply rate limited to 155 gallons per minute.

With the bulk flow rate constant at 155 gallons per minute, the following fluids were injected into the main stream: water and aqueous solutions of polyethylene oxide at concentrations of 25.0, 50.0, and 150.0 ppm. The water was injected at a rate of 537.0 mls/min. Since this rate of injection, the highest considered in this investigation, did not significantly change the shape of the velocity profiles, lower injection rates of water were not considered. Most of the studies were performed with solutions containing 50.0 ppm of polyethylene oxide. These solutions were injected at four different injection rates of 60.0, 134.0, 268.0, and 537.0 mls/min giving $\frac{\rho_w v_w}{\rho_\infty u_\infty}$ values of 0.62, 1.38, 2.75, and 5.51×10^{-5}, respectively. The 25.0 ppm solution was introduced at rates of 134.0 and 537.0 mls/min, while the 150.0 ppm solution was injected at 134.0 mls/min.

In the investigation, velocity profiles were obtained by means of a total pressure probe in combination with a wall static tap. The differen-

tial pressures were measured with a Foxboro Type 15A Differential-Pressure Cell Transmitter with a range of 0 to 2.4 inches of water. The velocity profiles were used to calculate skin-friction values and shear-stress distributions by an integral momentum-deficit analysis. Distributions of the injected polymer in the boundary layer were measured by analyzing samples, withdrawn from the test section, with a polarographic technique developed by Goren, et al[57].

The following conclusions were reached:

1. Introducing the drag-reducing additive in the boundary layer by distributed surface mass addition is very efficient. Drag reductions of up to 37 percent were attained while injecting aqueous solutions of polyethylene oxide at concentrations of 50.0 ppm. The injection ratio, $\frac{\rho_w v_w}{\rho_\infty u_\infty}$, at this drag reduction was 1.38×10^{-5} and the Reynolds number was 1.24×10^6.

2. Although no extensive investigation was made of injections at concentrations other than 50.0 ppm, the data obtained for the injection of solutions of 25.0 and 150.0 ppm indicate that the weight of the polymer injected per unit of time and unit area is the prime criterion in drag reduction.

3. The onset of drag reduction occurred at lower values of the wall shear stress than predicted by present hypotheses[53,54,67]. This agrees with the findings of Little[36] who investigated similar drag-reducing agents.

4. The shape of the velocity profiles was not significantly changed by injection of water at a rate of 537.0 mls/min. The effect of aqueous solutions of polyethylene oxide was to make the velocity profiles blunter at each axial location. This effect was found to increase with injection

rate (up to 134.0 mls/min) and with axial distance down the channel.

5. The boundary-layer thickness decreased with injection of water and aqueous solutions of polyethylene oxide. Injection of water reduced the thickness by a maximum amount of approximately 11 percent. Injection of the polymer solutions at concentrations of 50.0 ppm continued to decrease the boundary-layer thickness until an injection rate of 134.0 mls/min was attained. The reduction in thickness at that point was about 20 percent. Then a reversal occurred and the boundary layer increased in thickness with higher injection rate.

6. The shear stresses in the boundary layer were lowered by mass additions. Aqueous solutions of polyethylene oxide at concentrations of 50.0 ppm produced the largest reduction at the porous wall, except at a rate of 134.0 mls/min, which yielded a constant reduction of 37 percent from y = 0 to the edge of the boundary layer. Injections of water at 537.0 mls/min, however, produced the largest shear-stress reduction at the outer edge of the boundary layer. The two largest injection rates examined in this investigation--537.0 mls/min--produced a surprising result, both in the case of water injection and polymer addition. This was that the maximum shearing stress no longer occurred at the wall, but was displaced from it. The maximum shearing stress in the case of water injection occurred at a y value of 0.02 inch, whereas in the case of polymer addition the maximum was found at y = 0.05 inch. The reasons for the occurrence of these maxima were not clear, but they have been noticed previously in the case of gas injections in air boundary layers[68,69].

7. The non-dimensional mean-velocity profiles were shifted linearly in an upward direction by all injections considered in this investigation.

This implies that injections of water and aqueous solutions of polyethylene oxide at 50.0 ppm do not cause changes in the universal constant k (the mixing-length constant). These results agree with the findings of Ernst[27] and Meyer[52], but contradict those of Elata and Tirosh[25] and Wells[26].

8. Concentration measurements were made in the transpired boundary layer while injecting aqueous solutions of polyethylene oxide at 50.0 ppm. Sharp drops in concentration were observed in the laminar sub-layer--from 50.0 ppm at the wall to values of a few ppm at the edge. The concentrations in the turbulent portion of the boundary layer were found to be relatively constant at the value at the edge of the sub-layer.

CHAPTER I

INTRODUCTION

Various investigators have observed that the turbulent flow structure of fluids can be considerably modified by the addition of macroscopic particles. Sproull[1]* observed friction reductions in dusty air. Elata and Ippen[2] and Daily and Chu[3] reported reductions in friction caused by the presence of polystyrene particles in water. Daily and Bugliarello[4] and Bobkowicz and Gauvin[5] discovered drag reductions in various fiber suspensions.

Recently, attention has been focussed on the turbulent flow characteristics of solutions containing high-molecular-weight linear polymers, which show exceptionally large reductions in friction drag, even in extremely dilute solutions. Since Toms[6] was apparently the first to study quantitatively the drag-reducing characteristics of this type of solution, the phenomenon is often referred to as "Toms phenomenon." Further experiments with various polymer-solvent systems, conducted mainly during the past five years, have shown this same type of anomalous behavior.

Practically all of the published data, more fully discussed in Chapter III, deal with the dynamics of pre-mixed solutions in straight tubes or rotating disks. The preference of investigators for this type of experimental analysis is due to two reasons. First, it is the most direct method

---

* Superscript numbers refer to the Bibliography on page 139.

for studying the mechanism involved in the drag-reducing phenomenon. Second, it is clear that applications in pipe flow are relatively easy to achieve, because the unit of additive is used over and over again until the end of the pipe or until mechanical breakdown of the polymer molecules occurs. Some applications of this technique have already been developed. For example, oil companies use it in the drilling of muds, in oil-well fracturing operations, and in the pumping of crude oil.

It appears that many additional applications can be developed based on injection of dilute polymer solutions along solid-liquid interfaces with the object of reducing skin-friction drag. Some of these are used on warships during action, submarines, deep-submergence craft, submarine-rescue craft, torpedoes, depth charges, and hydrofoil boats which could become foil-borne with a lower expenditure of power. However, experimental investigations in this area are rather scarce. Only four investigations seem to have been concerned with this problem. Thurston and Jones[7] developed and studied a soluble, drag-reducing coating which can be applied to the surface of an underwater body. Love[8] investigated the drag-reducing effects of macromolecular polymer solutions ejected through slots at the leading edge of a flat plate. Forester and Francis[9] prepared concentrated dispersions of polymers in non-solvent carriers and ejected the slurries into turbulent streams of water. Wells and Spangler[10] investigated slot injections of drag-reducing fluids into water in turbulent pipe flow.

At the present time, it is difficult to foresee the economic aspects of drag-reducing schemes involving polymer additives. This is due to the fact that the drag-reducing phenomenon is incompletely understood and because it is presently not known how the effect can be optimized. Studies

performed by Pruitt and co-workers[11] and by Ousterhout and Hall[12] have shown, however, that friction-reducing additives can substantially lower the cost of a given hydraulic fracturing operation. Kowalski[13] has published some preliminary calculations of the amount of polymer necessary to provide a concentration of 20 ppm in the boundary layer of a typical merchant ship of 450 feet in length, operating at a speed of 18 knots. His computations show that an amount of 13,360 pounds per hour would be needed. Later studies conducted by Wells and Spangler[10], however, have indicated that the presence of polymer in the viscous sub-layer alone is sufficient to cause the reduction in drag. This newly discovered effectiveness makes the situation much more hopeful for boundary-layer applications.

The studies performed to date have shown fairly conclusively that the following rules can be applied to drag reductions in polymer solutions.

a. Friction reductions occur only in the turbulent flow regime.

b. The polymer solution must be dilute so that the polymer molecules exist as identities separated from each other by pure solvent.

c. The polymer must have a linear structure, be soluble, and have a high molecular weight.

The purpose of the present study was to investigate the distributed surface injection of dilute polymer solutions. In view of the results of Wells and Spangler[10], it was felt that this injection technique provided an approach to the most efficient use of polymeric additives. For ease of analysis, injection of dilute solutions into a two-dimensional, turbulent boundary layer was selected. The specific objectives were to:

(a) Determine how the additives affect the velocity profiles in

the turbulent boundary layer.

(b) Evaluate the effect of injections on the boundary-layer thickness.

(c) Determine the magnitude of the drag reductions by measuring velocity profiles at several stations along the flat plate and using these in a momentum-deficit integral analysis.

(d) Calculate the shear-stress distributions in the boundary layer and to investigate how they are influenced by the presence of the injected fluids.

(e) Determine the distribution of the additive in the boundary layer.

It is well known that, at present, fully developed, turbulent boundary-layer flow cannot be successfully analyzed for all flow details. This is apparently due to the fact that no mathematical model is available which describes the generation and maintenance of turbulence in this particular type of flow. Introduction of a second species into the boundary layer complicates the situation even more so as to preclude a detailed mathematical analysis. Although a complete delineation of the structural details is probably impossible, the completion of the objectives listed above will provide a contribution to the understanding of the effect of macromolecular additives on the turbulent flow structure.

CHAPTER II

TURBULENT BOUNDARY LAYERS AND DRAG

Turbulent Flow

The details of "ordinary" turbulent flows are described by the three Navier-Stokes equations, together with the continuity equation. These four equations, however, are insufficient for obtaining structural flow details due to the existence of ten variables: three time-averaged velocity components, pressure, and six Reynolds stresses. Introducing a second material into a turbulent flow field increases its complexity even more so as to preclude a detailed analysis. Fortunately, in many instances fluid-flow problems can be reduced to a two-dimensional case. This permits a simplification since the number of variables is reduced to six: two velocity components, pressure, and three Reynolds stresses. Even this simplification does not permit a solution of all flow details and, at present, investigators must resort to empirical relations which permit mean-flow solutions.

Turbulent Boundary Layer

The boundary-layer concept is due to Prandtl[14] who recognized the importance of this layer in determining drag and separation characteristics. Later it was found that this layer also plays an important role in heat- and mass-transfer operations.

Investigators have found that a boundary layer is comprised of different regions. Runstadler and co-workers[15] describe the boundary layer

as consisting of three regions*, each correlating with a distinct portion of the non-dimensional mean-velocity profile. These regions are:

(a) wall-layer region

(b) fully turbulent region

(c) wake or intermittent region.

This structural delineation was confirmed in investigations by Schraub and Kline[16].

Wall-Layer Region (Viscous Sub-layer)

In normal boundary layers, the viscous sub-layer is very thin. Although the region is not sharply defined, its thickness is usually taken to be y^+ less than 10. In this layer the mean viscous stress is nearly constant and equal to the value at the wall, and the following relationship holds:

$$\tau = \mu \frac{du}{dy} \approx \tau_w \quad . \tag{1}$$

The mean-velocity profile in this region is given by:

$$u^+ = y^+ \quad . \tag{2}$$

Fully Turbulent Region

The fully turbulent zone is the region which extends from a y^+ value of approximately 10 to 300. It is characterized by a shear-stress dependence on both molecular viscosity and turbulent motion. The mean-velocity profile in this region is given by the "Law of the Wall":

---

* Note that these regions are somewhat different from those in pipe flow.

$$\frac{u}{u^*} = \frac{1}{k} \ln \frac{yu^*}{\nu} + C \quad . \tag{3}$$

This relationship can be derived by integrating Prandtl's relation

$$\tau = - \rho \ell^2 \left|\frac{du}{dy}\right| \frac{du}{dy} \quad , \tag{4}$$

with the mixing length $l = ky$ and $u^* = \sqrt{\frac{\tau_w}{\rho}}$. The two empirical constants appearing in Equation (3) must be evaluated experimentally, and many different values have appeared over a period of years.

Wake Region

The outer portion of the boundary layer shows a velocity distribution which deviates considerably from the logarithmic profile given by the Law of the Wall. The reason for this behavior is that the shear stress has become primarily dependent on the turbulent motion. Experimental evidence has shown that the mean-velocity profile can be correlated with two parameters in a velocity-defect law:

$$\frac{u_\infty - u}{u^*} = F\left(\Pi, \frac{y}{\delta}\right) \quad , \tag{5}$$

where Π is a profile parameter independent of x and y. Hinze[17] has proposed the following equation for the mean-velocity profile in this region:

$$\frac{u_\infty - u}{u^*} = - 2.50 \ln \frac{y}{\delta} + 1.38 \left(2 - \omega\left(\frac{y}{\delta}\right)\right) \quad . \tag{6}$$

This relationship was derived from an equation suggested by Coles[18] which

is essentially the Law of the Wall expression with a correction function.

Drag

A body moving relative to a fluid encounters a resistance known as drag, which is comprised of form or pressure drag and skin-friction drag. The form drag is caused primarily by separation of the boundary layer from the body with formation of a turbulent wake. This results in a loss of energy, the magnitude of which is a function of the shape of the body. Friction drag, in contrast, is caused by shear stresses exerted in the boundary layer. A flat plate experiences only skin-friction drag at zero incidence. Drag on other immersed bodies consists of both form and friction drag. Usually, in the case of a stream-lined object, the major contribution to drag is skin friction. Any technique to materially reduce the skin-friction drag will therefore substantially reduce the overall drag.

Drag-Reducing Techniques Applicable to Turbulent Boundary Layers

A number of techniques have been suggested to change momentum transport in a turbulent boundary layer with the object of lowering skin-friction drag. Lumley[19] has discussed some of these techniques in detail. He concludes that most methods effect drag reduction by changing the boundary-layer structure, i.e., by violating one or more of the principles of similarity or by increasing the sub-layer-thickness Reynolds number. The similarity principles affected are the Reynolds number similarity and the principle of wall similarity. According to Lumley, they can be violated by introducing other length and time scales. The sub-layer-thickness Reynolds number, i.e., the value of y^+ where the sub-layer profile meets the logarithmic profile, can be increased by making the unsteady motions more

dissipative. This can be accomplished by introducing particles, fibers, viscoelastic non-Newtonian additives, and dilute macromolecular solutions into the sub-layer, or by utilizing compliant boundaries.

Alteration of the viscosity in the laminar sub-layer is one of the few drag-reducing techniques which do not affect the boundary-layer structure. However, Lumley states that to be effective the viscosity must vary from a low value at the wall to a higher value at the edge of the sub-layer.

Methods for Measuring Skin Friction

Several techniques are available to measure skin-friction drag. The first method uses velocity gradients in the viscous sub-layer to obtain the wall shear stress from Equation (7):

$$\tau_w = \mu \frac{\Delta u}{\Delta y} \quad . \tag{7}$$

The difficulty connected with this method is due to the fact that the sub-layer is very thin so that extremely small probes must be used to obtain meaningful measurements.

The second method consists of fitting velocity data in the wall-layer region to the universal equation

$$\frac{u}{u^*} = 2.5 \ln \frac{yu^*}{\nu} + 5.5 \quad . \tag{8}$$

This is a relatively straightforward method to obtain the shear stress at the wall, provided the boundary layer is a one-component boundary layer not subjected to mass addition or to pressure gradients[16].

The third is a direct method in which a floating element is used to

obtain the friction force at the wall. This method is fairly difficult to apply, especially in flows where distributed surface mass addition takes place.

The fourth technique uses an integral momentum equation to obtain the shear stress at the wall. If accurate velocity profiles are available, this is probably the most generally applicable method. This last method was used in the present investigation.

CHAPTER III

PREVIOUS STUDIES DEALING WITH POLYMERIC DRAG-REDUCING ADDITIVES

Studies with Pre-Mixed Solutions

In 1948, Toms[6] presented a classical paper entitled: "Some Observations on the Flow of Linear Polymer Solutions through Straight Tubes at Large Reynolds Numbers." In this paper, he described investigations of the flow rate-pressure drop relationship of a 0.01 percent (by weight) solution of polymethylmethacrylate in monochlorobenzene. Two pipes, 0.404 cm and 0.128 cm in internal diameter were used, and both the laminar and turbulent flow regions were studied. The results clearly showed that the presence of the polymer in the solvent decreased the flow rate in laminar flow, possibly due to an increase in viscosity. In the turbulent region, however, the flow rate increased with polymer concentration up to a certain optimum value. Later studies have confirmed that drag reduction in dilute polymer solutions, now called the Toms' phenomenon, is restricted to turbulent flow only.

Many additional investigations of the dynamics of polymer solutions in pipe flow have since been made using various polymer-solvent systems. Fabula[20] investigated the flow characteristics of aqueous solutions of six polyethylene oxides in a series of blowdown experiments. He was the first investigator to clearly recognize that only a few parts per million of the higher-molecular-weight polymers in water are sufficient to yield relatively large reductions in drag. A major complication in his studies was a rather

severe mechanical degradation of the polymer molecules at high flow rates.

Hoyt and Fabula[21] conducted a study to evaluate the friction-reducing effectiveness of various water-soluble polymer additives. The investigation was conducted in a rotating-disk apparatus. Most effective on a weight basis was polyethylene oxide. In additional pipe-flow tests, polyethylene oxide gave drag reductions of more than 40 percent in an aqueous solution of 2 parts per million by weight (ppm) and of more than 75 percent at a concentration of 100 ppm.

In order to elucidate the mechanism involved in the drag-reducing phenomenon, a few investigations have been made of the turbulent velocity profiles. Shaver and Merrill[22] studied the fluid dynamics of dilute solutions of four different polymers in a recirculating pipe-flow apparatus. The polymers were: sodium carboxymethylcellulose, ammonium alginate, carboxypolymethylene, and polyisobutylene. With the exception of the cyclohexane solutions of polyisobutylene, all were aqueous solutions. At a given Reynolds number, the velocity profiles in the solutions were found to be less blunt than those in the base fluids. In addition, photographic studies of dye injections in the polymer solutions were made at the tube wall and in the center of the tube. These studies showed the occurrence of a thicker laminar sub-layer in the polymer solutions and a lower rate of vortex formation at the tube wall. Studies conducted by Elata, Lehrer, and Kahanovitz[23] and by Pruitt and Crawford[24] have confirmed that the presence of polymers substantially increases the thickness of the laminar sub-layer in pipe flow.

Elata and Tirosh[25] investigated the drag-reducing abilities of Separan AP 30 and guar gum in water. Using their experimental data and

those available in the literature for several kinds of additives, they concluded that drag reduction practically always coincides with a decrease in the universal constant k^*. Velocity profile data in aqueous solutions of guar gum obtained by Wells[26] show the same type of behavior. His data indicates that the slope of the logarithmic velocity profile (the Law of the Wall profile) was increased and that the mixing-length constant was consequently decreased compared with purely viscous behavior. Again a thickening of the viscous sub-layer was noticed.

Ernst[27] measured velocity profiles in aqueous solutions of carboxymethylcellulose. The major effect of the polymer was found to be a linear upward shift of the velocity parameter in the universal Law of the Wall relationship. This indicated that the mixing-length constant had not been affected, contradicting the findings of Elata and Tirosh[25] and Wells[26].

The friction-reducing effects of dilute polymer solutions flowing in rough pipes were investigated by Lindgren[28]. The experiments, conducted in the turbulent flow region, showed that friction reductions similar in magnitude to those obtainable in smooth pipes were attained.

Couette flow of dilute polymer solutions has received some attention. Shin[29] and Lee[30] investigated the drag-reducing effects of several polymers and concluded that the concentration of polymer required to attain a given fractional drag reduction varied inversely with its terminal relaxation time, as calculated from the theory of Rouse[31]. The stability of this type of flow using dilute polymer solutions was investigated by

---

* See Equation (3), page 7.

Rubin and Elata[32]. Dye-injection experiments showed that the critical Taylor number increased with concentration while the wavelengths of the vortex cells remained unaltered.

Pruitt and Crawford[24] studied the effect of friction-reducing additives on the hydraulic fluid MIL H-5606 A. It was found that friction reductions as high as 60 percent could be achieved. Velocity profile data taken within 0.01 inch from the wall showed that the viscous sub-layer of the treated fluid is three to ten times thicker than that of the base fluid.

Wells and co-workers[33] conducted turbulence measurements in a 0.05 percent aqueous solution of sodium carboxymethylcellulose, and also in pure water for purposes of comparison. In this experimental study, the stream-wise component of turbulence was measured in pipe flow. It was found that the frequency-dependent turbulent energy spectra differ in that the low-frequency energy is less for the carboxymethylcellulose solution than for water. The reverse is true for the high-frequency energy.

Pruitt, Rosen, and Crawford[34] studied the effect of temperature on drag reduction. Testing aqueous solutions of polyethylene oxide (Polyox-701), polyacrylamide (K-PAM), and guar gum at four concentrations, relatively little change in drag reduction was found from 35° F to 105° F. A substantial loss in drag reduction, however, became apparent from 105° F to 140° F.

Hoyt and Fabula[35] conducted drag-reduction studies with a rotating-disk apparatus to determine the effect of sea water on the performance of polymer additives. Friction-reduction data taken in simulated sea-water solutions of guar gum and polyethylene oxide agree very closely with those obtained in fresh-water solutions.

Little[36] measured flow birefringence in dilute polymer solutions. It was discovered that Polyox macromolecules continue to deform with increasing velocity gradient in turbulent flow, even after alignment with the flow field. Also based on his experimental observations, Little suggested that adsorption of macromolecules on solid-liquid interfaces may play an important role in the drag-reduction phenomenon. This adsorption phenomenon has also been observed by Pruitt and co-workers[34].

Virk[37] studied the effect of polymer molecular weight and concentration on the onset and extent of turbulent drag reduction in two pipes. Five molecular-weight cuts of polyethylene oxide were used, covering a range from 80,000 to 6,000,000. Concentrations varied from 0.1 to 10,000 ppm. It was observed that for a given polymer-solvent system and pipe, the onset of drag reduction by the Toms' phenomenon occurred at a well-defined threshold stress, independent of concentration over the range investigated.

Goren and Norbury[38] summarized friction-reduction studies conducted at the University of Liverpool. These studies dealt with fully developed turbulent flow of Polyox WSR-301 in a 2-inch-diameter pipe. The mechanism of the flow was investigated by examining the friction drag, velocity profiles, and concentration distribution. It was found that the polymer was uniformly distributed over the pipe cross section. Even though the polymer was uniformly distributed, the additive was found to influence the flow only in the neighborhood of a solid boundary. There, the eddy viscosity was found to be much lower than that of water. A critical Reynolds number, below which no drag reduction occurs, was established. It was found to be independent of concentration over the range investigated. The

maximum drag reduction obtained was 71 percent at a Reynolds number of 1.5 x 10^5 in a solution having a concentration of 10 ppm. The data tend to support the premise that k is not a universal constant.

A few studies have been performed to evaluate the drag of bodies moving through polymer solutions. Kowalski[13] tested a flat plate and models of two ships in fresh water and aqueous solutions containing 10, 20, 30, and 50 ppm of polyethylene oxide (WSR-301). The drag measurements covered a Reynolds number range of 7 x 10^5 to 4 x 10^6, based on length dimension. The models were towed at constant speed in a towing tank and the drag was measured by means of a force block. Reductions in resistance of up to 40 percent were attained.

Merrill, Smith, and Chung[39] tested the drag-reducing capabilities of polyethylene oxide solutions (WSR-301) on two test bodies, one a flat plate the other a scale model of a torpedo. The concentrations investigated were: 0, 20, 50, and 100 ppm. The test apparatus consisted of an open column equipped with photo-electric cells to measure the terminal velocities of the test models. The models were placed on the bottom of the tank and were accelerated to terminal velocity by a system of counter-weights. The drag on the flat plate was in all instances reduced, the terminal velocity increasing with increasing concentration. The drag on the torpedo model also decreased with increasing concentration up to a concentration of approximately 30 ppm. Then the torpedo suffered a drag increase. The explanation was advanced that addition of the polymer caused early separation, thereby increasing the form drag.

Lang and Patrick[40] performed drop tests in plain water and in poly-ethylene oxide (Polyox WSR-301) solutions of 200 and 1,000 ppm to evaluate

the drag of blunt bodies in polymer solutions. Results show that sphere drag was reduced by as much as 69 percent for the case of a 2-inch-diameter steel sphere in a 1,000 ppm solution of Polyox at a Reynolds number of 1.4×10^5, while the drag of other models (cones, disks, and cylinders) was at most only slightly reduced. Dyed-wake photographs of falling spheres showed that the additives could shift the point of boundary-layer separation in a rearward direction. It was also found that the additives produced an apparent decrease in turbulent mixing in the near wake.

Ruszczycky[41] conducted sphere drop tests in various aqueous solutions of guar gum and Polyox WSR-301. Since the highest Reynolds number reached was only 5.19×10^4, all spheres experienced separated laminar flow only. Maximum reductions in the drag coefficient of 28 percent were achieved, under these conditions.

Studies with Injection

As was mentioned earlier, a few investigations have been made of drag reductions produced by injecting polymers into turbulent boundary layers.

Vogel and Patterson[42] evaluated the effect of injecting aqueous solutions of Polyox WSR-35, 205, and 301 into the three-dimensional boundary layer of a streamlined model. The fluids were injected through a nose slot. Since the boundary layer was too thin to probe, only measurements in the wake were performed. Preliminary results, using a hot-film probe, indicate a change in the mean square of the turbulence velocities.

Thurston and Jones[7] developed a soluble drag-reducing coating. In a test program, the coatings were applied to the stagnation region of a

torpedo-shaped test model which was dropped in a drop-tank facility. By accurately measuring the time-distance relationship, reductions of approximately 18 percent in total model drag were obtained, corresponding to a reduction in friction drag of approximately 30 percent.

Love[8] made an experimental investigation of the effects of injecting polymer solutions into the turbulent boundary layer of a flat plate. It was found that ejection of the solutions through slots at the leading edge of the flat plate decreased its drag by as much as 50 percent. The media ejected from the flat plate were: pure water, dilute aqueous solutions of sodium carboxymethylcellulose, polyethylene oxide (Polyox WSR-301), and suspensions of neutrally buoyant, spherical polystyrene particles. Ejection of the polystyrene particles, not too much larger than the macromolecules, had no effect on the drag of the plate.

Wells and Spangler[10] investigated injection of drag-reducing fluids into water, in turbulent pipe flow. They found that the local pressure gradient could be reduced by an amount comparable to the flow of a uniform concentration when the fluid was injected in the wall region. When the fluid was injected in the turbulent core, no reduction in local pressure gradient occurred until the injected fluid had diffused into the wall region. This confirmed earlier findings[22,23,24,34,36,38] that the significant changes in turbulent shear flow occur in the viscous sub-layer.

Forester and Francis[9] formulated concentrated dispersions of water-soluble polymers in non-solvent carriers. The polymer particles in such a slurry do not dissolve, but remain suspended as discrete particles and mixtures of relatively low viscosities result. The polymers investigated were: guar gum, polyethylene oxide, and polyacrylate. Carriers were:

glycerin/isopropyl alcohol and polypropylene glycol. Ten percent slurries were injected into turbulent water streams, and friction reductions as large as 49 percent were measured with mixing times as short as 1.5 seconds.

Baronet and Hoppmann[43] investigated the drag on cylindrical bodies with spherical ends which were suspended coaxially within straight tubes. Dynamometers measured the drag in water and in aqueous solutions of Polyox Coagulant and Polyox WSR-35. In the investigation, polymer solutions at concentrations of 0.10, 0.25, 0.50, and 1.00 percent were injected into the water by a tube located transversely in the stream and ahead of the test model. Drag reductions of approximately 35 percent were attained.

Explanations of the Drag Reduction

Although the exact mechanism responsible for drag reduction in dilute polymer solutions is still far from understood, some progress has been made in developing a physical model. The earlier explanations centered on wall effects. Oldroyd[44] postulated a solvent-rich layer near the wall which would cause effective slip. A photographic study of viscoelastic polymer solutions by Shaver and Merrill[22] lends some support to this theory. However, instead of assuming a discrete annular layer near the wall, Shaver and Merrill assumed the existence of a viscosity gradient in turbulent pipe flow with a higher viscosity at the center than at the wall. It was hypothesized that the increasing viscosity with increasing distance from the wall would resist migration of vortices from the wall. This then would decrease the rate of vortex formation and lead to a decrease in the intensity of the turbulence fluctuations inside the boundary layer. One objection against these physical models is the fact that later

studies have shown that even extremely dilute solutions of polymers show appreciable reductions in friction drag. These solutions have viscosities indistinguishable for all practical purposes from those of the pure solvents. In 1967, Little[36] suggested that adsorption of polymer molecules on the wall may be involved in drag reduction which would remove some of the objections. He based his suggestion on accummulated evidence [22,23,24,34,38] which indicates that drag-reducing effects apparently occur in the laminar sub-layer of the flow and on his experimental studies which showed unusually high values of Meyer's fluid-property parameter* at low concentrations.

Another explanation centers on hypothesized visco-elastic properties of dilute polymer solutions. Ward and Atkinson[45] were the first to advance this explanation in 1948. It was suggested that the elastic elements of the fluid store kinetic energy of turbulent fluctuations thus damping the turbulence and producing a lower Reynolds stress, conventionally denoted by $-\overline{\rho u'v'}$.

The theory of visco-elasticity was supported by Lumley[46] who examined dissipation of turbulent energy in incompressible, isotropic fluids, and by Gadd[47] who showed that dilute solutions of Polyox WSR-301 and of guar gum, not more than 60 ppm in concentration, show normal-stress differences.

Recently, Black[48,49] proposed a new theory of wall turbulence which can explain drag reductions when a visco-elastic coupling agent is present in the wall-layer region of the fluid. Supported by visual studies

---

* The reader is referred to Equation (11), page 23.

conducted by Kline and colleagues[15,16], he concluded that the classical division of the instantaneous motion into mean and turbulent components is inadequate. Instead, Black considers instantaneous flow as the sum of two unsteady periodic motions. One of these motions (the primary motion) is a large-scale, low-frequency, organized motion which is attached to the wall and which is described deterministically by the time-dependent equations of motion. The second (secondary) motion consists of random, high-frequency turbulent elements or eddies which are detached from the wall and which rotate in the primary motion with no direct interaction. This motion can only be described on a statistical basis. Thus, Black envisions turbulent shear flow as a time-dependent viscous phenomenon which is continuously striving to return to the laminar state, but is prevented by a periodic breakdown due to instability excited by the ambient turbulence. The periodic breakdown is accompanied by violent ejections of fluid from the wall in localized jet-like motions, which are believed to relieve viscous stress build-up in the sub-layer. It is thought that a visco-elastic material in the boundary layer will store quantities of elastic energy during high transient rates of shear and then release it at a rate depending on the elastic relaxation time in the fluid. In this manner some of the energy which is normally transferred to the mixing jets in primary motion breakdown is fed back into the primary motion during the period of viscous development. This procedure would reduce the rate of turbulence generated and subsequently depress the entire level of turbulence in the shear layer.

Empirical Relationships

It is useful at this point to consider some empirical relationships which have been developed for flow of dilute polymer solutions. It should be noted that the relations do not imply existence of any sort of physical mechanism, and that the expressions are strictly applicable only to the polymer-solvent systems for which they were developed, under the operating conditions specified in the references.

Oldroyd[44] has derived an expression for the pipe flow of dilute polymer solutions by altering the von Kármán-Nikuradse[50,51] relationship. The original relation, valid for turbulent pipe flow of Newtonian fluids, is:

$$\frac{1}{\sqrt{c_f}} = 4.00 \log \left(\mathrm{Re} \sqrt{c_f} \right) - 0.40 \quad . \tag{9}$$

To extend this expression to the flow of dilute polymer solutions, Oldroyd took two factors into consideration; namely, that the viscosity of these solutions is a function of the rate of shear and the suspected presence of a wall effect. It was assumed that the limiting value of the viscosity at high rates of shear, μ', adequately described the flow situation. The wall effect was treated quantitatively by replacing the volumetric rate of discharge, Q, by $Q-\pi R^2 v_s$, where v_s is the effective slip velocity at the wall. Then Equation (9) becomes:

$$\frac{1}{\sqrt{c_f}} = 4.00 \log \left(N_{Re} \sqrt{c_f} \right) - 0.40 + \frac{1}{4} \zeta \left(\frac{\mu' N_{Re} \sqrt{c_f}}{R} \right) \quad , \tag{10}$$

where N_{Re} = Modified Reynolds number, $N_{Re} = \frac{D\langle u \rangle \rho}{\mu'}$. By introducing the

function ζ into the von Kármán-Nikuradse equation, the unknown phenomena operating in tube flow of dilute polymer solutions are lumped in one term. It is obvious that in all cases where reduction in friction occurs, the function ζ must be positive.

Meyer[52] has suggested the following equation to describe the flow behavior of dilute polymer solutions in pipes:

$$\frac{1}{\sqrt{c_f}} = \left(4 + \frac{\alpha}{\sqrt{2}}\right) \log\left(Re\sqrt{c_f}\right) - \frac{\alpha}{\sqrt{2}} \log\left(\sqrt{\frac{2\tau_w}{\rho}}\,\frac{D}{\mu_w}\right) - 0.394 \,, \tag{11}$$

where: α = a fluid-property parameter.

Little[36] determined the value of the parameter α for the following four Polyox compounds: WSR-35, WSR-205, WSR-301, and Coagulant. The resulting relationship was:

$$\alpha = \left[\frac{834\left(C_{Cr} + 240\right) C}{\left(C_{Cr} + 240 - C\right)\left(C_{Cr} + 240 + 227\,C\right)}\right]^2 \,, \tag{12}$$

where: C_{Cr} = critical concentration as defined by Shin*.

Elata and co-workers[23] have proposed an equation similar to that of Meyer, namely:

---

* Shin[29] has defined a critical polymer concentration which divides the dilute and concentrated regimes. The critical concentration according to this principle is reached when the polymer molecules, having been assigned an effective spherical diameter which is of the order of magnitude of its root-mean-square end-to-end distance, are brought to a spherical packing of 74 percent with 26 percent void volume. When the concentration is less than the critical value, the polymer solution may be considered dilute.

$$\frac{1}{\sqrt{c_f}} = 2.0 \log Re \sqrt{c_f} - 0.8 + \frac{\alpha}{\sqrt{8}} \log \left(\frac{\tau_w^{\square} \lambda_{max}}{\mu} \right) , \qquad (13)$$

where: λ_{max} = largest relaxation time of the polymer molecule in the fluid.

Virk[37] has observed that the onset of drag reduction in a given pipe and polymer-solvent system occurs at a well-defined point. Drag reduction in turbulent flow of dilute polymer solutions is initiated at a constant value of the product $D_m k_d$, which is physically the ratio of macromolecule to dissipative eddy size. The best present value for $D_m k_d$ is approximately 0.0025, which was obtained from data on polyethylene oxides in water. In this expression, k_d is defined as the wavenumber where the dissipation is a maximum; D_m is the characteristic diameter of the macromolecule which is twice its root-mean-square radius of gyration.

The onset hypothesis can ideally be used to determine when a given macromolecule will produce a reduction in drag. Using the value of 0.0025 for $D_m k_d$ and making the necessary conversions in

$$\sqrt{\tau_w} = \frac{D_m u^* \rho^{\frac{1}{2}}}{2R_G} \quad . \qquad (14)$$

Virk, et al.[53] obtained

$$\tau_w^{\square} = \rho \left(0.625 \times 10^6 \frac{\nu}{R_G} \right)^2 \quad . \qquad (15)$$

This expression is dimensional and the following units must be used:

$\tau_w^{\square}$ = wall shear stress at the onset of drag reduction, dynes/cm^2

ρ = solvent density, gms/cm^3

ν = kinematic viscosity, cm^2/sec

R_G = Root-mean-square radius of gyration of the macromolecule, Å.

Ram and co-workers[54] concluded that a critical Reynolds number exists for each polymer, below which no friction reduction occurs. This Reynolds number can be calculated from

$$Re \sqrt{c_f} = D \sqrt{\frac{2}{\lambda_{max} \nu}} \quad . \tag{16}$$

Fabula, Lumley, and Taylor[55] questioned the hypothesis of Virk that the threshold stress is reached when the smallest significant scale of turbulence near the wall becomes small enough with respect to the coil diameter of the macromolecule. They concluded that the magnitude of this scale ratio was incompatible with present turbulence knowledge. Instead, they related the threshold stresses to macromolecular-coil characteristics. Data obtained by Virk[37] and Giles[56], however, indicate that Virk's relationship allows a much better fit of the data.

CHAPTER IV

EXPERIMENTAL APPARATUS AND PROCEDURES

Experimental Apparatus

Water Tunnel

To conduct the investigation, a water tunnel was built in the School of Chemical Engineering, Georgia Institute of Technology. A photograph of the tunnel is given in Figure 1 and a schematic diagram is presented in Figure 2. The apparatus was a single-pass, continuous-flow, low-speed water tunnel consisting of an inlet section, a test section, and an exit duct, all constructed of 0.250 inch aluminum plate. Water entered the apparatus through a 3 inch polyvinyl chloride pipe (Schedule 80) which originated at the bottom of a 500 gallon stainless steel overhead tank. This tank received water from a main line and discharged a major portion through the test section. The remainder of the water was discharged to a 500 gallon receiving tank through an overflow line, centered at 54.5 inches from the bottom of the overhead tank. In this manner, a constant head of approximately 16.6 feet was provided at the test apparatus. The water leaving the exit duct was discharged through a 3 inch polyvinyl chloride pipe to the receiving tank which emptied into a drain.

The 8.0-feet-long inlet section of the apparatus diverged from a 2.9 x 2.9 inch cross-sectional area to an area 6.0 x 12.0 inches in cross section. This section was designed such that the maximum angle between the

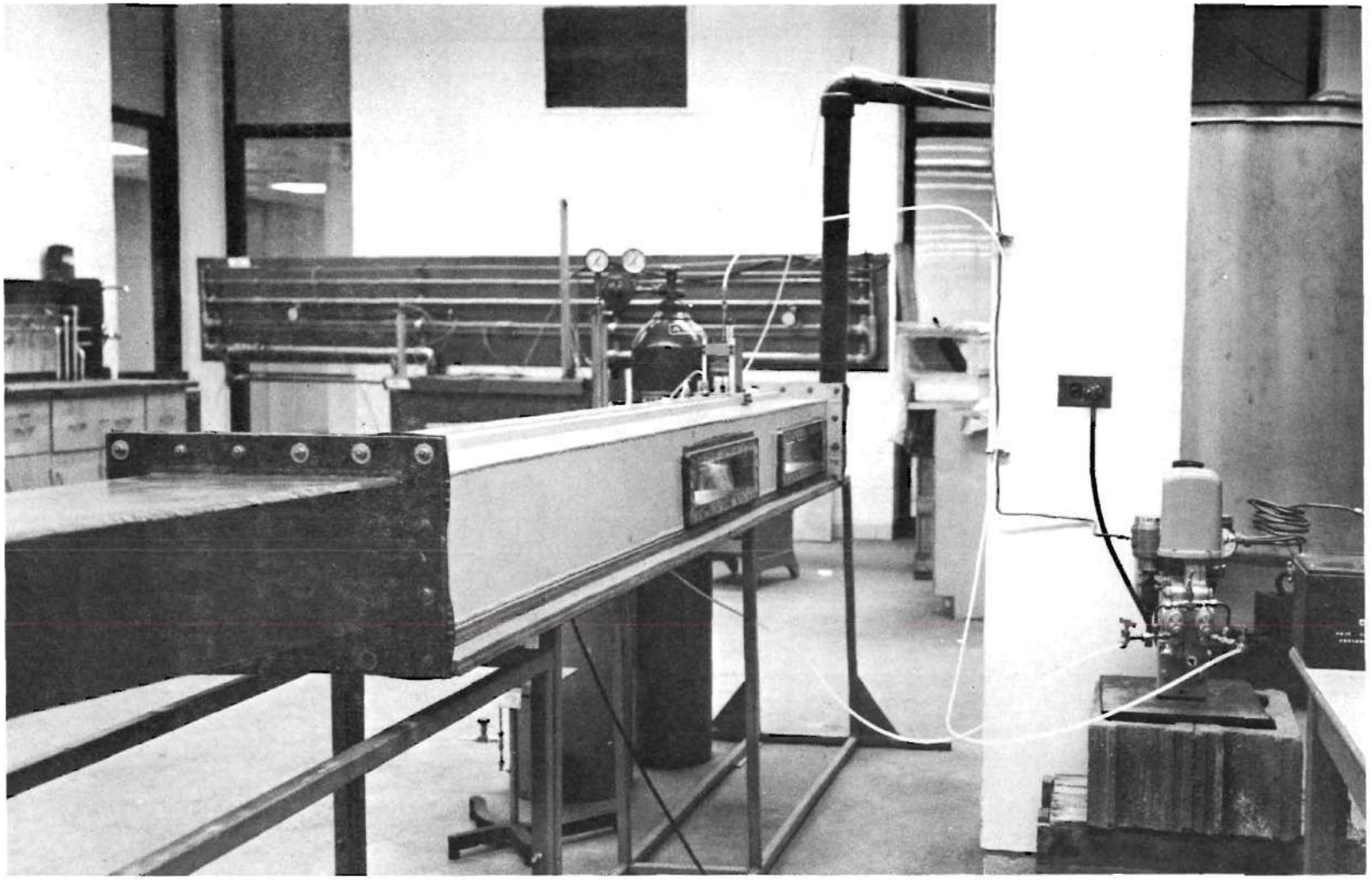

Figure 1. Experimental Apparatus.

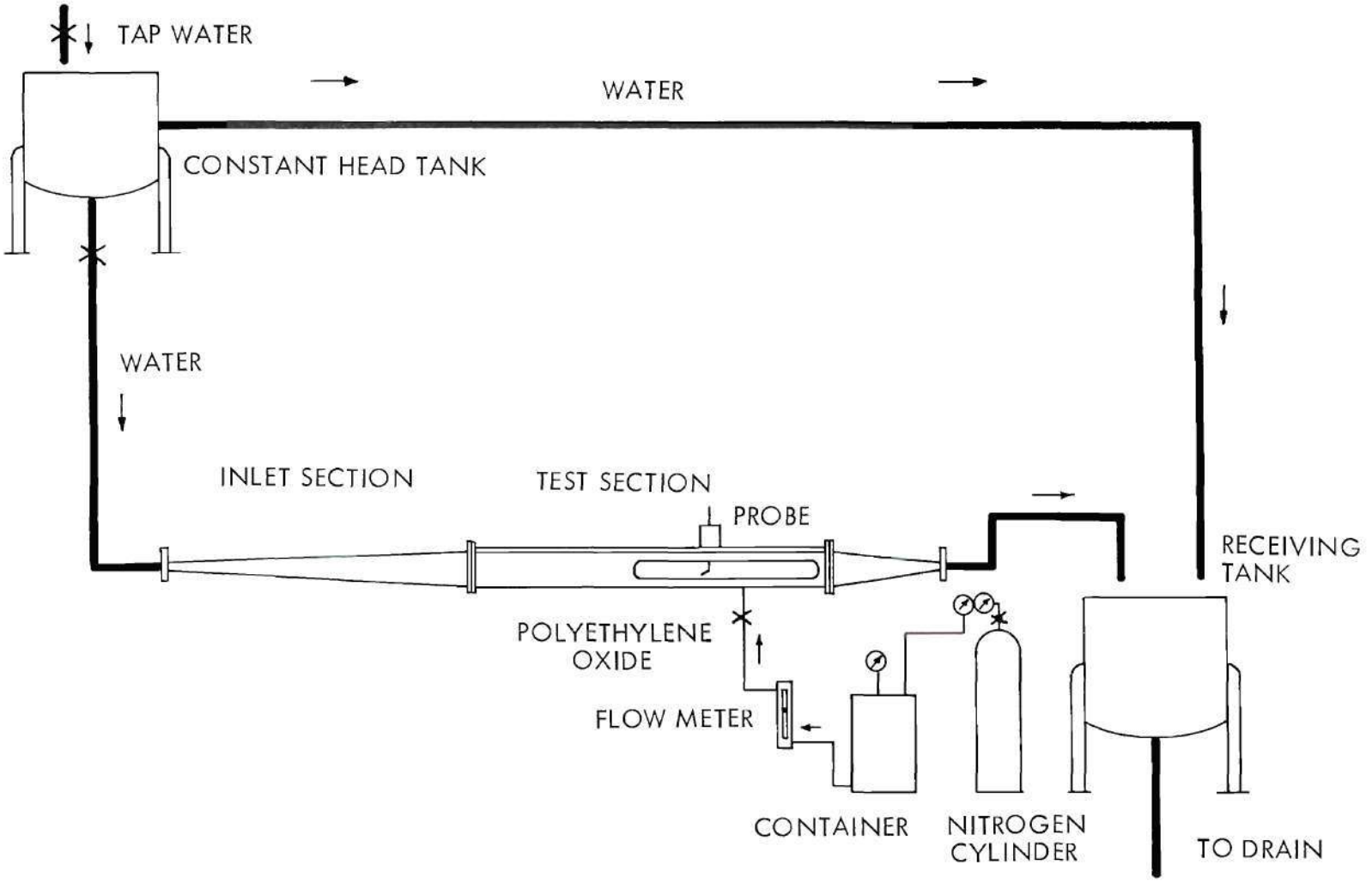

Figure 2. Schematic Layout of the Experimental Apparatus.

diverging walls was less than seven degrees to prevent separation and to maintain uniform flow*.

The test section, bolted to the inlet duct, was rectangular in cross section. It was 8.0 feet long and had an internal area of 7.0 x 12.0 inches. The bottom of this section carried an insert which served to distribute the injected fluid uniformly over the last half of the channel. The insert consisted of a 0.375-inch-thick aluminum plate, 96.0 inches long and 12.0 inches wide. The first 46.5 inches of this plate were covered with a sheet of 0.625-inch-thick aluminum. The top surface of the remaining 49.5 inches accommodated 0.75-inch-wide strips of 0.125-inch-thick aluminum which supported a 0.50-inch-thick porous plate, manufactured of rigid, high-density, linear polyethylene by the Porex Corporation**. This porous plate contained 30-micron pores and had a 200 micro-inch surface finish which was hydraulically smooth. It was attached to the aluminum strips with 0.125 inch stainless steel machine screws with countersunk heads.

The space between the porous plate and the aluminum was connected to a 40.0 liter aluminum container by means of three 0.250 inch lines, each provided with a needle valve. These lines terminated into one 0.250 inch line which was connected to the bottom of the container through a Fisher and Porter flowmeter, Model 10A4136 ND LK equipped with a 2L-150

---

* Chemical Engineers' Handbook, edited by J. H. Perry, McGraw-Hill Book Company, Inc., New York, Third Edition, p. 388 (1950).

** Porex Materials Corporation, Fairburn, Georgia.

tube and a glass float, with a capacity of 0 to 1200 mls/min. Selection of three connecting lines was based on dye experiments which had shown that one or two lines provided non-uniform injection.

The container, equipped with a relief valve, was pressurized by a nitrogen cylinder to eject the drag-reducing solution through the flow-meter and the porous plate directly into the boundary layer on the bottom surface. The test section contained two horizontal windows of plexiglass to facilitate initial adjustment of the probes. Two 12 volt light bulbs opposite and facing the plexiglass windows provided illumination.

The test section terminated into a 20.0-inch-long duct which converged from a 6.0 x 12.0 inch cross-sectional area to an area with a cross section of 2.9 x 2.9 inches. The water discharged from this section into a 500 gallon stainless steel tank through a 3 inch polyvinyl chloride pipe. The tank emptied into a drain.

With a water supply limited to approximately 170 gpm, it was decided to increase the flow of water in the channel in order to obtain more accurate measurements of the local velocities. The bulk flow rate of the main stream was increased by installing a section of rigid styrofoam backed with a sheet of aluminum in the top of the test section. This insert was 3.20 inches thick, 12.0 inches wide, and 96.0 inches long. Appropriate holes were provided to allow passage of the velocity probe into the channel.

Boundary-layer measurements were made with the probe assembly shown in Figure 3. This assembly was supported by an aluminum track, 4.5 inches wide by 96.0 inches long, which was attached to the top plate of the test section. This track contained eight ports located 6.0 inches apart,

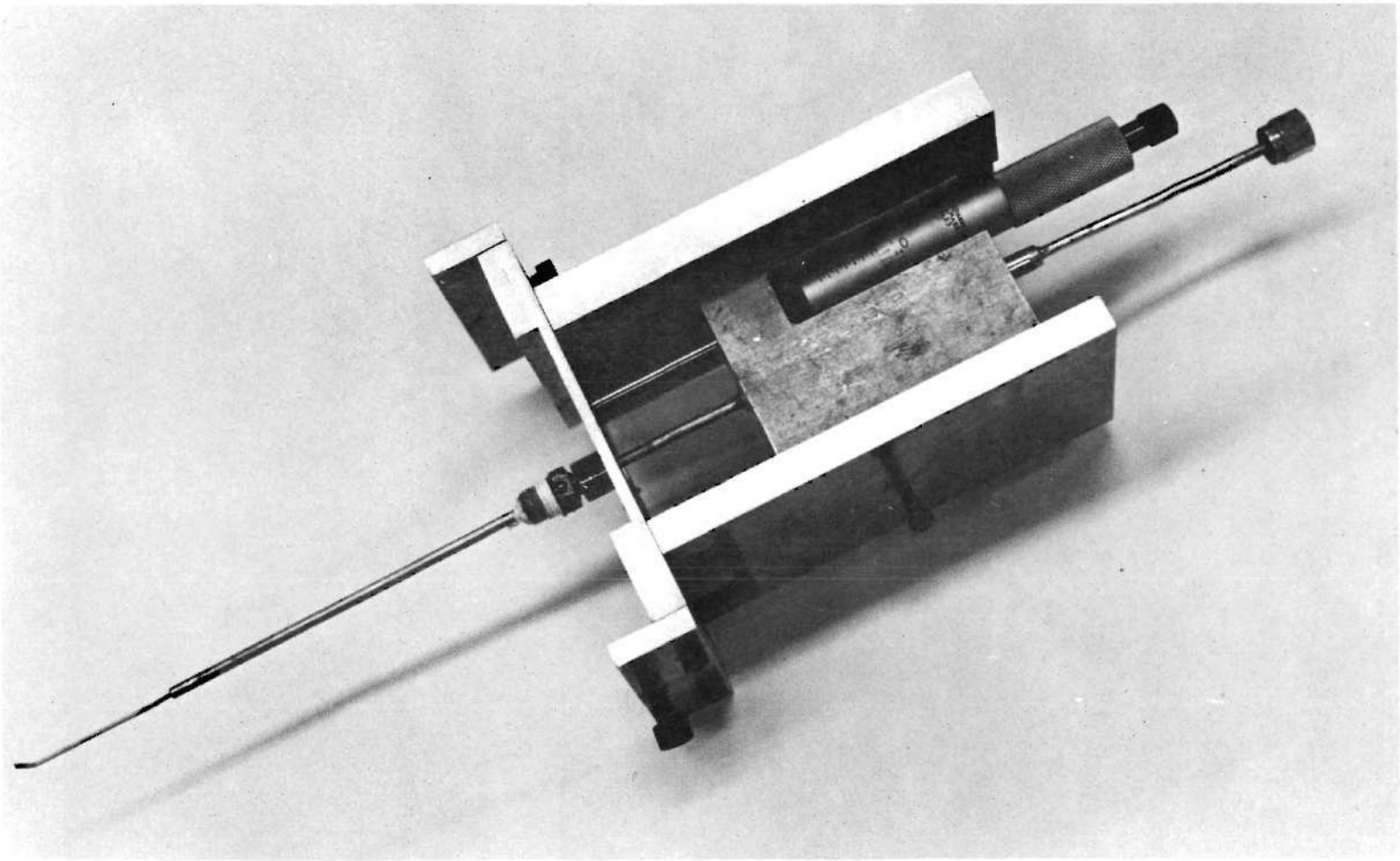

Figure 3. Probe for Measuring Velocity and Concentration Profiles.

starting at a distance of 48.0 inches from the inlet of the test section. Boundary-layer measurements at selected locations were made by probing through these ports. O-ring seals around the probe prevented water leakage from the test chamber. To obtain measurements in a vertical direction, a micrometer drive was employed to raise or lower a slide to which the probe was attached. The probe itself was constructed from 0.125-inch-diameter stainless steel tubing. Its tip was fabricated from 0.065-diameter stainless steel hypodermic tubing and telescoped into the bottom end of the larger tube. The probe tip had a 0.005 x 0.070 inch rectangular opening and was 0.010 inches high. Of the five probes that were made, the one having the most uniform opening was selected under a stereoscopic microscope at a magnification of 25X. This probe was used to conduct the measurements later described in this work. The top of the probe was connected to the differential-pressure cell during velocity measurements, or was left open to collect samples for concentration measurements.

Differential-Pressure Cell

To measure the relatively low differential pressures involved in this study, a Foxboro Type 15A Differential-Pressure Cell Transmitter with a range of from 0 to 2.4 inches of water was employed. Air required to operate the cell was supplied through an air filter and a regulator. The regulator was adjusted to provide air at a pressure of 20 psi. The high-pressure inlet of the differential-pressure cell was connected to the top of the velocity probe. The low-pressure side was connected to one of several static taps in the side wall of the channel. A balancing system was provided so that equal pressures could be applied to both inlets. The output of the cell was transmitted to a mercury manometer through a relay.

Polarograph

To analyze samples taken from the channel, a Sargent Model XV Polarograph was employed. This instrument produces a continuous record of the current-voltage curve of a solution undergoing electrolysis between a dropping-mercury electrode and a reference electrode. In the present application, it was used to measure concentrations of polyethylene oxide in water by determining the height of the oxygen peak, according to a technique described by Goren and co-workers[57].

The Drag-Reducing Agent Selected for this Investigation

The polymer selected for this investigation was polyethylene oxide (Polyox WSR-301), manufactured by Union Carbide Chemicals Company. The selection was based on the following considerations:

(1) The chemical is one of the best drag-reducing agents presently known.

(2) It is water soluble and the solutions are easily characterized, for example by intrinsic viscosity measurements.

(3) It is relatively inexpensive and is available in commercial quantities.

Polyox is one of the high-molecular-weight polymers of ethylene oxide, $H-[O-CH_2-CH_2]_n-O-H$. The lower members--n up to about 150--are known as polyethylene glycols. The higher members of the series, with n ranging from about 2,000 to 200,000 and more, differ considerably in properties from the glycols. They are called polyethylene oxides. Four different molecular-weight grades are manufactured. They are, in increasing molecular weight: WSR-35, WSR-205, WSR-301, and WSR-Coagulant grade.

Polyethylene oxides are soluble in a number of common solvents, such as methanol, ethylene dichloride, chloroform, acetone, benzene, and others. Of special importance, however, is their solubility in water. All aqueous solutions of polyethylene oxide, even though dilute, evidence a considerable degree of polymer-solvent interaction. At concentrations of the order of 1 percent, a stringy consistency is produced and the solutions are classed rheologically as pseudoplastic, i.e., the viscosity decreases in a reversible manner with increasing shear rate. Solutions over 5 percent in concentration are elastic gels which show a yield point.

Solutions of polyethylene oxide in water are characterized by a parameter called the intrinsic viscosity, $[\eta]$, which is defined as:

$$[\eta] = \lim_{c \to o} \frac{\mu - \mu_o}{c\mu_o} \quad . \tag{17}$$

It has been shown that a relationship exists between average molecular weight of the polymer in solution and its intrinsic viscosity. For polyethylene oxide in water at 30° C, this relation is[58]

$$[\eta] = 1.25 \times 10^{-4} M^{0.78} \quad , \tag{18}$$

when $[\eta]$ is expressed in units of dl/gm.

At 25° C, Shin[29] obtained a similar expression with a slightly lower constant having a value of 1.03. The relations hold over the molecular-weight range from somewhat below 10,000 to 10 million or more, and consequently cover the range of WSR-301 which has a maximum average molecular weight of about 4 million.

Polyethylene oxide is a polyether and as such is subject to oxidative attack. The polymer is also subject to degradation by shearing action. Possibilities of hazards in using Polyox resins seem to be remote. Standard feeding tests indicate that Polyox has a very low toxicity[59].

Viscosities of the aqueous solutions used in this investigation were measured at 76.0° F with a Cannon-Fenske viscometer having a range of from 0.6 to 1.6 centistokes. The solution concentrations were: 0, 25.0, 50.0, and 150.0 ppm. It was found that all viscosities agreed within 1.5 percent. The intrinsic viscosity of the injected solutions was measured as 16.98 dl/gm which indicated an average molecular weight of 3.8×10^6 for WSR-301. This implies that no degradation of the polymer occurred during preparation of the solutions.

Procedures

Prior to the experimental investigation, a short study was made to determine if any changes take place in the physical properties of the ejected solution, when it is forced through the porous polyethylene surface. The properties examined were: concentration and intrinsic viscosity. It was found that no changes were effected. This indicates that no adsorption of the polymer takes place and no mechanical breakdown of the macromolecules.

In the experimental investigation, runs were made without mass addition, with water addition, and with polymer injections at various injection rates. In these runs, velocity profiles and, where applicable, concentration profiles were obtained at one or more of six stations located at 48.0, 54.0, 60.0, 72.0, 78.0, and 90.0 inches from the inlet of the test section.

At each station measurements were made at 19 different vertical positions.

The system was operated at the maximum capacity of 155 gallons of water per minute. In the runs without injections, measurement of the differential pressures was started almost immediately after the gate valve in the main line had been opened. The measurements were made with a Foxboro Differential-Pressure Cell Transmitter. The static pressure was provided by a 1/32-inch hole in the wall of the test section adjacent to the dynamic probe. Since the meter was placed below the test section, the difference between the static and dynamic pressure with the water at standstill was zero, no matter where the probe was positioned in a vertical direction, because the same total head was applied to each connection of the pressure cell. With the main stream in motion, the difference in pressure between the static and dynamic connection was directly due to the velocity. Measurements were started at the porous surface, after the probe tip had been carefully located at this surface by visual inspection through the plexiglass windows. Measurements were continued until the differential pressure became constant.

Before the injection runs were started, the necessary polymer solutions were prepared by slowly adding the required amount of polyethylene oxide to 40.0 liters of tap water under gentle, manual agitation. The solution was usually left standing for at least 2 hours to allow complete dissolution of the additive. The solution was then poured into the 40.0 liter container.

The injection runs were started by providing water to the channel and pressurizing the storage container to approximately 25 psi. The float of the flowmeter was then adjusted to the desired rate. No difficulties

were experienced in maintaining the injection rates for the duration of the runs. Approximately 15 minutes were allowed to let the system reach equilibrium, then the differential-pressure measurements were started.

To obtain concentrations of polyethylene oxide in the boundary layer, samples of approximately 25 mls were withdrawn through the probe. One axial location, station 6, was probed at three different injection rates: 60.0, 134.0, and 537.0 mls/min. The concentration of the injected fluids was 50.0 ppm. Time allowed for sample taking varied from approximately 4 minutes at the wall to about 1 minute near the edge of the boundary layer. The samples were withdrawn at these slow rates so as not to disturb the flow field and were analyzed by a polarographic technique.

The polarographic technique, invented by Heyrovsky in 1922, is based on determination of the current flow when a solution containing oxidizable or reducible substances is electrolyzed in a cell. The apparatus in which the analysis is conducted, called a polarograph, is shown schematically in Figure 4. The solution to be analyzed is placed in the polarographic cell and a few drops of mercury are added. This relatively large pool of mercury forms the references electrode of the cell and is connected to one terminal of the polarograph. The other electrode in the solution is a dropping-mercury electrode, consisting of a very fine-bore capillary tube, which produces small drops of mercury just beneath the surface of the solution. The capillary tube is connected by flexible tubing to a mercury reservoir.

In operation, a variable voltage is impressed on the cell. As the voltage is increased from zero, the current remains nearly constant until a voltage is reached at which a component of the solution is reducible at

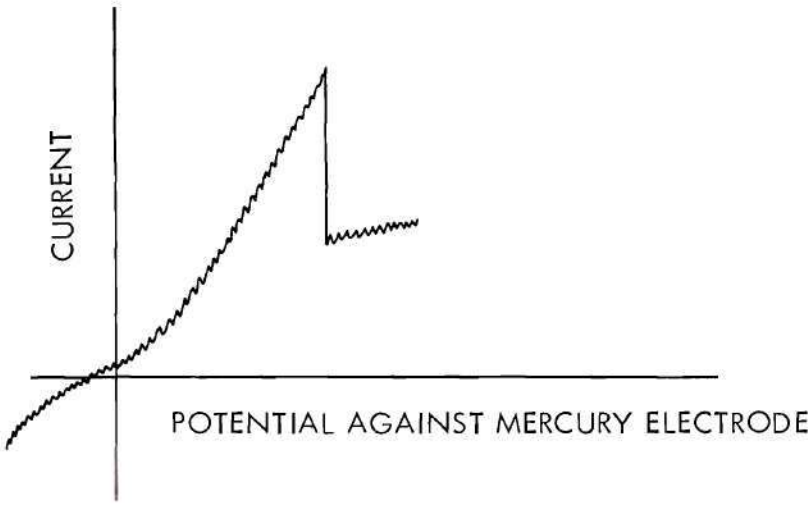

POLAROGRAM OF TAP WATER CONTAINING DISSOLVED OXYGEN

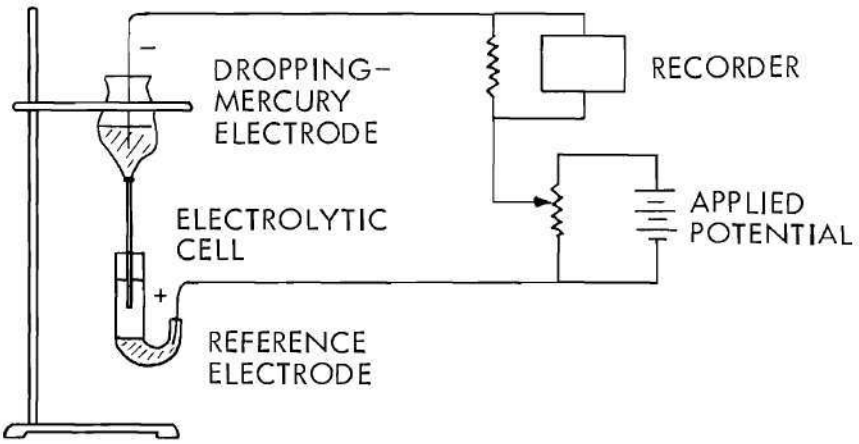

SCHEMATIC DIAGRAM OF POLAROGRAPH

Figure 4. Schematic Diagram of Polarograph and Polarogram of Tap Water.

the mercury cathode. The current then rises sharply to a new level. The current, measured as the drop potential across a fixed resistor, is recorded as a function of the voltage applied. In this manner a current-voltage curve, called a polarogram, is obtained. The height of the current wave is proportional to the concentration of a substance and the corresponding voltage indicates its nature.

It has been found that dissolved oxygen acts as a depolarizer of the dropping-mercury electrode in the following reaction:

$$\frac{1}{2} O_2 + 2e + H_2O \rightarrow 2\ OH^- \quad , \tag{19}$$

and a polarogram of tap water which contains some dissolved oxygen has the form shown in Figure 4. The reason for the maximum is still the subject of discussion but, from the analytical point of view, the important feature of it is that it can be suppressed by adding small concentrations of surface-active agents to the electrolyte. Polyox is a surfactant suitable for suppression of the oxygen maximum, and the method developed by Goren, et al.[57] utilizes suppression of the oxygen wave to determine concentrations of polyethylene oxide. In the present analysis, the following procedure was used. Five mls of sample were mixed with five mls of a 0.002 normal KCl solution, which had been saturated with oxygen and then left exposed to the atmosphere for approximately six hours. The solution was poured into a Sargent polarographic cell and approximately 1 ml of mercury was added. A voltage range of 0 to -1.0 volt was applied to the cell at two different current sensitivities. For samples containing up to

6 ppm, a sensitivity of 0.150 μa/mm was used, while for higher concentrations the sensitivity was changed to 0.040 μa/mm. Using samples of known concentrations, a calibration curve had been prepared by plotting the height of the oxygen peak as a function of concentration of polyethylene oxide. Using this calibration curve and the peak height of any unknown sample, its concentration could be determined. It is believed that the measurements obtained by this procedure are accurate to within 1.0 ppm.

CHAPTER V

DATA REDUCTION

Derivation of Equations

In this investigation it was desired to determine the effect of injections on the shear-stress distributions and on the wall shear stresses. Integrated boundary-layer equations were used which allowed calculation of these parameters in a binary boundary layer from measured velocity profiles. In the derivation, the following well-known, turbulent boundary-layer assumptions were made:

(1) The flow is steady, i.e, $\frac{\partial u}{\partial t} = 0$, $\frac{\partial v}{\partial t} = 0$. This is strictly applicable for laminar flow but applies to turbulent flow if mean velocities are considered.

(2) The velocity v is much smaller than the velocity u, so some terms which involve v are of such an order of magnitude that they may be neglected.

(3) $\frac{\partial p}{\partial x}$ is independent of y.

A control volume was considered of length Δx, height y, and unit width as shown in Figure 5. The equations of mass and momentum conservation can then be written as:

$$\rho_w v_w - \rho v - \frac{d}{dx} \int_0^y \rho u dy = 0 \quad , \tag{20}$$

and

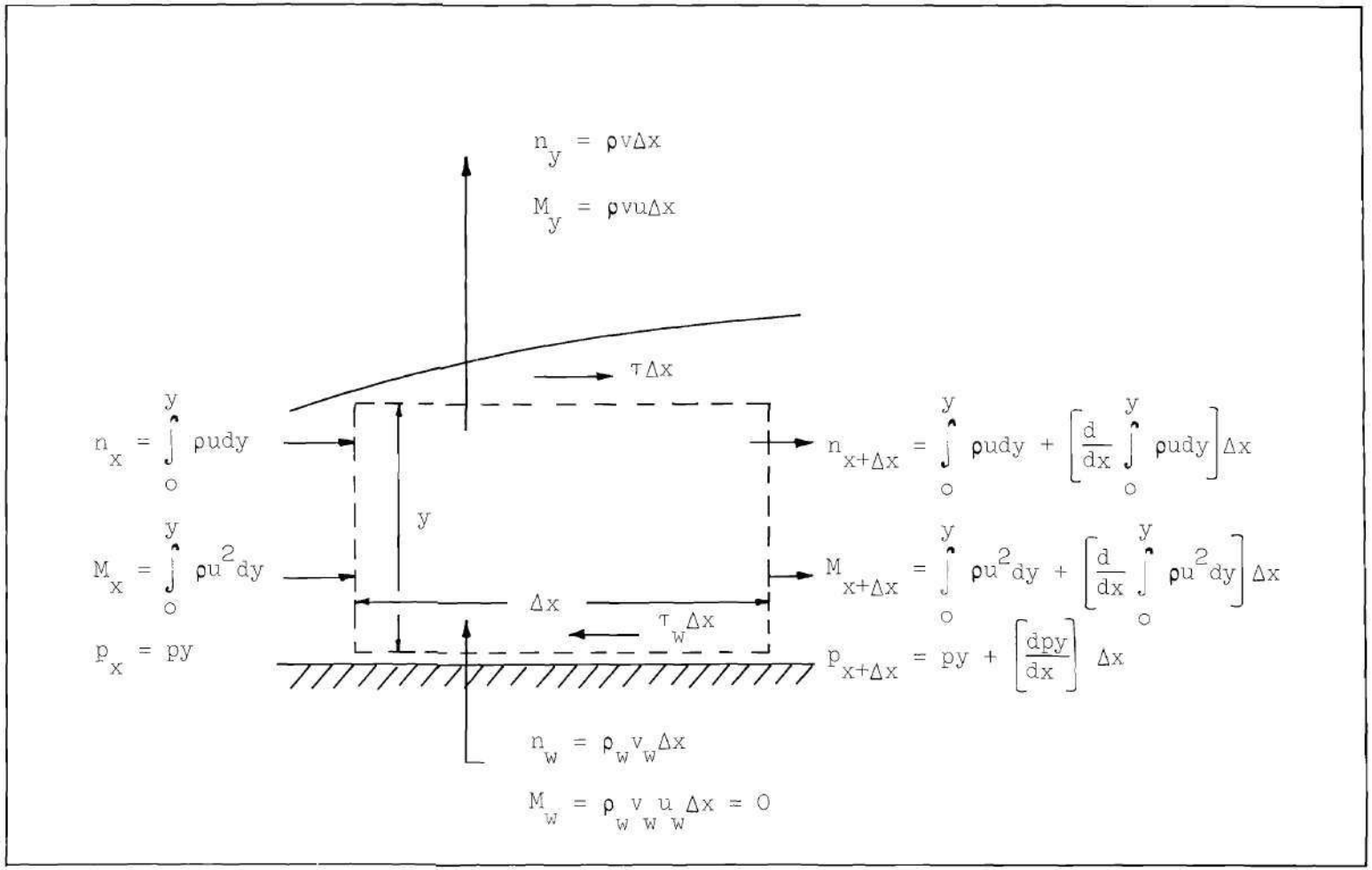

Figure 5. Imaginary Control Planes for Obtaining Shear-Stress Distributions in the Boundary Layer.

$$\tau - \tau_w - y \frac{dp}{dx} - \rho vu - \frac{d}{dx} \int_o^y \rho u^2 dy = 0 \quad . \tag{21}$$

Expressing the pressure-gradient term as

$$\frac{dp}{dx} = - \rho_\infty u_\infty \frac{du_\infty}{dx} \quad , \tag{22}$$

Equation (21) can be written as

$$\tau = \tau_w - y\rho_\infty u_\infty \frac{du_\infty}{dx} + \rho vu + \frac{d}{dx} \int_o^y \rho u^2 dy \quad . \tag{23}$$

Since

$$v = \frac{\rho_w v_w}{\rho} - \frac{1}{\rho} \frac{d}{dx} \int_o^y \rho u dy \quad , \tag{24}$$

Equation (23) becomes

$$\tau = \tau_w - y\rho_\infty u_\infty \frac{du_\infty}{dx} + \rho_w v_w u - u \frac{d}{dx} \int_o^y \rho u dy + \frac{d}{dx} \int_o^y \rho u^2 dy \quad . \tag{25}$$

This expression gives the shear-stress distribution in a compressible, turbulent boundary layer subjected to distributed surface mass addition.

To obtain the shear stress at the wall, the boundary conditions at $y = \delta$: $\tau = 0$, $u = u_\infty$ can be substituted in Equation (25) to obtain

$$\tau_w = \delta \rho_\infty u_\infty \frac{du_\infty}{dx} - \rho_w v_w u_\infty + u_\infty \frac{d}{dx} \int_0^\delta \rho u dy - \frac{d}{dx} \int_0^\delta \rho u^2 dy \quad . \tag{26}$$

Equation (26) can be re-arranged to give

$$\tau_w = \frac{d}{dx} \int_0^\delta \rho u(u_\infty - u) dy - \rho_w v_w u_\infty + \frac{du_\infty}{dx} \left(\delta \rho_\infty u_\infty - \int_0^\delta \rho u dy \right) \quad . \tag{27}$$

This relationship gives the shear stress at the wall. It has been derived previously in a slightly different manner by Eckert and Drake[60].

Calculations

Velocity profiles at various axial locations were obtained by measuring pitot pressures with a Foxboro Differential-Pressure Cell Transmitter, as was described earlier. Before and after each run, the balance pressure, i.e., the pressure reading with equal pressures applied to both sides of the twin-diaphragm capsule, was measured. Pitot-pressure readings were obtained by closing the balancing valve, thereby connecting the static pressure to one side of the capsule and the dynamic pressure to the other. The signal from the differential-pressure cell was fed into a mercury manometer. The readings were used to calculate the local mean velocities by

$$u = 2.32 \sqrt{\frac{P_A - P_{BP}}{10.18}} \quad , \tag{28}$$

where

P_A = output pressure, inches of mercury.

P_{BP} = balance pressure, inches of mercury.

The velocity data were used to obtain:

(a) Boundary-layer thicknesses.

(b) Free-stream velocities.

(c) Wall shear stresses.

(d) Shear-stress distributions.

(e) Universal velocity distributions.

Concentration data were obtained in the form of polarograms with peaks representing the oxygen wave. These peaks were measured with a scale. Using known concentrations, a calibration curve was prepared showing suppression of maximum current versus concentration of polyethylene oxide in aqueous solutions. With aid of this calibration curve, concentrations of samples taken from the channel were determined.

Most of the calculations were performed on a Burroughs B-5500 computer to speed up the data reduction. Values of u, ρu, ρu^2, and $\rho u(u_\infty - u)$ were calculated and printed for y values of from 0.000 to 0.100 in steps of 0.010, and from 0.100 to 1.400 in steps of 0.100. These values were used to determine the behavior of the parameters to facilitate curve fitting in later programs, and also to obtain free-stream velocities and boundary-layer thicknesses.

Free-stream velocities at the various axial locations were obtained by selecting the value where u became essentially constant. Since values of $\rho u(u_\infty - u)$ were available as functions of y, it was decided to use this parameter as a criterion for obtaining boundary-layer thicknesses. As the edge of the boundary layer is approached, this parameter is asymptotic to 0. In our case, the boundary-layer thickness was fixed at the

value where $u = 0.99\ u_\infty$, or where $\rho u(u_\infty - u) = 0.0099\ \rho u_\infty^2$.

In many of the calculations to follow, values of the integrals from 0 to y of ρu, ρu^2, and $\rho u(u_\infty - u)$ were required. The procedure used to obtain these integrals was to develop equations approximating the parameters by means of a least-squares fit and to integrate these equations to obtain expressions containing the independent variable y. By substituting various values of y, the values of the integrals were calculated.

In a first attempt, a polynomial of the tenth degree, $I = A_0 + A_1 y + A_2 y^2 + \ldots + A_{10} y^{10}$ was selected. The result was a curve which oscillated about the experimental curve and crossed it ten times. This indicated that the exponents in the expression were too large to give a proper fit. A careful examination of the data showed that an excellent fit could be obtained by using the following equation: $I = A_0 + A_1 y^{0.06} + A_2 y^{0.12} + A_3 y^{0.18} + \ldots$. Even so, it was found necessary to delete the bottom portion of the curve that corresponds to the laminar sub-layer. Since this was practically a straight line covering a distance of only 0.02 inches, no problems were encountered. The areas under the curves could be approximated by triangles which were, in all cases, added to the integral values.

Using the latter expression, a computer program was written to calculate the integral values, mentioned earlier, in a step-wise fashion. This program is presented in Appendix A. Initially, an equation with 11 coefficients was tried. This produced a coefficient matrix which was singular and all coefficients became zero. The procedure was then modified to lower the degree of the polynomial by one until the matrix became non-singular. The highest acceptable degree found in this manner was five.

To determine the accuracy of the fit, several measured velocity profiles were compared with the approximations. In all cases, the two curves were practically indistinguishable. In addition, expressions of the second and third degree were tried. Of these, the third-degree polynomial provided just as good an approximation as the fifth degree, and was used in successive calculations. A sample of the computer output is presented in Table 1 of Appendix A.

To calculate the wall shear stress, Equation (27) was used. First, values of the integral $\rho u(u_\infty - u)$ were plotted as a function of the axial distance x for each injection rate. It was found that the curves through the data points could be approximated by straight lines giving a constant slope at each axial location. The term $\rho_w v_w u_\infty$ was obtained by dividing the injection rate $\rho_w v_w A$ by the area of the porous plate, and multiplying this by the local free-stream velocity.

The shear-stress distributions in the boundary layer at station 6 were calculated with Equation (25) for the various injection rates. The integral values of ρu and ρu^2 were plotted as functions of x, one value for each y value. Slopes were then drawn to the curves at station 6.

With the skin-friction values known as functions of axial distance and injection rate, the velocity data were used to calculate the dependent variable $\frac{u}{u^*}$ and the independent variable $\frac{yu^*}{\nu}$ in the Law of the Wall expression. These calculations were also performed on a Burroughs B-5500 computer. The value of the kinematic viscosity, ν, was the value given by Bird and co-workers[61]: 1.0037×10^{-2} cm^2/sec or 1.0804×10^{-5} ft^2/sec.

CHAPTER VI

DISCUSSION OF RESULTS

Preliminary Considerations

In all test runs reported in this investigation, the bulk flow rate of the liquid moving through the test section was constant at a value of approximately 155 gpm. Although a globe valve was provided at the channel inlet for adjustment of the flow rate, in case of changes caused by drag-reducing additives, it was not needed for this purpose. After estimating the various resistances in the system, the reason became clear. Table 2 shows that the major losses occurred in the 3.0 inch plastic pipe, the five elbows, and in the globe valve. These three resistances contributed approximately 80 percent to the total and were essentially unaffected by drag-reducing effects. The one resistance which was primarily influenced was friction in the channel which added only approximately 0.1 percent to the total resistance in the system. Any changes in it were too small to cause changes in the bulk flow rate, which was checked in each test run by measuring the free-stream velocity at station 0, upstream of the porous plate.

The following fluids were injected into the main stream: water, and aqueous solutions of polyethylene oxide at concentrations of 25.0, 50.0, and 150.0 ppm. Water was introduced at a rate of 537.0 mls/min. The polyethylene oxide solutions were injected at one or more of four different rates of 60.0, 134.0, 268.0, and 537.0 mls/min, giving $\frac{\rho_w v_w}{\rho_\infty u_\infty}$

Table 2. Approximate Steady-State Mechanical Energy Balance on the Experimental System

Equation:

$$\Delta \tfrac{1}{2} \langle u \rangle^2 + g\Delta h + \int_{p_1}^{p_2} \frac{g_c}{\rho}\, dp + g_c W + \sum_i \left(\tfrac{1}{2} \langle u \rangle^2 \frac{L}{R_H} c_f \right)_i + \sum_i \left(\tfrac{1}{2} \langle u \rangle^2 e_v \right)_i = 0$$

Head Available	16.6 ft	or	534.5 ft^2/sec^2
Head Used			
(a) friction in plastic pipe			57.1 ft^2/sec^2
(b) conversion into flow energy			30.4
(c) friction in channel			0.5
(d) 5 ells			106.1
(e) 1 gate valve (open)			6.1
(f) 1 globe valve (partially closed)			264.0*
(g) sudden contraction (overhead tank)			13.7
(h) sudden expansion (lower tank)			30.4
(i) slow expansion			13.0
(j) slow contraction			13.0
(k) sudden contraction due to styrofoam			0.2
Total:			534.5 ft^2/sec^2

* This value was obtained by subtraction. It is slightly higher than the amount contributed by an open globe valve which is 230.0. The values of e_v were obtained from Reference 61.

values of 0.62, 1.38, 2.75, and 5.51 x 10^{-5}, respectively.

All computations performed in this investigation were based on measured mean-velocity profiles. Consequently, it is important to discuss the errors inherent in measurements of local mean velocities. These errors are:

(1) Error in the probe position. With the micrometer drive used in this investigation, the error in the probe location is believed to be less than 0.0005 inch, which represented one-half of a scale division on the micrometer.

(2) Viscous effects. At low probe Reynolds numbers, i.e., the Reynolds number based on probe height, the viscous effects in the fluid increase the stagnation pressure inside the probe. At the lowest velocity measured in this investigation, this Reynolds number was approximately 35, giving a correct velocity reading according to an investigation performed by MacMillan[62]. At the highest velocity measured, 1.67 ft/sec, the probe Reynolds number was 220 which made the indicated velocity approximately 0.2 percent low.

(3) Effective displacement of the center of the probe. A total pressure probe placed in a fluid with a transverse velocity gradient experiences a displacement of the effective center of total pressure from the geometric center. This displacement for the present probe dimensions was about 0.004 inches in the direction of the region with the higher velocity, according to a study by Young and Haas[63].

(4) Effect of the turbulence level. Goldstein[64] has shown that dynamic probes in turbulent flows do not give an exact indication of the total pressure due to the effect of velocity fluctuations. The result is

an increase in the dynamic pressure at the tip of the probe.

(5) Effect of the hole dimension of the static tap. Shaw[65] investigating the influence of hole dimensions on static pressure measurements concluded that the observed static pressure was always greater than the true static pressure. In the present investigation, the diameter of the static tap was 0.031 inches, and the effect is therefore believed to be negligible.

(6) Possible viscoelastic effects. Although it has not been definitely proven that the very dilute solutions of polyethylene oxide considered in this investigation are viscoelastic, the possibility cannot be excluded. If this type of solution were found to be viscoelastic, the simple Bernoulli expression used in calculating velocities from differential-pressure measurements could no longer be used without correction. Since the errors in the magnitude of the local mean velocities are small, it was decided to make no corrections in the velocity readings and to just list them in Appendix B for individual interpretation.

Analysis of the Data

The velocity profiles on which the conclusions in this investigation were based are presented in Appendix B, Tables 3 through 9. Table 3 lists the profiles without mass addition. The velocity profiles with addition of water at a rate of 537.0 mls/min are given in Table 4. Tables 5, 6, 7, and 8 present the profiles in the boundary layer subjected to addition of aqueous solutions of polyethylene oxide at concentrations of 50.0 ppm and at rates of 60.0, 134.0, 268.0, and 537.0 mls/min, respectively. Table 9 gives the velocity data obtained during injection of polyethylene oxide

solutions having concentrations different from 50.0 ppm.

Although some scatter in the data occurred primarily due to low velocities, the following observations were made. In the runs without mass addition, the velocity profiles became less blunt in the axial direction. This trend was expected since the boundary layer--the region of lower-velocity fluid--increased with axial distance. To maintain the same bulk flow rate, the free-stream velocity had to increase.

The velocity profiles with addition of water at a rate of 537.0 mls/min were very similar to those without mass addition. This was expected since the injection ratio, i.e., the mass flux of the injected material divided by the mass flux of the main stream, was very small--5.51×10^{-5}.

The addition of aqueous solutions of polyethylene oxide made the velocity profile blunter at each axial location. The effect increased with injection rate (up to 134.0 mls/min) and with axial distance in the downstream direction of the channel.

The effect of injection on the free-stream velocity is presented in Figure 6. It was found that, within 2.5 percent, all experimental values of the free-stream velocity could be represented by one curve. This applied to all of the cases investigated in this study. Actually, the presence of the polymeric additives should have caused a decrease in the free-stream velocity at a constant value of the bulk flow rate. However, this change was possibly too small for measurement with the present apparatus and instrumentation. The free-stream velocity over the measured portion of the test section varied from 1.58 ft/sec at the beginning to 1.67 ft/sec at the end, the increase in velocity being due to the growth of

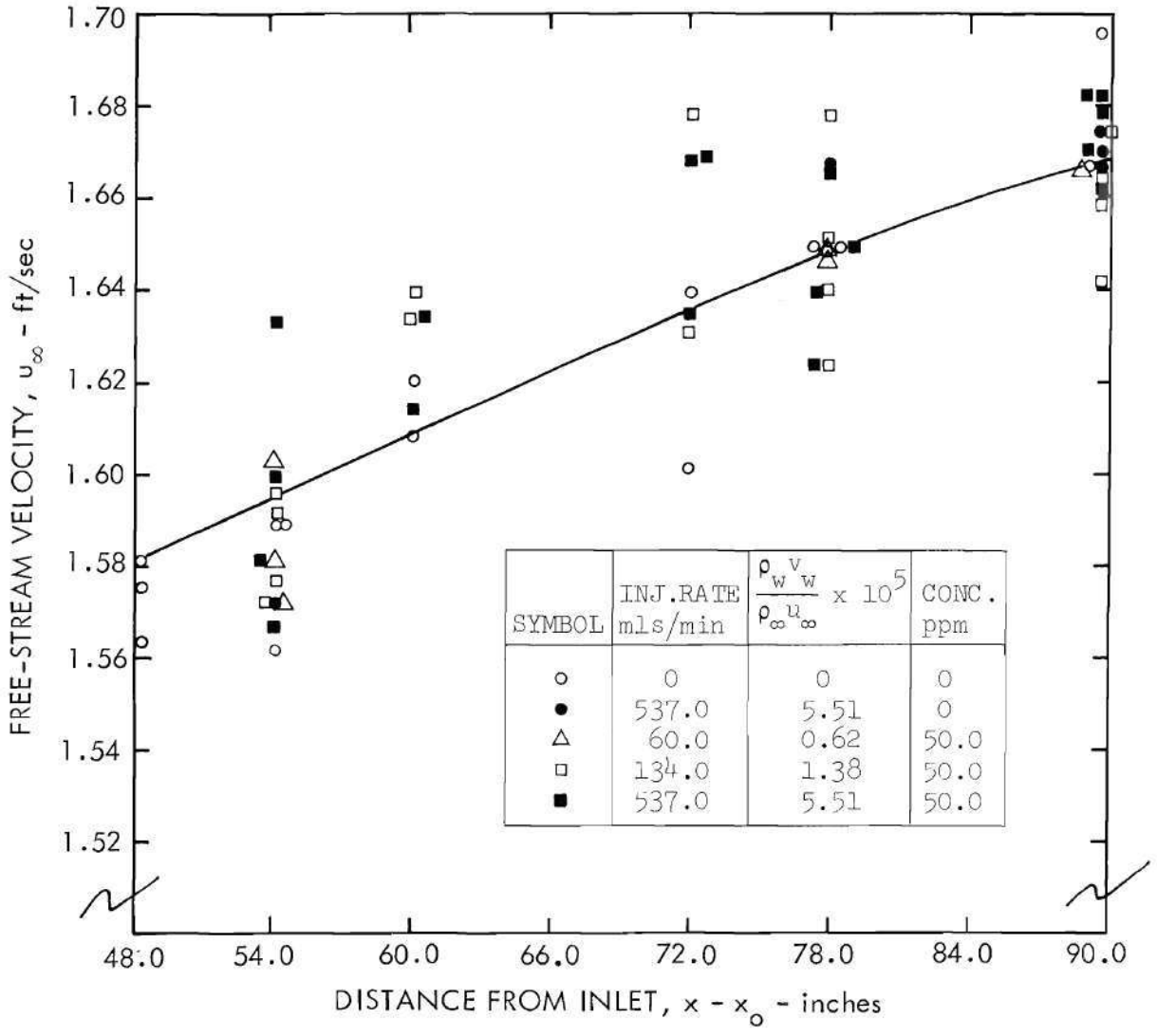

Figure 6. Effect of Injections on the Free-Stream Velocity Distribution.

the boundary layer in the axial direction.

The effect of injections on the boundary-layer thickness is shown in Tables 10 through 14 of Appendix C, and graphically in Figure 7. The boundary-layer thickness without mass addition increased from 0.81 inch at station 1 to 1.27 inches at station 8. Within 2.2 percent, the thickness could be represented as a function of axial distance and Reynolds number by the relation

$$\delta = \frac{0.235\ x}{Re_x^{\frac{1}{5}}} \quad . \tag{29}$$

This relationship is similar to one presented by Schlichting[66] for flow past a flat plate at zero incidence, except for the coefficient: 0.235 instead of 0.37. This lower coefficient was also evident in a recent investigation by Schraub and Kline[16], who studied the flow of water in a recirculating tunnel. The deviations from the flat-plate expression may be due to the geometry of the test section and possibly the pressure gradient.

Figure 7 shows that all injections decreased the thickness of the boundary layer. Water injections at a rate of 537.0 mls/min decreased the thickness by a maximum amount of 11 percent. Injections of aqueous solutions of polyethylene oxide at 50.0 ppm continued to decrease the thickness with increasing injection rates, up to a rate of 134.0 mls/min. The reduction in the boundary-layer thickness at that point was approximately 20 percent. Then a reversal occurred which was evident in many of the later results of this investigation. Similar reversals have occurred previously; for example, in the studies of Toms[6], Goren and

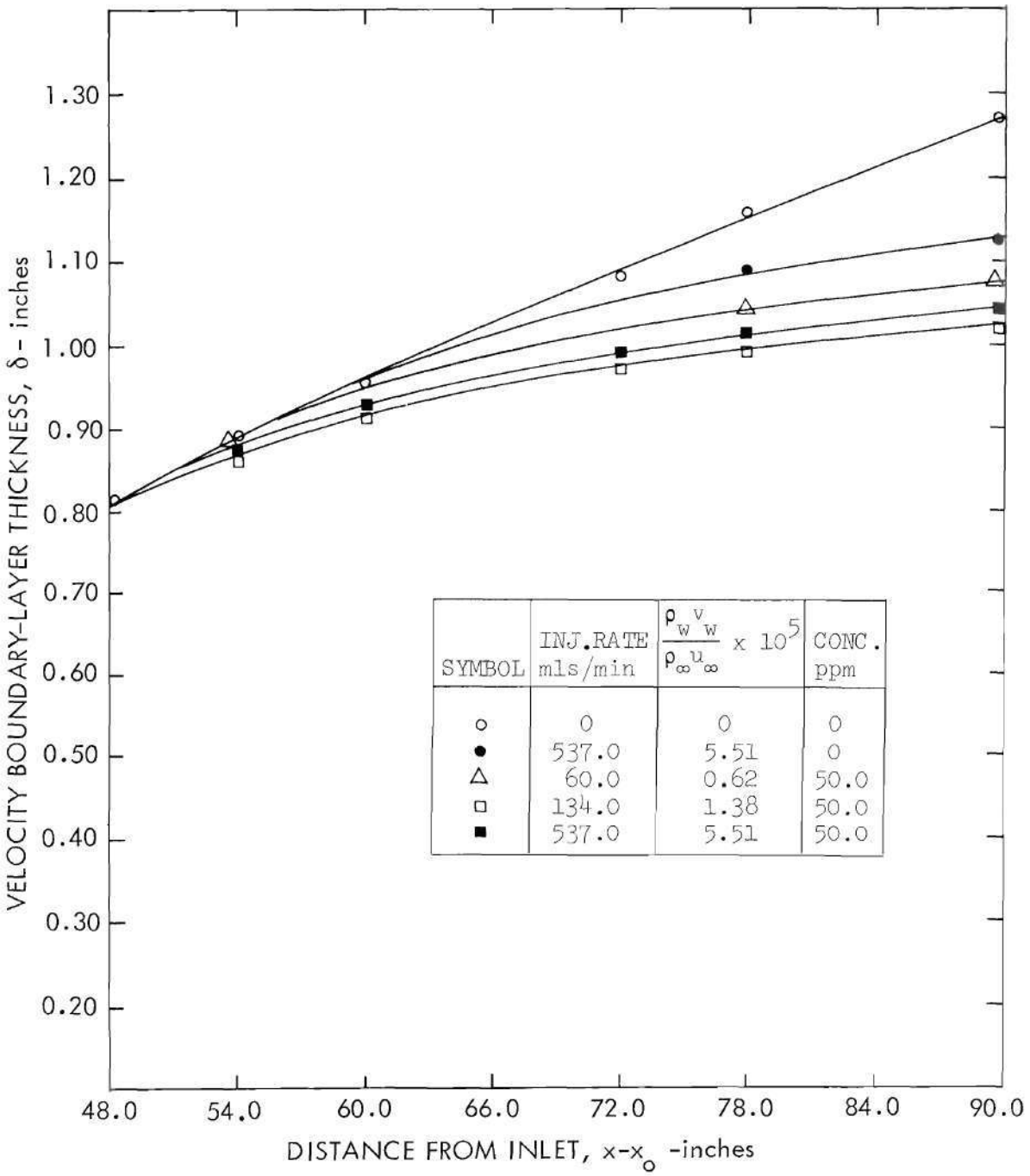

Figure 7. Effect of Injections on the Velocity Boundary-Layer Thickness.

Norbury[38], and Baronet and co-workers[43].

A very important parameter in this investigation was the effect of injections on the shear stress at the wall, since this would be the parameter to consider in cost evaluation studies and in commercial applications. It was interesting to consider compatibility of the present initiation of drag reduction with recent hypotheses.

Virk and co-workers[53] hypothesized that drag reduction is initiated when

$$\tau_w^{\square} \geq \rho\left(0.625 \times 10^6 \frac{\nu}{R_G}\right)^2 \quad , \tag{15}$$

where

$\tau_w^{\square}$ = wall shear stress at the onset of drag reduction, dynes/cm^2

ρ = solvent density, gms/cm^3

ν = kinematic viscosity, cm^2/sec

R_G = Rms radius of gyration of the macromolecule, Å .

Since this expression is independent of concentration, it was felt that the relationship could be applied to the present investigation. Substituting: ρ = 1.0 gms/cm^3, ν = 1.0037 x 10^{-2} cm^2/sec, and R_G = 2350 Å*, it followed that

$$\tau_w^{\square} \geq 7.13 \text{ dynes/cm}^2 \quad , \tag{30}$$

or

---

* This value of R_G was taken from Virk, et al.[67], p. 312.

$$\tau_w^{\square} \geq 0.0149 \text{ lb}_f/\text{ft}^2 \quad . \tag{31}$$

Virk and co-workers[67] also obtained the following relationship to determine the onset of drag reduction in aqueous solutions of Polyox WSR-301:

$$\frac{(u^*)^{\square}}{\nu} \geq 210 \text{ cm}^{-1} \quad . \tag{32}$$

Substituting the values listed above and making the necessary conversions, the shear stress at the beginning of drag reduction was calculated to be

$$\tau_w^{\square} \geq 0.0093 \text{ lb}_f/\text{ft}^2 \quad . \tag{33}$$

According to Ram and co-workers[54], drag reduction is initiated when

$$\text{Re}\sqrt{c_f} \geq D\sqrt{\frac{2}{\lambda\nu}} \quad , \tag{16}$$

or when

$$c_f \geq \left(\frac{D}{\text{Re}}\right)^2 \frac{2}{\lambda\nu} \quad . \tag{34}$$

Replacing D by the hydraulic diameter D_H, and with Re = 51,900, ν = 1.0804×10^{-5} ft^2/sec, $\lambda = 2.1 \times 10^{-3}$ sec*, and D_H = 0.379 ft, it follows that

$$c_f \geq \left(\frac{0.379}{51{,}900}\right)^2 \frac{2 \times 10^8}{(2.1)(1.0804)} = 0.00470 \quad . \tag{35}$$

---

* The value of λ was taken from Little, op. cit., p. 2.

Since

$$\tau_w = \frac{c_f \rho \langle u \rangle^2}{2 g_c} \tag{36}$$

$$\tau_w^{\square} \geq \frac{(0.00470)(62.4)(1.48)^2}{64.4} = 0.00997 \text{ lb}_f/\text{ft}^2 \quad . \tag{37}$$

The predicted values of the wall shear stress at the onset of drag reduction varied from a high value of 0.0149 to a low value of 0.0093 lb_f/ft^2. In the present investigation, drag reduction occurred at a value of 0.0059 lb_f/ft^2, which was considerably lower than the predicted values. Little[30] obtained similar low values with WSR-35 and WSR-205 in water. His experimental values were approximately 0.207 and 0.307, respectively, of those predicted by Equation (16). In the present case the ratio was 0.592 which is in line with Little's findings, since the ratio seems to increase with molecular weight and WSR-301, used in the present investigation, has a higher molecular weight than WSR-205.

The skin-friction values, based on the momentum-deficit values listed in Tables 15 through 19 of Appendix C, are shown in Tables 20 through 24 and graphically in Figure 8. Without mass addition, the wall shear stress varied from a value of 5.9×10^{-3} at station 1 to 5.8×10^{-3} lb_f/ft^2 at station 8. From the generalized expression, which applies to flow past a flat plate, we calculated for station 1:

$$\tau_w = \frac{0.0585}{Re_x^{0.20}} \frac{62.4}{(32.2)(2)} u_\infty^2 \tag{38}$$

or

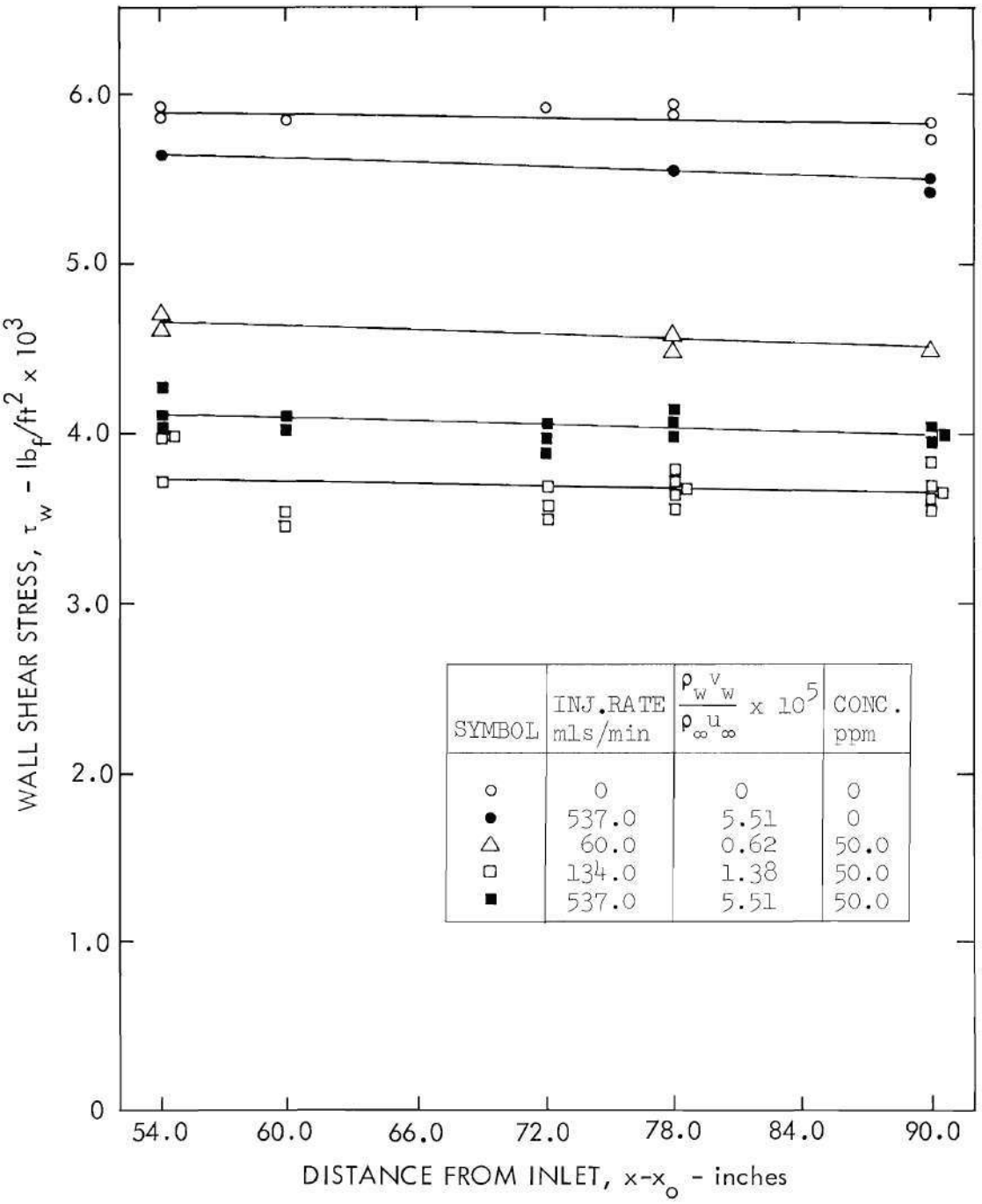

Figure 8. Effect of Injections on the Wall Shear Stress.

$$\tau_w = \frac{0.0585}{14.23} \frac{62.4}{(32.2)(2)} (1.581)^2 = 0.00995 \text{ lb}_f/\text{ft}^2 \quad . \qquad (39)$$

A comparison shows that the experimental value of the skin friction at station 1 is appreciably lower than the value calculated from Equation (38). An explanation is not obvious, but a similar behavior was evident in the study conducted by Schraub and Kline[16], referred to earlier.

Figure 8 shows that injection of water at a rate of 537.0 mls/min reduced the skin friction drag to 5.85 and 5.54 x 10^{-3} lb_f/ft^2 at stations 2 and 8, respectively. This amounted to a maximum decrease of 3.5 percent. Injections of aqueous solutions of polyethylene oxide at 50.0 ppm gave maximum drag reductions of approximately 37 percent at station 8, for an injection rate of 134.0 mls/min. Higher rates of addition lowered the amount of drag reduction.

The effectiveness of distributive surface mass addition may be seen qualitatively by considering the studies performed by Love[8], who investigated slot injections of polyethylene oxide solutions over a flat plate. A quantitative comparison is impossible because there are indications that the magnitude of the effect is dependent on the Reynolds number. Qualitatively, the results show that homogeneous addition is much more effective than slot injection per unit weight of injected polymer.

A few exploratory test runs were made with injection of solutions having concentrations different from 50.0 ppm. This was done to determine if any gross differences in drag reduction occurred. In each of these runs, the velocity profiles were measured and the values of $\int_0^\delta \rho u(u_\infty - u)dy$ were computed. These values were then plotted in Figure 9, which also shows the values of this parameter for injection of solutions containing

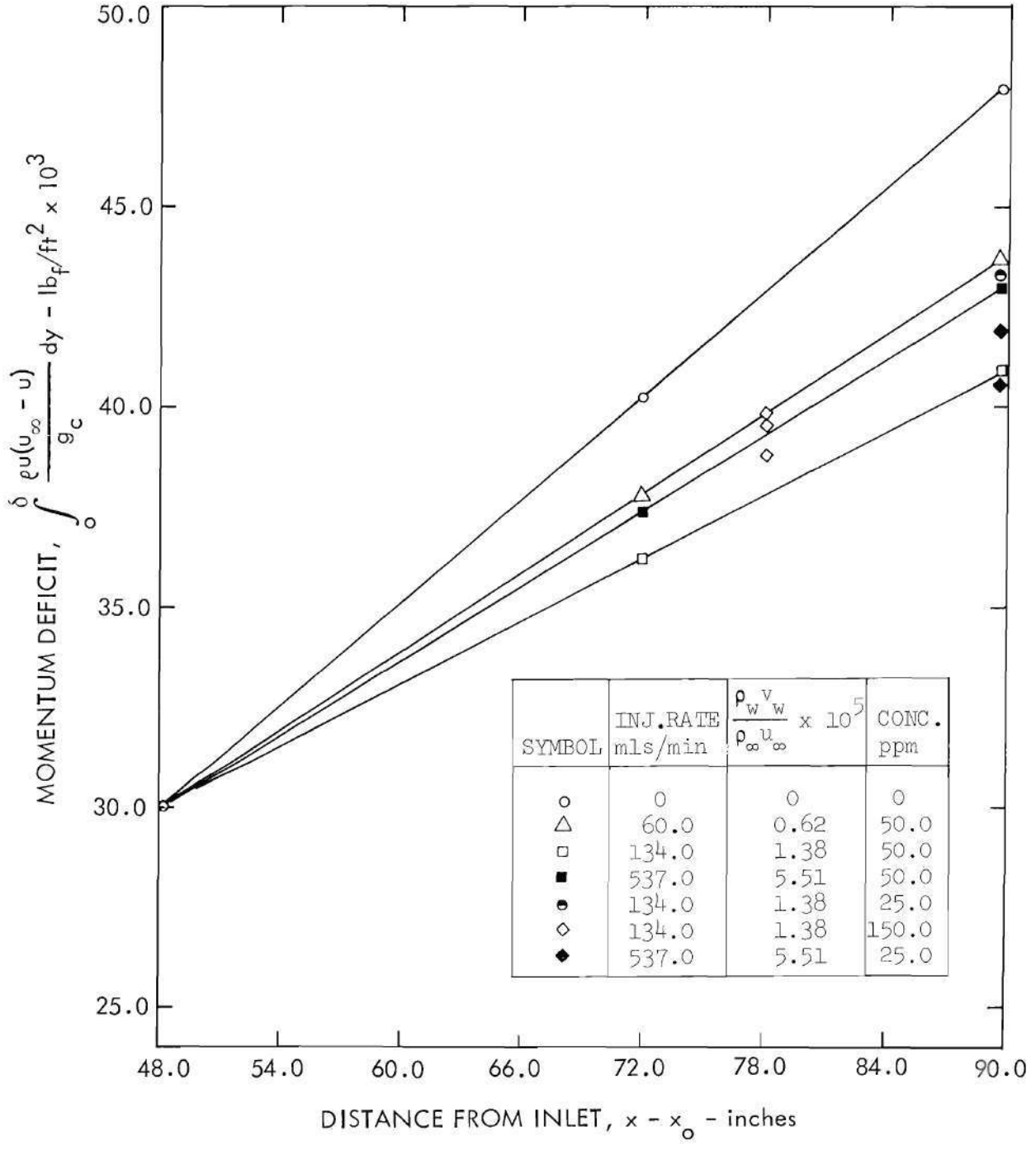

Figure 9. Effect of Injections on the Momentum Deficit in the Boundary Layer.

50.0 ppm. Since the term $\left[\frac{du_\infty}{dx}\right]\left[\delta\rho_\infty u_\infty - \int_0^\delta \rho u dy\right]$ was practically constant at each station, and because the term $\rho_w v_w u$ was very small, a different value of τ_w would have required a change in the value of $\int_0^\delta \rho u(u_\infty - u)dy$. With this and the limited number of runs in mind, the following conclusions were drawn based on Figure 9:

(a) Injection of 537.0 mls/min at 25.0 ppm gave practically the same skin friction as 134.0 mls/min at 50.0 ppm.

(b) Injection of 134.0 mls/min at 150.0 ppm produced approximately the same drag as 537.0 mls/min at 50.0 ppm.

(c) Introducing 134.0 mls/min at 25.0 ppm gave nearly the same value of τ_w as 60.0 mls/min at 50.0 ppm.

Therefore, it appears that the amount of polymer injected per square foot of surface per unit time is the prime criterion in obtaining drag reduction.

Shear-stress distributions in the boundary layer are presented in Tables 25 through 29 of Appendix C. The effect of injections on the shear stress is shown graphically in Figures 10 and 11. The distributions shown are for station 6. In all cases, the shear stress remained relatively constant in the laminar sub-layer, which had a thickness of approximately 0.02 inches. When aqueous solutions of polyethylene oxide at 50.0 ppm were injected into the boundary layer, the largest reduction in shear stress occurred at the wall. Injection at a rate of 134.0 mls/min produced a constant reduction of 37 percent throughout the boundary layer; reductions in shear stress at the other two injection rates decreased gradually as the edge of the boundary layer was approached. Injection of water at 537.0 mls/min, on the other hand, yielded the largest reduction

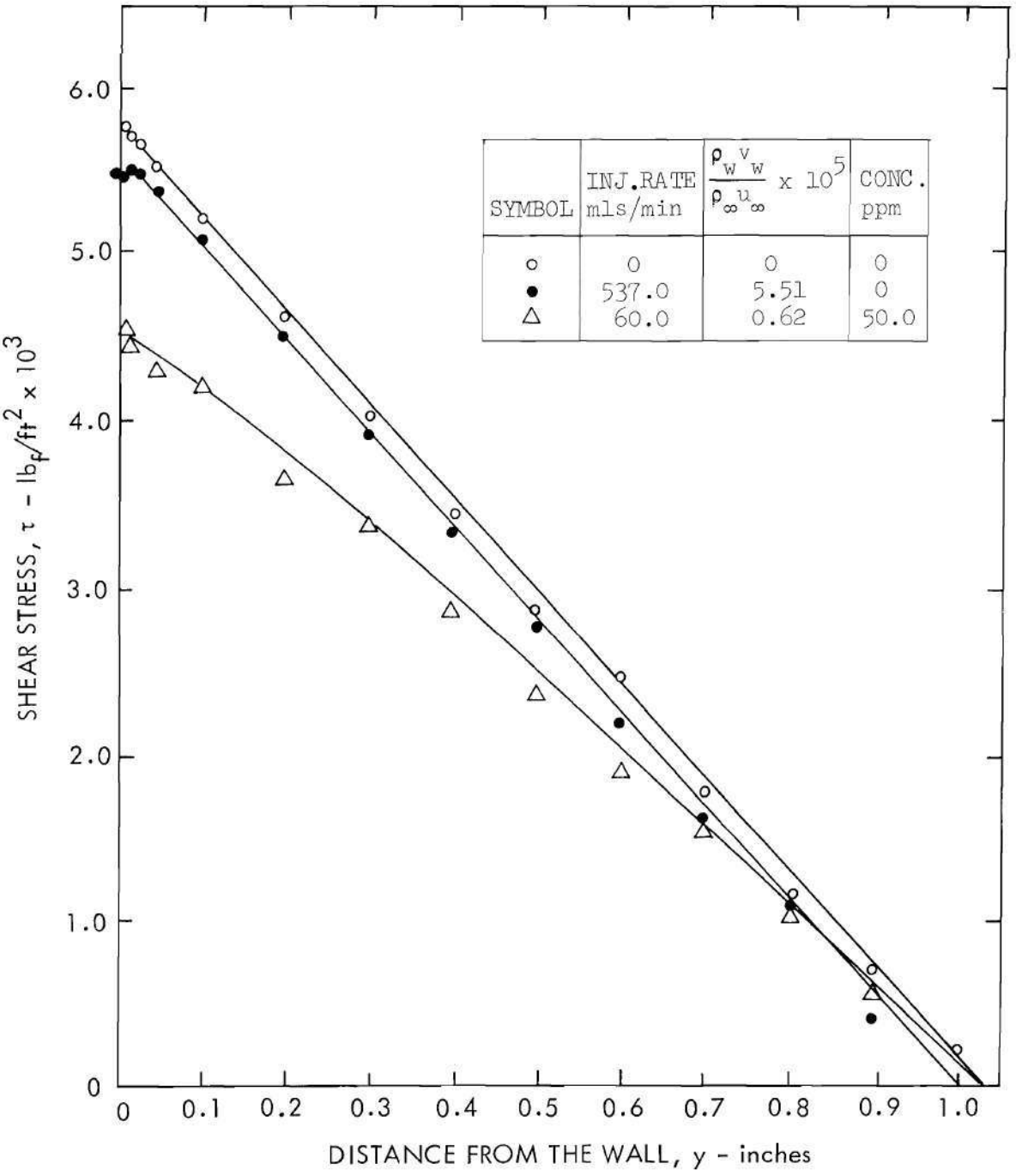

Figure 10. Effect of Injections on the Shear-Stress Distribution.

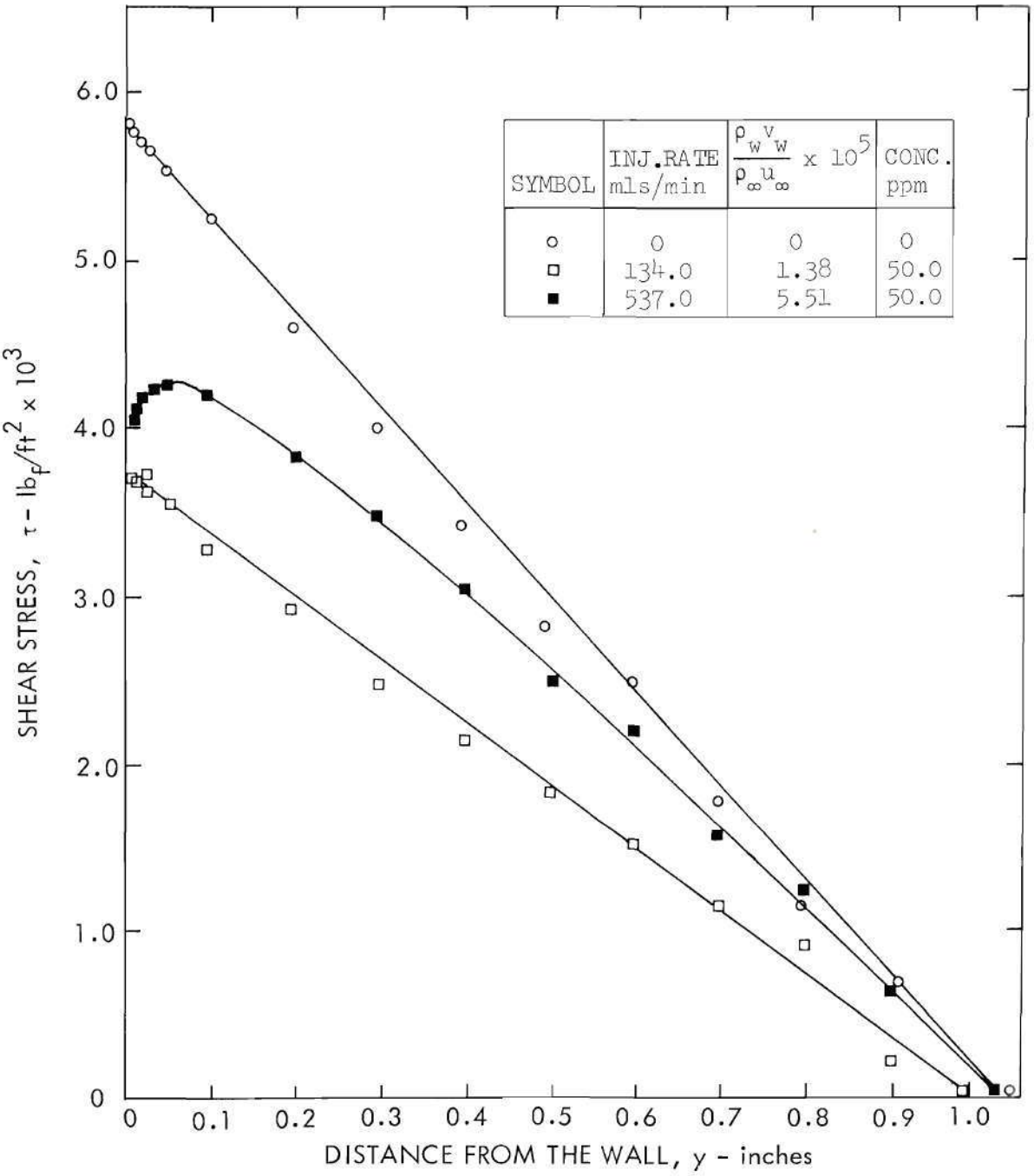

Figure 11. Effect of Injections on the Shear-Stress Distribution (Continued).

in shear stress at the outer edge of the boundary layer. The two largest injection rates examined in this investigation--537.0 mls/min--produced a curious result, both in the case of water injection and polymer addition. This is that the maximum shearing stress no longer occurred at the wall, but was displaced from it. The maximum shearing stress in the case of water injection occurred at a y value of 0.02 inch, whereas in the case of polymer addition the maximum was found at y = 0.05 inch. The reasons for the occurrence of these maxima were not clear, but they have been noticed previously in the case of gas injections in air boundary layers[68,69].

Logarithmic velocity profiles are shown individually, one for each injection rate, in Figures 12 through 16 and combined in Figure 17. The data shown represent all stations investigated. The usual pattern was followed. Above a y^+ value of approximately 10, a straight-line relationship of $u^+ = 1/k \ln y^+ + C$ was attained. All of the mean-velocity profiles were combined in Figure 17. The important feature of this figure is that injections cause a linear shift of the non-dimensional mean-velocity profiles in an upward direction. This means that injection of polymeric additives does not cause a decrease in the universal constant k as suggested by Elata and Tirosh[25] and by Wells[26]. The results of the present study agree with the findings of Ernst[27] and Meyer[52]. The data indicated that the laminar sub-layer thickness had increased with addition of the drag-reducing additives, possibly because it had become less sensitive to disturbances being impressed upon it from above. The results did not support the contention of Fabula and co-workers[55] that the buffer zone increases in thickness with drag-reducing additives, since this would have resulted in lines with dissimilar slopes, at least for the lower values

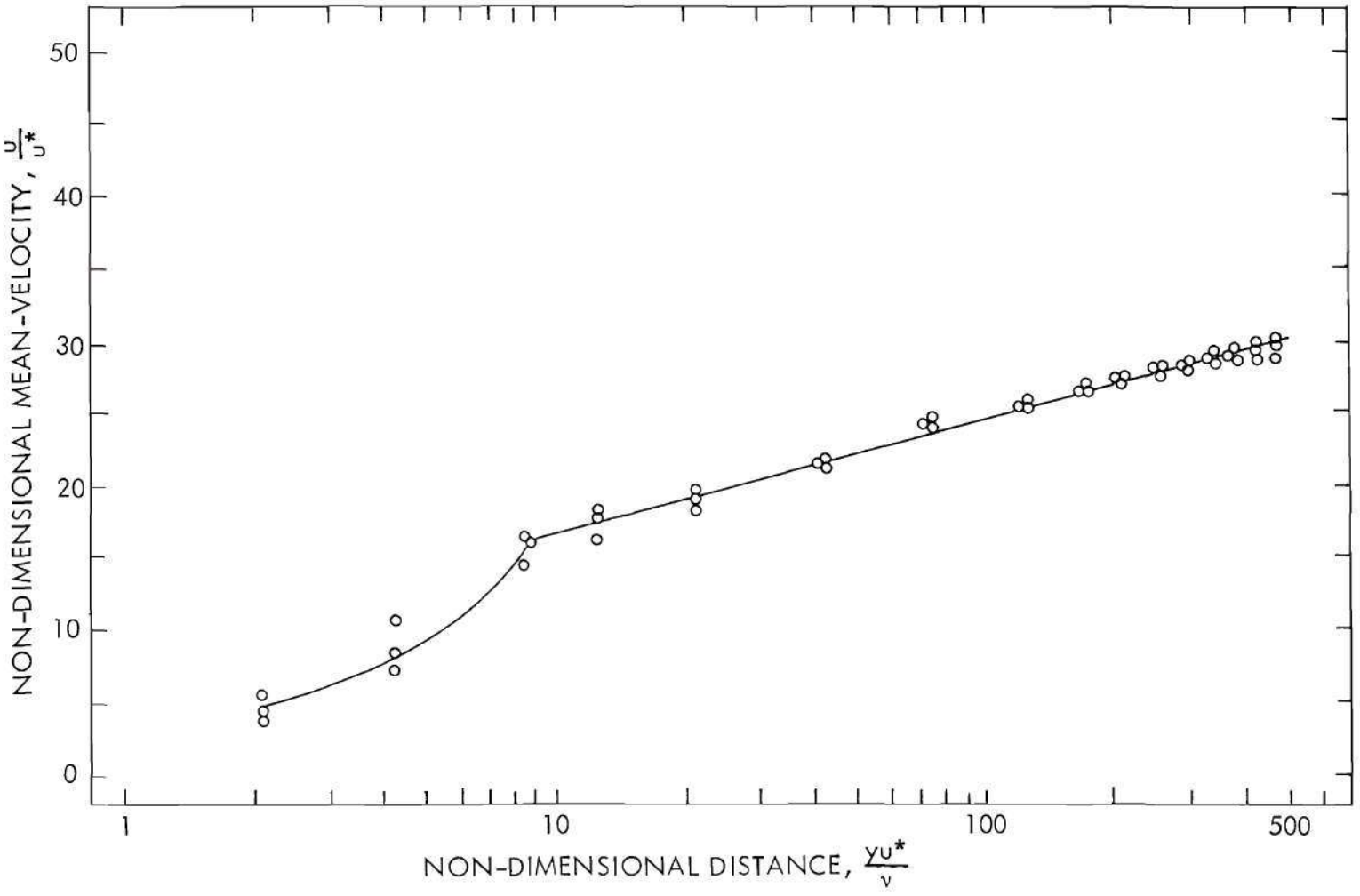

Figure 12. Non-Dimensional Mean-Velocity Profiles.
Injected Fluid: None.
Injection Rate: -- mls/min. Concentration: -- ppm.

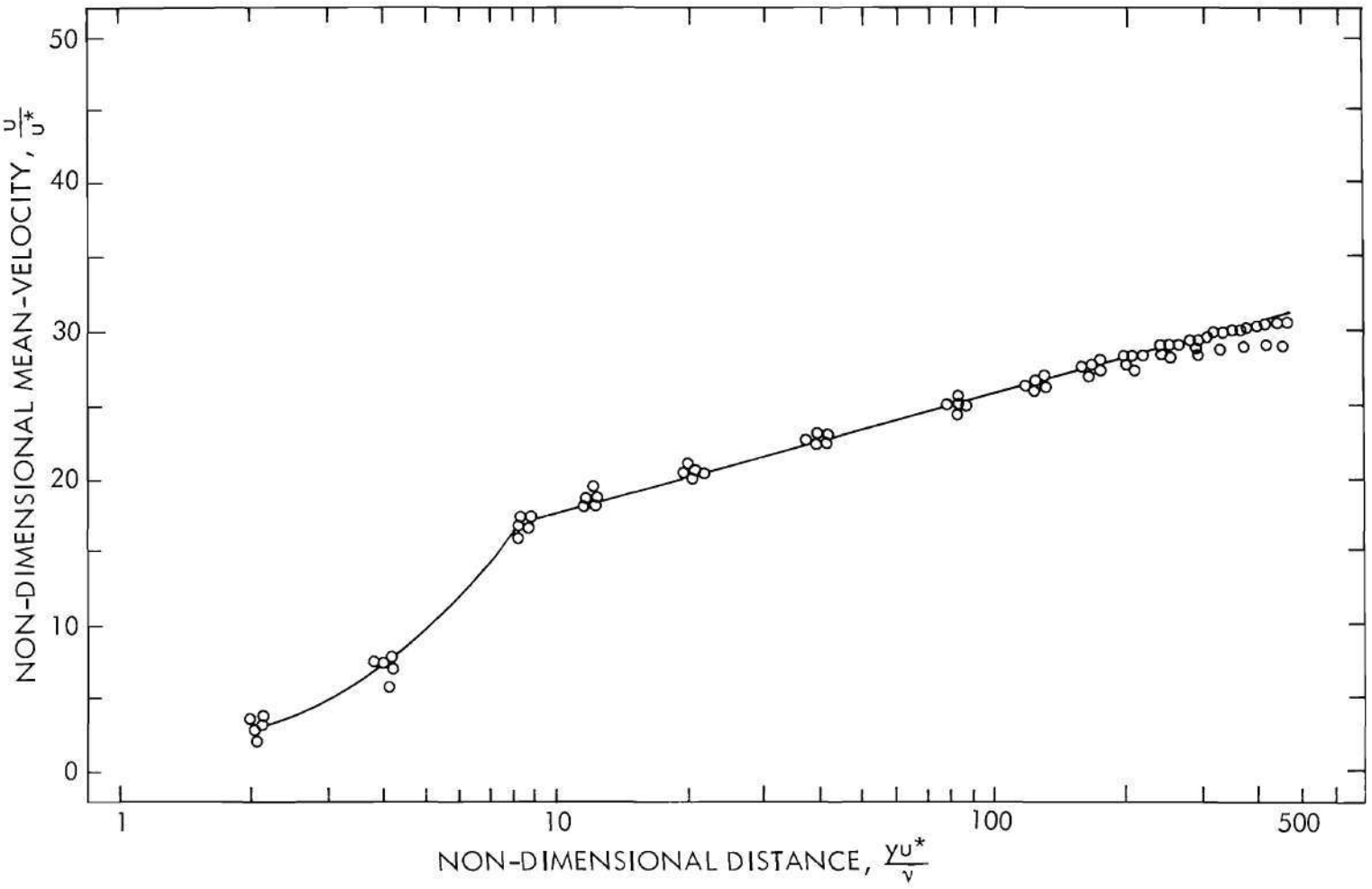

Figure 13. Non-Dimensional Mean-Velocity Profiles.
Injected Fluid: Water.
Injection Rate: 537.0 mls/min. Concentration: -- ppm.

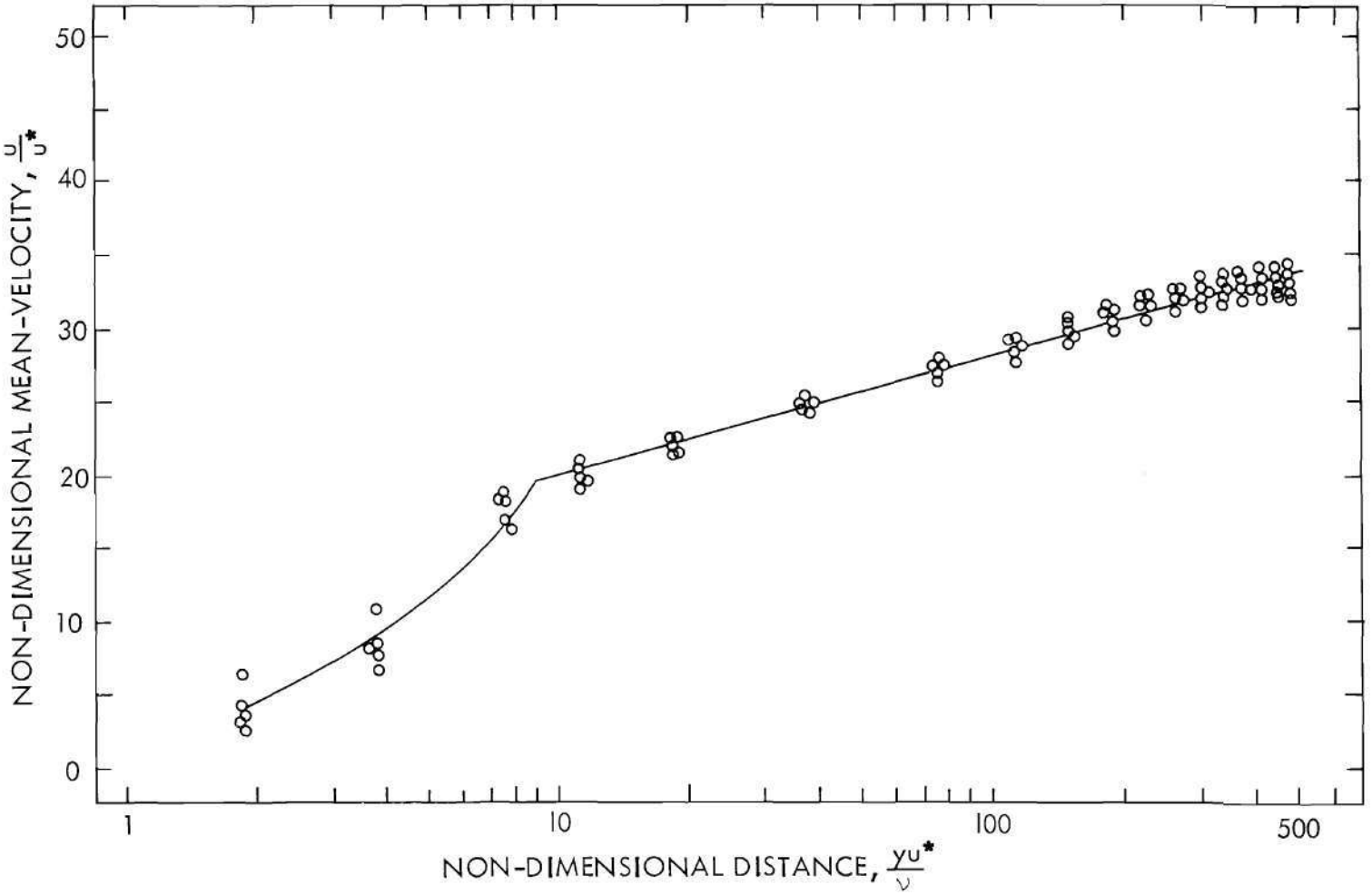

Figure 14. Non-Dimensional Mean-Velocity Profiles.
Injected Fluid: Aqueous Solution of Polyethylene Oxide.
Injection Rate: 60.0 mls/min. Concentration: 50.0 ppm.

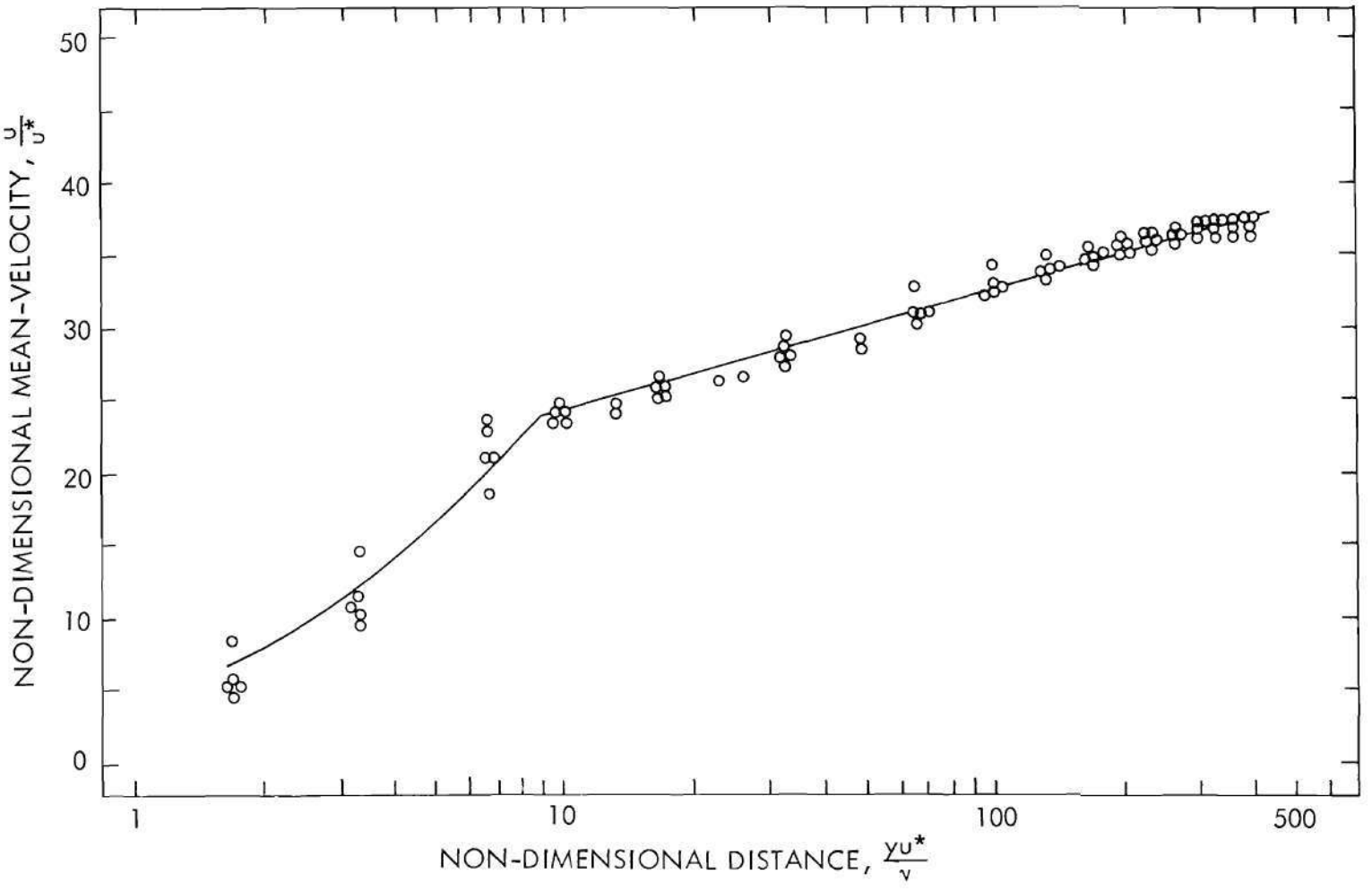

Figure 15. Non-Dimensional Mean-Velocity Profiles.
Injected Fluid: Aqueous Solution of Polyethylene Oxide.
Injection Rate: 134.0 mls/min. Concentration: 50.0 ppm.

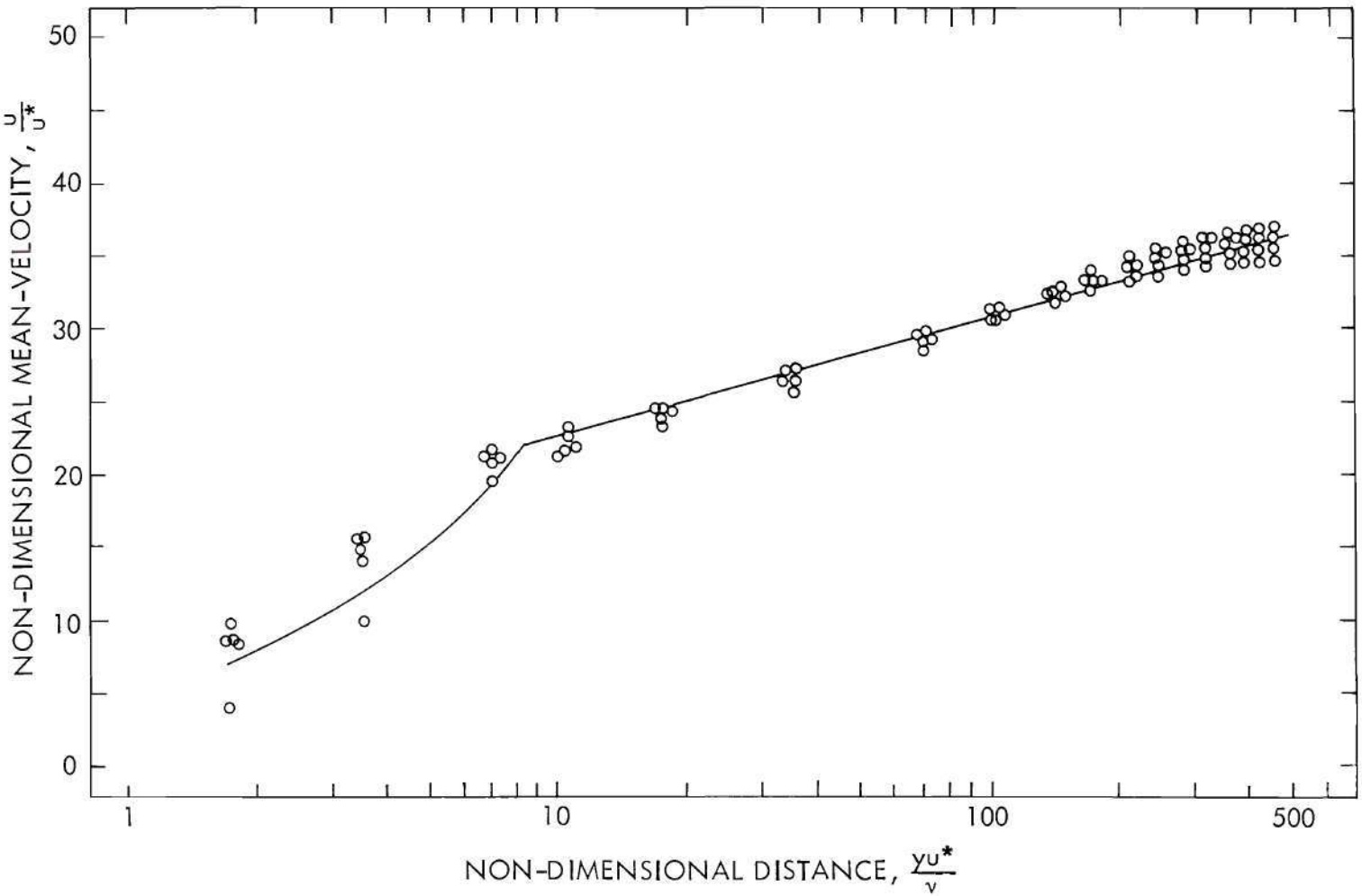

Figure 16. Non-Dimensional Mean-Velocity Profiles.
Injected Fluid: Aqueous Solution of Polyethylene Oxide.
Injection Rate: 537.0 mls/min. Concentration: 50.0 ppm.

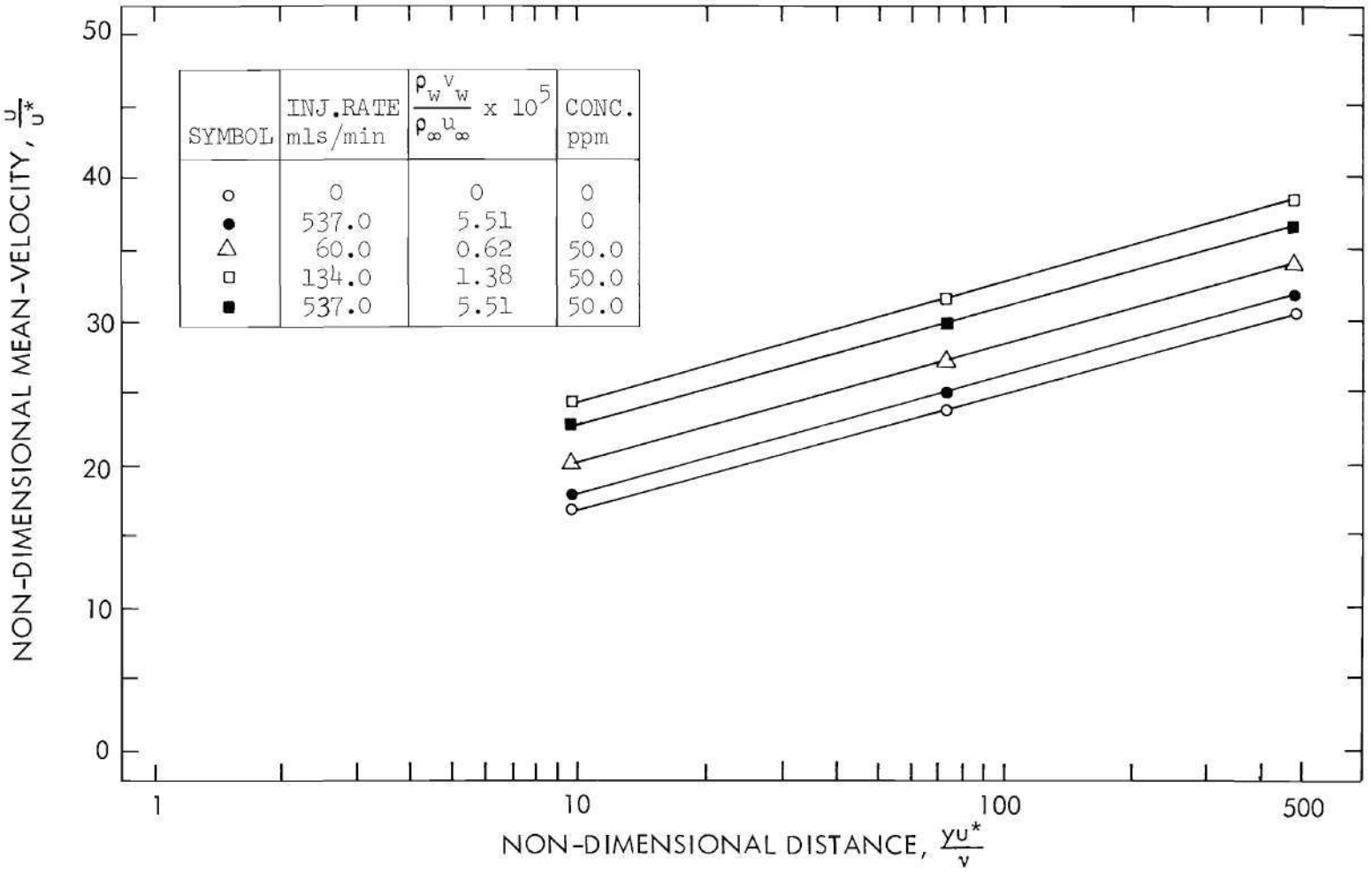

Figure 17. Effect of Injections on the Non-Dimensional Mean-Velocity Profiles.

of y^+.

Table 30 in Appendix C presents the non-dimensional skin friction, $\frac{\tau_w}{\tau_{w_o}}$, as a function of the injection parameter, $\frac{2\,\rho_w v_w}{\rho_\infty u_\infty c_{f_o}}$. The functional relationship, shown graphically in Figure 18, was based on the film theory described by Bird and co-workers[61], the principal result of which is:

$$1 + \frac{(u_\infty - 0)(N_{AW}M_A + N_{BW}M_B)}{\tau_w} = \exp. \frac{N_{AW}M_A + N_{BW}M_B}{\frac{1}{2}\rho u_\infty c_{f_o}} \quad . \qquad (40)$$

This equation shows how the wall shear stress depends on the molar fluxes: N_{AW} and N_{BW}. The dimensionless quantity on the right of Equation (40) is called the rate factor, since it varies directly with the mass-transfer rate. It is the abscissa used in Figure 18. The ordinate of this figure is a correction factor for the effect of mass transfer on the wall shear stress. Figure 18 shows that it varies almost linearly with the rate factor for injection of water. The correction factor for injection of the polymer solutions drops off sharply at first, shows an inversion, and then increases slowly with the rate parameter.

Concentration data were obtained in the boundary layer at station 6 during injection of aqueous solutions of polyethylene oxide at 50.0 ppm. In these measurements, it was impractical to take samples right at the surface because calculations, based on the highest injection rate and the inside diameter of the probe, had shown that it would take several hours to collect enough of a sample to run a polarographic analysis. The first samples were therefore collected at a distance of 0.001 inches from the porous surface. The boundary-layer concentrations are presented in Table 31

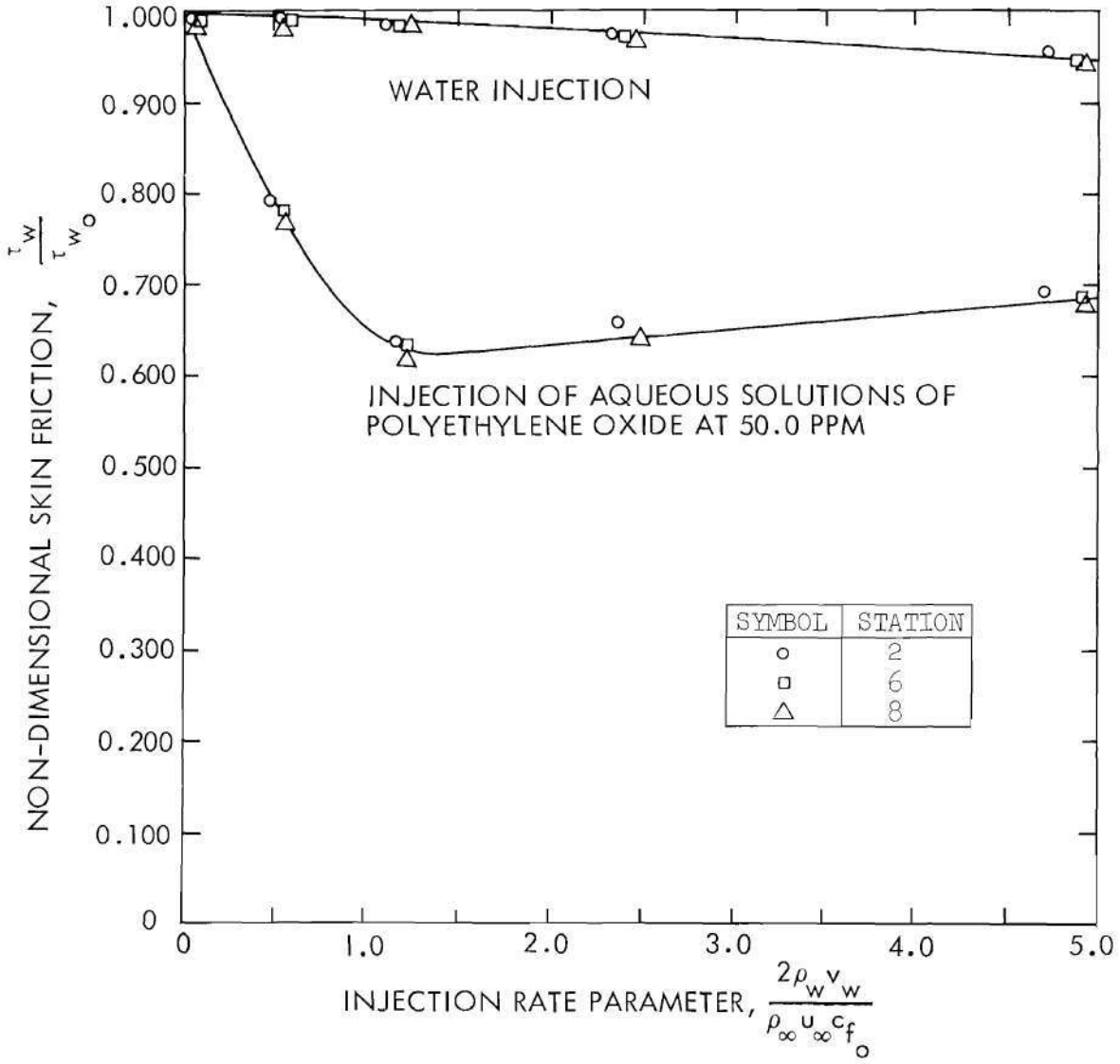

Figure 18. Non-Dimensional Skin Friction as a Function of the Injection Rate Parameter.

of Appendix C. A graphical presentation of the data in Figure 19 shows the sharp drop in concentration in the laminar sub-layer--from 50.0 ppm at the wall to a few ppm at the edge. Although the data has not been plotted, Table 31 shows that the concentrations remained relatively constant in the turbulent portion of the boundary layer.

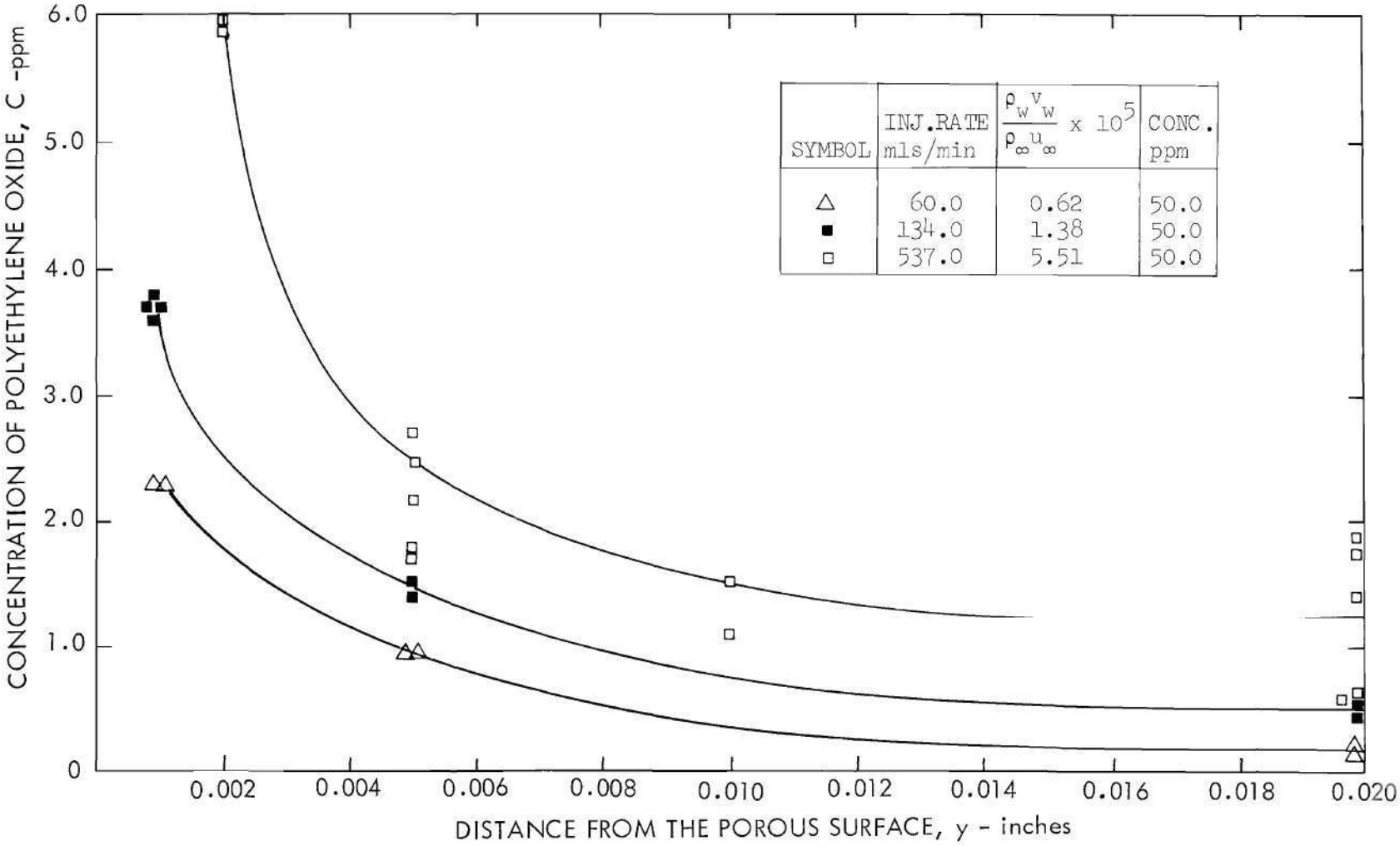

Figure 19. Effect of Injections on the Concentration of Polyethylene Oxide in the Boundary Layer.

CHAPTER VII

CONCLUSIONS

The results of this investigation may be summarized as follows.

1. A new technique for introducing drag-reducing solutions in the boundary layer was developed and investigated. This method, which employs distributed surface mass addition through a porous sheet of rigid, high-density, linear polyethylene has proven to be very efficient. Drag reductions of up to 37 percent were attained while injecting aqueous solutions of polyethylene oxide at concentrations of 50.0 ppm. The injection ratio, $\frac{\rho_w v_w}{\rho_\infty u_\infty}$, at this drag reduction was 1.38×10^{-5} and the Reynolds number was 1.24×10^6.

2. Although no extensive investigation was made of injections at concentrations other than 50.0 ppm, the data obtained for the injection of solutions of 25.0 and 150.0 ppm indicate that the weight of the polymer injected per unit of time and unit area is the prime criterion in drag reduction.

3. The onset of drag reduction occurred at lower values of the wall shear stress than predicted by present hypotheses[53,54,67]. This agrees with the findings of Little[36] who investigated similar drag-reducing agents.

4. The shape of the velocity profiles was not influenced appreciably by injection of water at a rate of 537.0 mls/min. The effect of aqueous solutions of polyethylene oxide was to make the velocity profiles blunter at each axial location. This effect was found to increase with injection

rate (up to 134.0 mls/min) and with axial distance down the channel.

5. The effect of injections on the free-stream velocity was essentially zero.

6. The boundary-layer thickness decreased with injection of water and aqueous solutions of polyethylene oxide. Injections of water reduced the boundary-layer thickness by a maximum amount of approximately 11 percent. Injection of the polymer solutions at concentrations of 50.0 ppm continued to decrease the boundary-layer thickness until an injection rate of 134.0 mls/min was attained. The reduction in thickness at that point was about 20 percent. Then a reversal occurred and the boundary layer increased in thickness with higher injection rate.

7. The shear stresses in the boundary layer were lowered by mass additions. Aqueous solutions of polyethylene oxide at concentrations of 50.0 ppm produced the largest reduction at the porous wall, except at a rate of 134.0 mls/min, which yielded a constant reduction of 37 percent from y = 0 to the edge of the boundary layer. Injections of water at 537.0 mls/min, however, produced the largest shear-stress reduction at the outer edge of the boundary layer. The two largest injection rates examined in this investigation--537.0 mls/min--produced a surprising result, both in the case of water injection and polymer addition. This was that the maximum shearing stress no longer occurred at the wall, but was displaced from it. The maximum shearing stress in the case of water injection occurred at a y value of 0.02 inch, whereas in the case of polymer addition the maximum was found at y = 0.05 inch. The reasons for the occurrence of these maxima were not clear, but they have been noticed previously in the case of gas injections in air boundary layers[68,69].

8. The non-dimensional mean-velocity profiles were shifted linearly in an upward direction by all injections considered in this investigation. This implies that injections of water and aqueous solutions of polyethylene oxide at 50.0 ppm do not cause changes in the universal constant k (the mixing-length constant). These results agreed with the findings of Ernst[27] and Meyer[52], but contradicted those of Elata and Tirosh[25] and Wells[26].

9. Concentration measurements were made in the transpired boundary layer while injecting aqueous solutions of polyethylene oxide at 50.0 ppm. Sharp drops in concentration were observed in the laminar sub-layer--from 50.0 ppm at the wall to values of a few ppm at the edge. The concentrations in the turbulent portion of the boundary layer were found to be relatively constant at the value at the edge of the sub-layer.

CHAPTER VIII

RECOMMENDATIONS

It is recommended that the following items be given consideration in future investigations of this nature.

1. The feasibility of measuring wall pressure fluctuations to obtain wall shear-stress values in turbulent boundary layers with and without mass addition should be evaluated.

2. The feasibility of using the hydrogen-bubble technique to measure instantaneous velocity profiles in a two-component liquid boundary layer should be examined.

3. The practicability of using a hot-film probe to measure mean velocities and velocity fluctuations in turbulent boundary layers subjected to distributed surface mass addition should be studied.

4. Investigations should be extended to include higher bulk flow rates.

5. Investigations should be continued to determine the exact distribution of additives in the boundary layer, with the object of optimizing the drag-reducing effect.

6. The effect of stream-wise, adverse pressure gradients on the magnitude of drag reduction should be studied.

7. The effect of surface roughness on drag reduction should be fully investigated.

8. Combinations of tangential and normal injections should be

studied.

9. The feasibility of recovering a portion of the injected solution, aft of the injection area, should be investigated.

APPENDICES

APPENDIX A

COMPUTER PROGRAM

Appendix A presents a list of symbols and the Algol program written for the Burroughs B-5500 computer. This program computes velocities from differential-pressure input data. The velocities are used to calculate the following parameters at various values of y:

$$\int_0^y \frac{\rho u}{g_c}\,dy, \quad \int_0^y \frac{\rho u^2}{g_c}\,dy, \quad \int_0^y \frac{\rho u(u_\infty - u)}{g_c}\,dy, \quad \text{and,} \quad \rho_w v_w u \ .$$

Part of the output for Test Run 108 is shown in Table 1.

List of Symbols for Computer Program

A[I]	Coefficient in polynomial
B1	Balance pressure at beginning of profile measurement
B2	Balance pressure at end of profile measurement
B	Average value of balance pressure
C	Concentration
CI1	Correction of integral values at y = 0.010 inch
CI2	Correction of integral values at y = 0.020 inch
D	Boundary-layer thickness
F	Value of integral under consideration
F1	Value of integral from y = 0 to y = 0.020 inch
G	Dimensional constant, g_c
H	Independent variable in polynomial used for curve fitting, $H = Y^{0.0600}$
M	Degree of polynomial
N	Number of data points
P1	Pressure in left side of manometer, inches of mercury above zero mark
P2	Pressure in right side of manometer, inches of mercury below zero mark
POS	Position
PU	ρu
PU*2	ρu^2 (also PU2)
Q	$\rho_w v_w u/g_c$
R	Injection rate
S	Distance from the wall
U	Velocity in the axial direction

UM	u_∞
V	u/u_∞
W	Dummy variable
X	Distance from the beginning of the test section
Y	Distance from the wall
YL	First data point used for curve fitting
Z	$\rho u(u_\infty - u)/12\ g_c$

Algol Program

```
BEGIN
FILE IN JJH1IN (2,10);
FILE OUT JJH1OUT 16(2,15);
REAL      S,P1,P2,B1,B2,C,R,D,B,UM,X,V,W,Q,F,YL,FL,CI1,CI2;
REAL ARRAY U1,PU1,PU21,Z1,Y[0:25],
          U2,PU2,PU22,Z2,H[0:25],A[0:11];
INTEGER   I,POS,N,M,J,K,RUN;
ALPHA     D1,D2;
FORMAT    HD("  Y      U       U/UM     Z        PU        PU*2       Q"//);     08
FORMAT    H10("     X                 Y          VELOCITY");
FORMAT    F9("YL= ",F5.3,"INTEGRAL 0 TO YL= ",E15.5);
FORMAT    F1(F5.3,4F6.2,I3,F8.1,F6.1,F7.3);
FORMAT    RN("RUN NO.",I3," DATE ",2A4//);
FORMAT    R1(I3,X2,2A4);
FORMAT    F2(F5.3,2F6.2);
FORMAT    CO(F5.3);
FORMAT    KEY("RATE=",F8.1," MLS/MIN"//
              "CONCENTRATION=",F6.1,"PPM"//
              "POSITION",I3//);
FORMAT    F4(F5.3,2F7.3,3F9.4,F12.8);
FORMAT    F6(F7.3,X9,F6.3,E20.6);
FORMAT    FMT6("    X                 Y          INT 0 TO Y PU*2"//);
FORMAT    FMT7("    X                 Y          INT 0 TO Y PU"//);
FORMAT    FMT8("    X                 Y          INT 0 TO D PU(UM-U)/G"//);
FORMAT     FMT5("Z=",2E15.6," xH",E15.6," xH*2"F15.6," xH*3"/
          F15.6," xH*4",E15.6," xH*5",E15.6," xH*6",E15.6," xH*7"/
          F15.6," xH*8",E15.6," xH*9",E15.6," xH*10"//);
FORMAT     FTT5("U=",2E15.6," xH",E15.6," xH*2"E15.6," xH*3"/
          F15.6," xH*4",E15.6," xH*5",E15.6," xH*6",E15.6," xH*7"/
          F15.6," xH*8",E15.6," xH*9",E15.6," xH*10"//);
FORMAT     FM5("PU=",2F15.6," xH",F15.6," xH*2"F15.6," xH*3"/
          F15.6," xH*4",E15.6," xH*5",E15.6," xH*6",E15.6," xH*7"/
          F15.6," xH*8",E15.6," xH*9",E15.6," xH*10"//);
FORMAT    F5("PU*2=",2E15.6," xH",F15.6," xH*2"F15.6," xH*3"/
          F15.6," xH*4",E15.6," xH*5",E15.6," xH*6",E15.6," xH*7"/
          F15.6," xH*8",E15.6," xH*9",E15.6," xH*10"//);
LABEL     L1,L2,L3,L4,L5,L6,L,LF;
```

```
LIST      OUT4(Y[I],U1[I],V,Z1[I],PU1[I],PU21[I],Q);
LIST      OUT5(FOR K←0 STEP 1 UNTIL M DO A[K]);
$$ A A066                                                                    00000000
                                                                             99999999
LABEL     TEST:
DUMP JJH1OUT(M,N,H,PU22,A)TEST:1;
          WRITE(JJH1OUT[NO]);
L1:       READ(JJH1IN,R1,RUN,D1,D2)[LE];
          I←0;
L2:       READ(JJH1IN[NO],CO,S)[LE];
          IF S=5.00 THEN READ(JJH1IN,CO,S)
          ELSE IF S<3.00 THEN
                         READ(JJH1IN,F2,S,P1,P2)
          ELSE READ(JJH1IN,F1,S,P1,P2,B1,B2,POS,R,C,D);
          IF S=5.00 THEN GO TO L6;
          IF S<3.00 THEN GO TO L3;
          READ(JJH1IN,CO,YL);
          B←(B1+B2)/2.036;
          UM←2.32 × SQRT(0.2×(((P1+P2)/2.036)-B));
          IF POS=01 THEN X← 48.000       ELSE
          IF POS=02 THEN X← 54.000       ELSE
          IF POS=03 THEN X← 60.000       ELSE
          IF POS=04 THEN X← 66.000       ELSE
          IF POS=05 THEN X← 72.000       ELSE
          IF POS=06 THEN X← 78.000       ELSE
          IF POS=07 THEN X← 84.000       ELSE
          X← 90.000;
          WRITE(JJH1OUT[PAGE]);
          WRITE(JJH1OUT,RN,RUN,D1,D2);
          WRITE(JJH1OUT,KEY,R,C,POS);
          WRITE(JJH1OUT,HD);
          GO TO L5;
L3:       IF I>2 THEN GO TO L4 ELSE GO TO L5;
L4:       Y[I]←S;
          H[I]←S*0.0600;
          U2[I]←U1[I]←2.32 × SQRT(0.2×(((P1+P2)/2.036)-B));
          PU2[I]←PU1[I]←1.9379 ×U1[I]/12;
```

```
          PU22[I]←PU21[I]←U1[I] × PU1[I];
          Z2[I]←Z1[I]←PU1[I] ×(UM-U1[I]);
          Q←(3.259×@-7) ×R ×U1[I];
          V←U1[I]/UM;
          WRITE(JJH10UT,F4,OUT4);
          I←I+1;
          GO TO L2;
L5:       Y[I]←S; Y[0]←0;
          U1[I]←2.32 × SQRT(0.2×(((P1+P2)/2.036)-B));
          PU1[I]←1.9379 ×U1[I]/12;
          PU21[I]←U1[I] × PU1[I];
          Z1[I]←PU1[I] ×(UM-U1[I]);
          Q←(3.259×@-7) ×R ×U1[I];
          V←U1[I]/UM;
          WRITE(JJH10UT,F4,OUT4);
          I←I+1;
          GO TO L2;
L6:       N←I-2; M←3; FOR J←0 STEP 1 UNTIL M DO A[J]←0;
L:        LSQPOLY(M,N,H,PU22,A);
TEST:
           FOR I←0 STEP 1 WHILE I≤M AND A[I]=0 DO;
          IF I≥M THEN BEGIN M←M-1; GO TO L END;
          WRITE(JJH10UT[PAGE]);
          WRITE(JJH10UT,F5,OUT5);
BEGIN
INTEGER   DUM;
          FL←A[0]×YL +A[1]×(YL*1.0600)/1.0600
          +A[2]×(YL*1.1200)/1.1200 +A[3]×(YL*1.1800)/1.1800
          +A[4]×(YL*1.2400)/1.2400 +A[5]×(YL*1.3000)/1.3000
          +A[6]×(YL*1.3600)/1.3600 +A[7]×(YL*1.4200)/1.4200
          +A[8]×(YL*1.4800)/1.4800 +A[9]×(YL*1.5400)/1.5400
          +A[10]×(YL*1.6000)/1.6000;
          WRITE(JJH10UT,F9,YL,FL);
          WRITE(JJH10UT,FMT6);
          END;
          CI1←0.5000×Y[2]×PU21[2];
          WRITE(JJH10UT,F6,X,Y[2],CI1);
```

```
        CI2←0.500×Y[3]×PU21[3];
        WRITE(JJH1OUT,F6,X,Y[3],CI2);
        FOR W←0.03 STEP 0.01 UNTIL 0.10 DO
    BEGIN
        F←A[0]×W +A[1]×(W*1.0600)/1.0600    -FL+CI2
        +A[2]×(W*1.1200)/1.1200 +A[3]×(W*1.1800)/1.1800
        +A[4]×(W*1.2400)/1.2400 +A[5]×(W*1.3000)/1.3000
        +A[6]×(W*1.3600)/1.3600 +A[7]×(W*1.4200)/1.4200
        +A[8]×(W*1.4800)/1.4800 +A[9]×(W*1.5400)/1.5400
        +A[10]×(W*1.6000)/1.6000;
        WRITE(JJH1OUT,F6,X,W,F);
        END;
        FOR W←0.20 STEP 0.10 UNTIL 1.4 DO
    BEGIN
        F←A[0]×W +A[1]×(W*1.0600)/1.0600    -FL+CI2
        +A[2]×(W*1.1200)/1.1200 +A[3]×(W*1.1800)/1.1800
        +A[4]×(W*1.2400)/1.2400 +A[5]×(W*1.3000)/1.3000
        +A[6]×(W*1.3600)/1.3600 +A[7]×(W*1.4200)/1.4200
        +A[8]×(W*1.4800)/1.4800 +A[9]×(W*1.5400)/1.5400
        +A[10]×(W*1.6000)/1.6000;
        WRITE(JJH1OUT,F6,X,W,F);
        END;
        FOR J←0 STEP 1 UNTIL M DO A[J]←0;
        LSQPOLY(M,N,H,PU2,A);
        WRITE(JJH1OUT[PAGE]);
        WRITE(JJH1OUT,FM5,OUT5);
BEGIN
INTEGER DUM;
        FL←A[0]×YL +A[1]×(YL*1.0600)/1.0600
        +A[2]×(YL*1.1200)/1.1200 +A[3]×(YL*1.1800)/1.1800
        +A[4]×(YL*1.2400)/1.2400 +A[5]×(YL*1.3000)/1.3000
        +A[6]×(YL*1.3600)/1.3600 +A[7]×(YL*1.4200)/1.4200
        +A[8]×(YL*1.4800)/1.4800 +A[9]×(YL*1.5400)/1.5400
        +A[10]×(YL*1.6000)/1.6000;
        WRITE(JJH1OUT,F9,YL,FL);
        WRITE(JJH1OUT,FMT7);
        END;
```

```
      CI1←0.500×Y[2]×PU1[2];
      WRITE(JJH1OUT,F6,X,Y[2],CI1);
      CI2←0.500×Y[3]×PU1[3];
      WRITE(JJH1OUT,F6,X,Y[3],CI2);
      FOR W←0.03 STEP 0.01 UNTIL 0.10 DO
BEGIN
      F←A[0]×W +A[1]×(W*1.0600)/1.0600    -FL+CI2
      +A[2]×(W*1.1200)/1.1200 +A[3]×(W*1.1800)/1.1800
      +A[4]×(W*1.2400)/1.2400 +A[5]×(W*1.3000)/1.3000
      +A[6]×(W*1.3600)/1.3600 +A[7]×(W*1.4200)/1.4200
      +A[8]×(W*1.4800)/1.4800 +A[9]×(W*1.5400)/1.5400
      +A[10]×(W*1.6000)/1.6000;
      WRITE(JJH1OUT,F6,X,W,F);
      END;
      FOR W←0.20 STEP 0.10 UNTIL 1.4 DO
BEGIN
      F←A[0]×W +A[1]×(W*1.0600)/1.0600    -FL+CI2
      +A[2]×(W*1.1200)/1.1200 +A[3]×(W*1.1800)/1.1800
      +A[4]×(W*1.2400)/1.2400 +A[5]×(W*1.3000)/1.3000
      +A[6]×(W*1.3600)/1.3600 +A[7]×(W*1.4200)/1.4200
      +A[8]×(W*1.4800)/1.4800 +A[9]×(W*1.5400)/1.5400
      +A[10]×(W*1.6000)/1.6000;
      WRITE(JJH1OUT,F6,X,W,F);
      END;
      FOR J←0 STEP 1 UNTIL M DO A[J]←0;
      LSQPOLY(M,N,J,Z2,A);
      WRITE(JJH1OUT[PAGE]);
      WRITE(JJH1OUT,FMT5,OUT5);
      FL←A[0]×YL +A[1]×(YL*1.0600)/1.0600
      +A[2]×(YL*1.1200)/1.1200 +A[3]×(YL*1.1800)/1.1800
      +A[4]×(YL*1.2400)/1.2400 +A[5]×(YL*1.3000)/1.3000
      +A[6]×(YL*1.3600)/1.3600 +A[7]×(YL*1.4200)/1.4200
      +A[8]×(YL*1.4800)/1.4800 +A[9]×(YL*1.5400)/1.5400
      +A[10]×(YL*1.6000)/1.6000;
      WRITE(JJH1OUT,F9,YL,FL);
      WRITE(JJH1OUT,FMT8);
      CI1←0.500×Y[2]×Z1[2];
```

```
        WRITE(JJH10UT,F6,X,Y[2],CI1);
        CI2←0.500×Y[3]×Z1[3];
        WRITE(JJH10UT,F6,X,Y[3],CI2);
        F←A[0]×D +A[1]×(D*1.0600)/1.0600    -FL+CI2
        +A[2]×(D*1.1200)/1.1200 +A[3]×(D*1.1800)/1.1800
        +A[4]×(D*1.2400)/1.2400 +A[5]×(D*1.3000)/1.3000
        +A[6]×(D*1.3600)/1.3600 +A[7]×(D*1.4200)/1.4200
        +A[8]×(D*1.4800)/1.4800 +A[9]×(D*1.5400)/1.5400
        +A[10]×(D*1.6000)/1.6000;
        WRITE(JJH10UT,F6,X,D,F);
        FOR J←0 STEP 1 UNTIL M DO A[J]←0;
        LSQPOLY(M,N,H,U2,A);
        WRITE(JJH10UT[PAGE]);
        WRITE(JJH10UT,FTT5,OUT5);
        WRITE(JJH10UT,H10);
        FOR W←0.02 STEP 0.01 UNTIL 0.10 DO
    BEGIN
        F←A[0] +A[1]×(W*0.0600) +A[2]×(W*0.1200)
        +A[3]×(W*0.1800) +A[4]×(W*0.2400) +A[5]×(W*0.3000)
        +A[6]×(W*0.3600) +A[7]×(W*0.4200) +A[8]×(W*0.4800)
        +A[9]×(W*0.5400) +A[10]×(W*0.6000);
        WRITE(JJH10UT,F6,X,W,F);
         END;
        FOR W←0.20 STEP 0.10 UNTIL 1.4 DO
BEGIN
        F←A[0] +A[1]×(W*0.0600) +A[2]×(W*0.1200)
        +A[3]×(W*0.1800) +A[4]×(W*0.2400) +A[5]×(W*0.3000)
        +A[6]×(W*0.3600) +A[7]×(W*0.4200) +A[8]×(W*0.4800)
        +A[9]×(W*0.5400) +A[10]×(W*0.6000);
        WRITE(JJH10UT,F6,X,W,F);
        END;
        FOR J←0 STEP 1 UNTIL M DO A[J]←0;
        GO TO L1;
LE:
END.
```

```
PROCEDURE      LSQPOLY(M,N,XH,YH,AH) ; %                                    100
VALUE          M,N ; %                                                      200
INTEGER        M,N ; %                                                      300
ARRAY          XH,YH,AH[0] ;%                                               400
%                                                                           500
%         THIS PROCEDURE FITS A LEAST SQUARES POLYNOMIAL OF DEGREE M        600
%                        M                                                  700
%              P(X) = SIGMA AH[K]x(X*K)                                     800
%                       K=0                                                 900
%    TO THE N POINTS OF THE TABULATION (XH[I],YH[I]), I = 1,2,3,...,N,      1000
%    BY COMPUTING THE COEFFICIENTS AH[K], K = 0,1,2,...,M. DOUBLE PRE-      1100
%    CISION ARITHMETIC IS USED INTERNALLY TO IMPROVE ACCURACY. IF THE       1200
%    COEFFICIENT MATRIX FOR THE SYSTEM WHICH DETERMINES THE COEFFICIENTS    1300
%    OF THE POLYNOMIAL TURNS OUT TO BE SINGULAR, THE COEFFICIENTS AH[K],    1400
%    K = 0,1,...,M, ARE ALL SET TO ZERO PRIOR TO EXIT.                      1500
%                                                                           1600
BEGIN %                                                                    1700
INTEGER        I,J,K ;%                                                    1800
REAL           SH,SL,TH,TL ; %                                             1900
ARRAY          AL[0:M], XL,YL[0:N], ZH,ZL[0:2xM], %                        2000
               RH,RL[0:M+1], GH,GL[0:M+1,0:M+1] ; %                        2100
LABEL          SING,RETURN ; %                                             2200
PROCEDURE      DPWR(N,XH,XL,ZH,ZL) ; %                                     2300
VALUE          N,XH,XL ; %                                                 2400
INTEGER        N ;%                                                        2500
REAL           XH,XL ; %                                                   2600
ARRAY          ZH,ZL[0] ; %                                                2700
BEGIN %                                                                    2800
INTEGER        I ; %                                                       2900
REAL           TH,TL ; %                                                   3000
DEFINE         D = DOUBLE # , T = TH,TL # , %                              3100
               X = XH,XL  # , ZI = ZH[I],ZL[I] # ; %                       3200
               TH ← ZH[0] ← 1.0 ; TL ← ZL[0] ← 0 ; %                       3300
               FOR I ← 1 STEP 1 UNTIL N DO %                               3400
               BEGIN D(T,X,x,←,T) ; D(T,←,ZI) END ; %                      3500
END DPWR ; %                                                               3600
PROCEDURE      DINVERT(N,AH,AL,RH,RL,LEBAL) ;                              3700
```

```
VALUE          N ; %                                                              3800
INTEGER        N ; %                                                              3900
REAL ARRAY     AH,AL,RH,RL[0,0] ; %                                               4000
LABEL          LEBAL ; %                                                          4100
%                                                                                 4200
%        THIS PROCEDURE COMPUTES THE INVERSE OF THE N-TH ORDER REAL               4300
%   DOUBLE PRECISION MATRIX A = AH[,],AL[,] AND STORES THE RESULT IN              4400
%   THE ARRAY R = RH[,],RL[,]. IF THE MATRIX A IS SINGULAR, EXIT IS               4500
%   MADE TO THE EXTERNALLY DECLARED LABEL "LEBAL". THE MATRIX PAIR                4600
%   A,R = A,A = AH,AL,AH,AL IS VALID IN A PROCEDURE CALL STATEMENT.               4700
%   THAT IS, THE MATRIX A CAN BE REPLACED BY ITS INVERSE.                         4800
%                                                                                 4900
BEGIN %                                                                           5000
INTEGER        I,I1,J,K,L,M,N1,SGN ; %                                            5100
REAL           BH,BL,EH,EL,GH,GL,QH,QL,TH,TL ; %                                  5200
INTEGER ARRAY  F[0:N] ; %                                                         5300
REAL ARRAY     CH,CL[0:N,0:N] ; %                                                 5400
LABEL          L1,L2,L3,L4,L5,L6 ; %                                              5500
DEFINE         D = DOUBLE #, UPTO = STEP 1 UNTIL # , %                            5600
               I1NDO  = FOR I ← 1 UPTO N  DO # , B = BH,BL # , %                  5700
               J1NDO  = FOR J ← 1 UPTO N  DO # , E = EH,EL # , %                  5800
               JINDO  = FOR J ← I UPTO N  DO # , G = GH,GL # , %                  5900
               J1IDO  = FOR J ← 1 UPTO I  DO # , Q = QH,QL # , %                  6000
               K1NDO  = FOR K ← 1 UPTO N  DO # , T = TH,TL # , %                  6100
               KINDO  = FOR K ← I UPTO N  DO # , CIJ = CH[I,J],CL[I,J] #,         6200
               KJNDO  = FOR K ← J UPTO N  DO # , CJK = CH[J,K],CL[J,K] #,         6300
               I1N1DO = FOR I ← 1 UPTO N1 DO # , CKI = CH[K,I],CL[K,I] #,         6400
               K1I1DO = FOR K ← 1 UPTO I1 DO # , CJI = CH[J,I],CL[J,I] #,         6500
               KJI1DO = FOR K ← J UPTO I1 DO # , CIK = CH[I,K],CL[I,K] #,         6600
               KI1LDO = FOR K ←I1 UPTO L  DO # , CMK = CH[M,K],CL[M,K] #,         6700
               CII = CH[I,I],CL[I,I] # , CKJ = CH[K,J],CL[K,J] # , %              6800
               CKM = CH[K,M],CL[K,M] # , AIJ = AH[I,J],AL[I,J] # , %              6900
               RIJ = RH[I,J],RL[I,J] # ; %                                        7000
%                                                                                 7100
               I1NDO J1NDO D(AIJ,←,CIJ) ; %                                       7200
%                                                                                 7300
    L1:        I1NDO %                                                            7400
```

```
        BEGIN I1 ← I-1 ;                                                    7500
              JINDO %                                                       7600
        BEGIN QH ← QL ← 0 ; %                                               7700
              K1I1DO D(CJK,CKI,×,Q,+,←,Q) ; %                               7800
              D(CJI,Q,-,←,CJI) ; %                                          7900
        END ; %                                                             8000
        BH ← BL ← 0 ; M ← I ; %                                             8100
                                                                            8200
   L2:        KINDO %                                                       8300
        BEGIN                                                               8400
              IF ABS(CH[K,I]) > BH THEN %                                   8500
        BEGIN SGN ← SIGN(CH[K,I]) ; %                                       8600
              D(SGN,0,CKI,×,←,B) ; %                                        8700
              M ← K ; %                                                     8800
        END ; %                                                             8900
        END ; %                                                             9000
              EH ← 1.0@-10 ; EL ← 0 ; %                                     9100
              IF BH ≤ EH THEN GO TO LEBAL ; %                               9200
              F[I] ← M ; %                                                  9300
              IF M ≠ I THEN %                                               9400
                                                                            9500
   L3:        K1NDO %                                                       9600
        BEGIN                                                               9700
              D(CIK,←,T) ; %                                                9800
              D(CMK,←,CIK) ; %                                              9900
              D(T,←,CMK) ; %                                               10000
        END ; %                                                            10100
              D(CII,←,G) ; %                                               10200
              FOR J ← I+1 UPTO N DO %                                      10300
        BEGIN QH ← QL ← 0 ; %                                              10400
              K1I1DO D(CIK,CKJ,×,Q,+,←,Q) ; %                              10500
              D(CIJ,Q,-,G,/,←,CIJ) ; %                                     10600
        END ; %                                                            10700
        END ; %                                                            10800
%                                                                          10900
   L4:        I1NDO %                                                      11000
        BEGIN I1 ← I-1 ; %                                                 11100
```

```
            D(CII,←,G) ; %                                              11200
            J1IDO %                                                     11300
        BEGIN %                                                         11400
            IF I = J THEN D(1,0,G,/,←,CIJ) ELSE %                       11500
        BEGIN QH ← QL ← 0 ; %                                           11600
            KJI1DO D(CIK,CKJ,×,Q,+,←,Q) ; %                             11700
            D(0,0,Q,-,G,/,←,CIJ) ; %                                    11800
        END ; %                                                         11900
        END ; %                                                         12000
        END ; %                                                         12100
            N1 ← N-1 ; %                                                12200
            FOR I ← N1 STEP -1 UNTIL 1 DO %                             12300
        BEGIN I1 ← I+1 ; %                                              12400
            FOR J ← N STEP -1 UNTIL I1 DO %                             12500
        BEGIN QH ← QL ← 0 ; %                                           12600
            L ← J-1 ; %                                                 12700
            KI1LDO D(CIK,CKJ,×,Q,+,←,Q) ; %                             12800
            D(0,0,CIJ,-,Q,-,←,CIJ) ; %                                  12900
        END ; %                                                         13000
        END ; %                                                         13100
            I1N1DO J1NDO %                                              13200
        BEGIN QH ← QL ← 0 ;%                                            13300
            IF I ≥ J THEN %                                             13400
        BEGIN %                                                         13500
            FOR K ← I+1 STEP 1 UNTIL N DO %                             13600
            D(CIK,CKJ,×,Q,+,←,Q) ; %                                    13700
            D(CIJ,Q,+,←,CIJ) ; %                                        13800
        END    ELSE %                                                   13900
        BEGIN %                                                         14000
            KJNDO D(CIK,CKJ,×,Q,+,←,Q) ; %                              14100
            D(Q,←,CIJ) ; %                                              14200
        END ; %                                                         14300
        END ; %                                                         14400
%                                                                       14500
    L5:     FOR J ← N STEP -1 UNTIL 1 DO                                14600
        BEGIN M ← F[J] ; %                                              14700
            IF F[J] = J THEN GO TO L6 ; %                               14800
```

```
            K1NDO %                                                          14900
        BEGIN D(CKM,←,T) ; D(CKJ,←,CKM) ; D(T,←,CKJ) END ; %                 15000
    L6: END ; %                                                              15100
            I1NDO J1NDO %                                                    15200
            BEGIN RH[I,J] ← CH[I,J] ; RL[I,J] ← CL[I,J] END ; %              15300
END DINVERT ; %                                                              15400
%                                                                            15500
DEFINE      D = DOUBLE # , %                                                 15600
            UPTO = STEP 1 UNTIL # , %                                        15700
            YI = YH[I],YL[I] # , RK1 = RH[K+1],RL[K+1] # , %                 15800
            ZK = ZH[K],ZL[K] # , GIJ = GH[I,J],GL[I,J] # , %                 15900
            RJ = RH[J],RL[J] # , ZJK = ZH[J+K],ZL[J+K] # , %                 16000
            AIM1 = AH[I-1],AL[I-1] # , S = SH,SL # , %                       16100
            GJ1K1 = GH[J+1,K+1],GL[J+1,K+1] # ; %                            16200
            FOR I ← 1 UPTO N DO XL[I] ← YL[I] ← 0 ; %                        16300
            FOR K ← 0 UPTO M DO %                                            16400
        BEGIN RH[K+1] ← RL[K+1] ← 0 ; %                                      16500
            FOR J ← 0 UPTO M DO %                                            16600
            GH[J+1,K+1] ← GL[J+1,K+1] ← 0 ; %                                16700
        END ; %                                                              16800
            FOR I ← 1 UPTO N DO %                                            16900
        BEGIN %                                                              17000
            DPWR(2×M,XH[I],XL[I],ZH,ZL) ; %                                  17100
            FOR K ← 0 UPTO M DO %                                            17200
        BEGIN %                                                              17300
            D(YI,ZK,×,RK1,+,←,RK1) ;%                                        17400
            FOR J ← 0 UPTO M DO %                                            17500
            D(ZJK,GJ1K1,+,←,GJ1K1) ; %                                       17600
        END ; %                                                              17700
        END ; %                                                              17800
            DINVERT(M+1,GH,GL,GH,GL,SING) ; %                                17900
            FOR I ← 1 UPTO M+1 DO %                                          18000
        BEGIN %                                                              18100
            SH ← SL ← 0 ; %                                                  18200
            FOR J ← 1 UPTO M+1 DO D(GIJ,RJ,×,S,+,←,S) ;%                     18300
            D(S,←,AIM1) ; %                                                  18400
        END ; GO TO RETURN ; %                                               18500
```

```
        SING: FOR I ← 0 UPTO M DO AH[I] ← AL[I] ← 0 ; %                    18600
RETURN: %                                                                  18700
END LSQPOLY ; %                                                            18800
```

Table 1. Computer Output for Test Run 108

RUN NO.108 DATE 07-10-68

RATE= 60.0 MLS/MIN

CONCENTRATION= 50.0PPM

POSITION 6

Y	U	U/UM	Z	PU	PU*2	Q
1.045	1.650	1.000	0.0000	0.2665	0.4397	0.00003227
0.005	0.163	0.099	0.0391	0.0263	0.0043	0.00000318
0.010	0.405	0.245	0.0814	0.0654	0.0265	0.00000792
0.020	0.894	0.541	0.1092	0.1443	0.1289	0.00001747
0.030	0.962	0.583	0.1069	0.1553	0.1494	0.00001881
0.050	1.051	0.637	0.1017	0.1698	0.1785	0.00002056
0.100	1.188	0.720	0.0886	0.1919	0.2280	0.00002323
0.200	1.351	0.818	0.0653	0.2181	0.2946	0.00002641
0.300	1.427	0.865	0.0515	0.2304	0.3287	0.00002790
0.400	1.481	0.898	0.0404	0.2392	0.3543	0.00002897
0.500	1.524	0.923	0.0312	0.2460	0.3748	0.00002979
0.600	1.554	0.942	0.0240	0.2510	0.3902	0.00003040
0.700	1.581	0.958	0.0175	0.2554	0.4039	0.00003092
0.800	1.601	0.970	0.0126	0.2586	0.4141	0.00003131
0.900	1.621	0.982	0.0076	0.2618	0.4244	0.00003170
1.000	1.628	0.986	0.0059	0.2628	0.4278	0.00003183
1.100	1.640	0.994	0.0026	0.2649	0.4346	0.00003208
1.200	1.644	0.996	0.0017	0.2654	0.4363	0.00003214
1.300	1.650	1.000	0.0000	0.2665	0.4397	0.00003227
1.400	1.650	1.000	0.0000	0.2665	0.4397	0.00003227

Table 1. (Continued)

PU*2= 1.475339@-05 -2.321500@+00 xH 4.553749@+00 xH*2 -1.804620@+00 xH*3

YL= 0.020INTEGRAL 0 TO YL= 1.08793@-03

X	Y	INT 0 TO Y PU*2
78.000	0.010	1.323458@-04
78.000	0.020	1.289304@-03
78.000	0.030	2.639035@-03
78.000	0.040	4.236620@-03
78.000	0.050	6.022366@-03
78.000	0.060	7.960284@-03
78.000	0.070	1.002618@-02
78.000	0.080	1.220262@-02
78.000	0.090	1.447642@-02
78.000	0.100	1.683725@-02
78.000	0.200	4.392127@-02
78.000	0.300	7.522477@-02
78.000	0.400	1.093057@-01
78.000	0.500	1.454645@-01
78.000	0.600	1.832840@-01
78.000	0.700	2.224861@-01
78.000	0.800	2.628720@-01
78.000	0.900	3.042921@-01
78.000	1.000	3.466302@-01
78.000	1.100	3.897929@-01
78.000	1.200	4.337040@-01
78.000	1.300	4.782995@-01

Table 1. (Continued)

PU= 4.064829@-06 -1.151703@+00 xH 2.696047@+00 xH*2 -1.281463@+00 xH*3

YL= 0.020INTEGRAL 0 TO YL= 2.18182@-03

Y	Y	INT 0 TO Y PU
78.000	0.010	3.269001@-04
78.000	0.020	1.442955@-03
78.000	0.030	2.930894@-03
78.000	0.040	4.533333@-03
78.000	0.050	6.220848@-03
78.000	0.060	7.975974@-03
78.000	0.070	9.787112@-03
78.000	0.080	1.164600@-02
78.000	0.090	1.354643@-02
78.000	0.100	1.548361@-02
78.000	0.200	3.627619@-02
78.000	0.300	5.871492@-02
78.000	0.400	8.217579@-02
78.000	0.500	1.063668@-01
78.000	0.600	1.311187@-01
78.000	0.700	1.563210@-01
78.000	0.800	1.818966@-01
78.000	0.900	2.077884@-01
78.000	1.000	2.339528@-01
78.000	1.100	2.603553@-01
78.000	1.200	2.869682@-01
78.000	1.300	3.137686@-01

Table 1. (Continued)

```
Z=  -8.045897@-06   4.210424@-01 xH  -1.049254@-01 xH*2  -3.099575@-01 xH*3

YL= 0.020INTEGRAL 0 TO YL=     2.51236@-03
   X              Y         INT 0 TO D PU(UM-U)/G


 78.000           0.010        4.070814@-04
 78.000           0.020        1.091757@-03
 78.000           1.045        3.965554@-02
```

Table 1. (Continued)

U= 2.517052@-05 -7.131655@+00 xH 1.669465@+01 xH*2 -7.935163@+00 xH*3

X	Y	VELOCITY
78.000	0.020	8.762765@-01
78.000	0.030	9.603147@-01
78.000	0.040	1.020846@+00
78.000	0.050	1.067315@+00
78.000	0.060	1.105154@+00
78.000	0.070	1.137016@+00
78.000	0.080	1.164493@+00
78.000	0.090	1.188616@+00
78.000	0.100	1.210092@+00
78.000	0.200	1.348075@+00
78.000	0.300	1.425116@+00
78.000	0.400	1.477552@+00
78.000	0.500	1.516705@+00
78.000	0.600	1.547582@+00
78.000	0.700	1.572827@+00
78.000	0.800	1.594008@+00
78.000	0.900	1.612126@+00
78.000	1.000	1.627860@+00
78.000	1.100	1.641637@+00
78.000	1.200	1.653961@+00
78.000	1.300	1.664945@+00

APPENDIX B

EXPERIMENTAL VELOCITY DATA

Appendix B lists the velocity data in Tables 3 through 9. The data were obtained during injection of the following fluids: (a) no injection, (b) water, and (c) aqueous solutions of polyethylene oxide at concentrations of 25.0, 50.0, and 150.0 ppm. The injection rates were 60.0, 134.0, 268.0, and 537.0 mls/min. These rates give $\frac{\rho_w v_w}{\rho_\infty u_\infty}$ values of approximately 0.62, 1.38, 2.75, and 5.51×10^{-5}, respectively.

Table 3. Experimental Velocity Data
Injected Fluid: None
Injection Rate: -- mls/min
Concentration: -- ppm

y (inches)	u(ft/sec) Station 1 Run No. 101	u(ft/sec) Station 1 Run No. 102	u(ft/sec) Station 2 Run No. 101	u(ft/sec) Station 2 Run No. 102	u(ft/sec) Station 2 Run No. 103	u(ft/sec) Station 3 Run No. 101
0.000	0.000	0.000	0.000	0.000	0.000	0.000
0.005	0.226	0.213	0.192	0.192	0.241	0.218
0.010	0.438	0.443	0.392	0.392	0.418	0.405
0.020	0.944	0.970	0.888	0.888	0.857	0.800
0.030	1.033	1.031	0.967	1.005	0.973	1.031
0.050	1.116	1.102	1.046	1.071	1.071	1.110
0.100	1.227	1.223	1.157	1.184	1.175	1.240
0.200	1.332	1.333	1.286	1.331	1.311	1.358
0.300	1.408	1.414	1.370	1.404	1.397	1.423
0.400	1.454	1.459	1.430	1.456	1.456	1.471
0.500	1.485	1.497	1.471	1.492	1.499	1.510
0.600	1.513	1.524	1.499	1.524	1.527	1.537
0.700	1.534	1.547	1.524	1.544	1.548	1.558
0.800	1.547	1.563	1.541	1.561	1.568	1.578
0.900	1.556	1.566	1.554	1.575	1.578	1.588
1.000	1.562	1.575	1.561	1.581	1.585	1.598
1.100	-----	-----	1.561	1.588	1.588	1.605
1.200	-----	-----	-----	-----	-----	1.608
1.300	-----	-----	-----	-----	-----	-----
1.400	-----	-----	-----	-----	-----	-----

(continued)

Table 3. (Continued)

y (inches)	u(ft/sec) Station 5 Run No. 101	u(ft/sec) Station 6 Run No. 101	u(ft/sec) Station 6 Run No. 102	u(ft/sec) Station 6 Run No. 103	u(ft/sec) Station 8 Run No. 101	u(ft/sec) Station 8 Run No. 102
0.000	0.000	0.000	0.000	0.000	0.000	0.000
0.005	0.241	0.163	0.300	0.073	0.241	0.218
0.010	0.519	0.349	0.604	0.262	0.466	0.454
0.020	0.967	0.723	0.793	0.509	0.899	0.701
0.030	1.041	0.945	0.888	0.813	0.984	0.934
0.050	1.129	1.041	1.000	1.056	1.086	1.021
0.100	1.240	1.170	1.170	1.197	1.206	1.170
0.200	1.347	1.319	1.343	1.323	1.319	1.335
0.300	1.408	1.404	1.419	1.401	1.397	1.430
0.400	1.456	1.460	1.471	1.460	1.456	1.495
0.500	1.488	1.503	1.510	1.503	1.503	1.544
0.600	1.517	1.541	1.541	1.537	1.537	1.581
0.700	1.541	1.568	1.565	1.568	1.571	1.608
0.800	1.561	1.605	1.585	1.588	1.595	1.634
0.900	1.571	1.605	1.605	1.605	1.618	1.653
1.000	1.581	1.618	1.624	1.618	1.637	1.669
1.100	1.591	1.631	1.640	1.631	1.653	1.679
1.200	1.598	1.640	1.644	1.640	1.660	1.688
1.300	1.601	1.647	1.650	1.644	1.669	1.691
1.400	-----	1.650	1.650	1.650	1.669	1.698

Table 4. Experimental Velocity Data
Injected Fluid: Water
Injection Rate: 537.0 mls/min
Concentration: -- ppm

y (inches)	u(ft/sec) Station 2 Run No. 104	u(ft/sec) Station 6 Run No. 104	u(ft/sec) Station 8 Run No. 104	u(ft/sec) Station 8 Run No. 105	u(ft/sec) Station 8 Run No. 106
0.000	0.000	0.000	0.000	0.000	0.000
0.005	0.192	0.126	0.192	0.163	0.192
0.010	0.430	0.317	0.405	0.405	0.405
0.020	0.911	0.899	0.899	0.940	0.870
0.030	1.021	0.994	1.066	1.010	1.000
0.050	1.110	1.105	1.138	1.100	1.110
0.100	1.219	1.240	1.228	1.219	1.232
0.200	1.339	1.370	1.339	1.343	1.354
0.300	1.412	1.445	1.416	1.423	1.430
0.400	1.460	1.499	1.481	1.481	1.488
0.500	1.495	1.541	1.537	1.524	1.534
0.600	1.524	1.575	1.571	1.558	1.568
0.700	1.544	1.601	1.601	1.585	1.591
0.800	1.558	1.618	1.621	1.608	1.614
0.900	1.568	1.634	1.640	1.624	1.628
1.000	1.571	1.644	1.650	1.640	1.644
1.100	1.571	1.653	1.660	1.650	1.657
1.200	-----	1.660	1.666	1.660	1.666
1.300	-----	1.666	1.669	1.669	1.672
1.400	-----	-----	1.672	1.669	1.676

Table 5. Experimental Velocity Data
Injected Fluid: Aqueous Solution of Polyethylene Oxide
Injection Rate: 60.0 mls/min
Concentration: 50.0 ppm

y (inches)	u(ft/sec) Station 2 Run No. 107	u(ft/sec) Station 2 Run No. 108	u(ft/sec) Station 6 Run No. 107	u(ft/sec) Station 6 Run No. 108	u(ft/sec) Station 8 Run No. 107
0.000	0.000	0.000	0.000	0.000	0.000
0.005	0.103	0.192	0.218	0.163	0.317
0.010	0.325	0.392	0.405	0.405	0.529
0.020	0.797	0.819	0.911	0.894	0.940
0.030	0.965	0.934	1.000	0.962	1.021
0.050	1.079	1.061	1.100	1.051	1.100
0.100	1.208	1.188	1.232	1.188	1.210
0.200	1.329	1.303	1.358	1.351	1.331
0.300	1.399	1.370	1.438	1.427	1.412
0.400	1.451	1.427	1.499	1.481	1.478
0.500	1.490	1.471	1.541	1.524	1.524
0.600	1.525	1.506	1.571	1.554	1.561
0.700	1.556	1.527	1.595	1.581	1.588
0.800	1.576	1.548	1.611	1.601	1.611
0.900	1.586	1.561	1.628	1.621	1.631
1.000	1.596	1.568	1.637	1.628	1.644
1.100	1.603	1.571	1.640	1.640	1.657
1.200	-----	-----	1.644	1.644	1.663
1.300	-----	-----	1.647	1.650	1.669
1.400	-----	-----	-----	-----	-----

Table 6. Experimental Velocity Data
Injected Fluid: Aqueous Solution of Polyethylene Oxide
Injection Rate: 134.0 mls/min
Concentration: 50.0 ppm

y (inches)	u(ft/sec) Station 2 Run No. 109	u(ft/sec) Station 2 Run No. 110	u(ft/sec) Station 3 Run No. 109	u(ft/sec) Station 3 Run No. 110	u(ft/sec) Station 5 Run No. 109	u(ft/sec) Station 5 Run No. 110
0.000	0.000	0.000	0.000	0.000	0.000	0.000
0.005	0.192	0.192	0.364	0.262	0.430	0.262
0.010	0.364	0.418	0.646	0.509	0.701	0.509
0.020	0.752	0.813	1.041	1.026	0.899	1.010
0.030	0.951	1.031	1.091	1.115	1.086	1.071
0.050	1.051	1.100	1.170	1.179	1.215	1.129
0.100	1.161	1.201	1.295	1.286	1.299	1.253
0.200	1.311	1.343	1.423	1.408	1.393	1.347
0.300	1.389	1.427	1.495	1.478	1.471	1.419
0.400	1.411	1.481	1.530	1.527	1.527	1.481
0.500	1.481	1.517	1.554	1.558	1.571	1.517
0.600	1.510	1.541	1.581	1.581	1.605	1.551
0.700	1.530	1.561	1.601	1.601	1.631	1.575
0.800	1.548	1.575	1.618	1.611	1.660	1.601
0.900	1.561	1.585	1.631	1.624	1.672	1.611
1.000	1.568	1.588	1.640	1.628	1.676	1.621
1.100	1.571	1.591	1.640	1.631	1.679	1.631
1.200	-----	-----	1.640	1.634	1.679	1.631
1.300	-----	-----	-----	-----	-----	-----
1.400	-----	-----	-----	-----	-----	-----

(continued)

Table 6. (Continued)

y (inches)	u(ft/sec) Station 6 Run No. 109	u(ft/sec) Station 6 Run No. 110	u(ft/sec) Station 6 Run No. 111	u(ft/sec) Station 6 Run No. 112	u(ft/sec) Station 8 Run No. 109	u(ft/sec) Station 8 Run No. 110
0.000	0.000	0.000	0.000	0.000	0.000	0.000
0.005	0.364	0.192	0.241	0.262	0.241	0.241
0.010	0.604	0.430	0.454	0.509	0.466	0.430
0.020	0.984	0.832	0.899	0.934	0.911	0.773
0.030	1.041	0.989	1.010	1.010	1.010	1.010
0.050	1.124	1.081	1.091	1.100	1.100	1.081
0.100	1.232	1.215	1.219	1.206	1.201	1.197
0.200	1.362	1.331	1.339	1.347	1.311	1.319
0.300	1.460	1.419	1.412	1.438	1.389	1.423
0.400	1.506	1.474	1.471	1.506	1.449	1.499
0.500	1.548	1.524	1.510	1.548	1.499	1.548
0.600	1.571	1.551	1.544	1.571	1.534	1.575
0.700	1.608	1.578	1.571	1.591	1.565	1.595
0.800	1.624	1.591	1.595	1.614	1.535	1.618
0.900	1.644	1.605	1.611	1.628	1.601	1.637
1.000	1.657	1.611	1.621	1.637	1.614	1.657
1.100	1.672	1.614	1.631	1.650	1.624	1.660
1.200	1.679	1.624	1.640	1.653	1.631	1.663
1.300	-----	-----	-----	-----	1.640	1.666
1.400	-----	-----	-----	-----	-----	-----

(continued)

Table 6. (Continued)

y (inches)	u(ft/sec) Station 8 Run No. 111	u(ft/sec) Station 8 Run No. 112
0.000	0.000	0.000
0.005	0.262	0.192
0.010	0.498	0.454
0.020	0.899	0.851
0.030	0.989	1.000
0.050	1.076	1.091
0.100	1.201	1.197
0.200	1.323	1.339
0.300	1.401	1.441
0.400	1.463	1.510
0.500	1.520	1.558
0.600	1.568	1.591
0.700	1.591	1.621
0.800	1.608	1.640
0.900	1.631	1.660
1.000	1.647	1.669
1.100	1.650	1.676
1.200	1.653	1.676
1.300	1.660	1.676
1.400	-----	-----

Table 7. Experimental Velocity Data
Injected Fluid: Aqueous Solution of Polyethylene Oxide
Injection Rate: 268.0 mls/min
Concentration: 50.0 ppm

y (inches)	u(ft/sec) Station 2 Run No. 114	u(ft/sec) Station 6 Run No. 114	u(ft/sec) Station 8 Run No. 114	u(ft/sec) Station 8 Run No. 115
0.000	0.000	0.000	0.000	0.000
0.005	0.218	0.163	0.349	0.333
0.010	0.405	0.333	0.773	0.793
0.020	0.832	0.549	0.894	0.945
0.030	0.967	0.752	1.021	1.051
0.050	1.051	0.951	1.110	1.138
0.100	1.179	1.091	1.210	1.232
0.200	1.339	1.262	1.323	1.343
0.300	1.412	1.362	1.404	1.427
0.400	1.463	1.430	1.471	1.488
0.500	1.510	1.471	1.520	1.534
0.600	1.537	1.503	1.554	1.571
0.700	1.561	1.530	1.591	1.588
0.800	1.578	1.551	1.621	1.614
0.900	1.588	1.568	1.637	1.637
1.000	1.598	1.578	1.653	1.640
1.100	1.601	1.585	1.663	1.657
1.200	-----	1.591	1.666	1.660
1.300	-----	1.595	1.666	1.666
1.400	-----	-----	-----	-----

Table 8. Experimental Velocity Data
Injected Fluid: Aqueous Solution of Polyethylene Oxide
Injection Rate: 537.0 mls/min
Concentration: 50.0 ppm

y (inches)	u(ft/sec) Station 2 Run No. 116	u(ft/sec) Station 2 Run No. 117	u(ft/sec) Station 2 Run No. 118	u(ft/sec) Station 3 Run No. 116	u(ft/sec) Station 3 Run No. 117	u(ft/sec) Station 5 Run No. 116
0.000	0.000	0.000	0.000	0.000	0.000	0.000
0.005	0.192	0.405	0.405	0.405	0.442	0.333
0.010	0.405	0.723	0.738	0.646	0.694	0.701
0.020	0.752	0.967	0.940	1.010	1.000	0.928
0.030	0.928	1.010	1.036	1.071	1.056	1.061
0.050	1.041	1.081	1.105	1.143	1.129	1.175
0.100	1.170	1.188	1.219	1.249	1.232	1.286
0.200	1.307	1.331	1.358	1.382	1.362	1.416
0.300	1.382	1.419	1.449	1.452	1.434	1.485
0.400	1.430	1.471	1.503	1.499	1.481	1.537
0.500	1.463	1.506	1.541	1.537	1.520	1.571
0.600	1.495	1.530	1.568	1.568	1.548	1.601
0.700	1.520	1.554	1.591	1.588	1.568	1.618
0.800	1.534	1.571	1.608	1.601	1.581	1.637
0.900	1.551	1.585	1.621	1.611	1.591	1.647
1.000	1.561	1.591	1.628	1.621	1.601	1.657
1.100	1.565	1.598	1.634	1.628	1.608	1.663
1.200	-----	-----	-----	1.634	1.614	1.669
1.300	-----	-----	-----	-----	-----	-----
1.400	-----	-----	-----	-----	-----	-----

(continued)

Table 8. (Continued)

y (inches)	u(ft/sec) Station 5 Run No. 117	u(ft/sec) Station 6 Run No. 116	u(ft/sec) Station 6 Run No. 117	u(ft/sec) Station 6 Run No. 118	u(ft/sec) Station 8 Run No. 116	u(ft/sec) Station 8 Run No. 117
0.000	0.000	0.000	0.000	0.000	0.000	0.000
0.005	0.073	0.454	0.163	0.192	0.364	0.126
0.010	0.192	0.723	0.349	0.349	0.678	0.317
0.020	0.851	0.882	0.888	0.654	0.967	0.731
0.030	0.978	0.989	0.967	0.857	1.021	0.994
0.050	1.138	1.100	1.061	1.000	1.100	1.100
0.100	1.266	1.206	1.188	1.179	1.201	1.240
0.200	1.401	1.339	1.319	1.323	1.319	1.370
0.300	1.471	1.430	1.404	1.416	1.412	1.449
0.400	1.520	1.488	1.467	1.478	1.478	1.506
0.500	1.554	1.534	1.510	1.517	1.527	1.551
0.600	1.585	1.568	1.544	1.554	1.568	1.585
0.700	1.611	1.598	1.571	1.578	1.595	1.608
0.800	1.631	1.618	1.591	1.601	1.618	1.628
0.900	1.644	1.631	1.608	1.618	1.637	1.644
1.000	1.657	1.647	1.618	1.628	1.650	1.657
1.100	1.666	1.657	1.628	1.637	1.657	1.663
1.200	1.669	1.660	1.637	1.650	1.663	1.669
1.300	-----	1.666	1.640	1.650	1.669	1.679
1.400	-----	-----	-----	-----	-----	-----

(continued)

Table 8. (Continued)

y (inches)	u(ft/sec) Station 8 Run No. 118	u(ft/sec) Station 8 Run No. 119	u(ft/sec) Station 8 Run No. 120
0.000	0.000	0.000	0.000
0.005	0.163	0.192	0.300
0.010	0.349	0.454	0.509
0.020	0.752	0.967	0.978
0.030	0.951	1.041	1.026
0.050	1.051	1.129	1.086
0.100	1.201	1.232	1.201
0.200	1.351	1.354	1.323
0.300	1.430	1.434	1.412
0.400	1.488	1.499	1.471
0.500	1.541	1.548	1.520
0.600	1.591	1.591	1.558
0.700	1.621	1.618	1.588
0.800	1.640	1.640	1.611
0.900	1.660	1.657	1.631
1.000	1.669	1.669	1.644
1.100	1.679	1.676	1.650
1.200	1.679	1.679	1.660
1.300	1.682	1.682	1.663
1.400	-----	-----	-----

Table 9. Experimental Velocity Data
Injected Fluid: Aqueous Solutions of Polyethylene Oxide
Injection Rate: Indicated
Concentration: Indicated

y (inches)	u(ft/sec) Station 6 Run No. 121 134.0 @ 150.0*	u(ft/sec) Station 6 Run No. 122 134.0 @ 150.0	u(ft/sec) Station 6 Run No. 123 134.0 @ 150.0	u(ft/sec) Station 8 Run No. 124 134.0 @ 25.0	u(ft/sec) Station 8 Run No. 125 537.0 @ 25.0	u(ft/sec) Station 8 Run No. 126 537.0 @ 25.0
0.000	0.000	0.000	0.000	0.000	0.000	0.000
0.005	0.241	0.241	0.282	0.300	0.192	0.163
0.010	0.498	0.454	0.509	0.488	0.378	0.378
0.020	0.923	0.940	0.905	-----	0.928	0.813
0.030	1.000	1.051	0.989	1.041	1.010	0.994
0.050	1.100	1.110	1.091	1.138	1.110	1.076
0.100	1.219	1.201	1.223	1.249	1.219	1.197
0.200	1.358	1.327	1.358	1.370	1.347	1.339
0.300	1.441	1.412	1.438	1.452	1.438	1.423
0.400	1.495	1.471	1.488	1.517	1.499	1.485
0.500	1.534	1.513	1.530	1.561	1.541	1.530
0.600	1.565	1.548	1.561	1.598	1.575	1.568
0.700	1.591	1.571	1.585	1.624	1.601	1.598
0.800	1.611	1.591	1.605	1.647	1.621	1.618
0.900	1.628	1.608	1.621	1.663	1.637	1.631
1.000	1.637	1.618	1.631	1.672	1.650	1.644
1.100	1.640	1.628	1.640	1.682	1.657	1.650
1.200	1.650	1.637	1.647	1.688	1.660	1.657
1.300	1.653	1.640	1.650	1.691	1.663	1.660
1.400	1.657	1.644	1.657	1.698	1.669	1.666

* 134.0 mls/min at a concentration of 150.0 ppm.

APPENDIX C

EFFECT OF INJECTIONS ON THE TURBULENT BOUNDARY-LAYER PARAMETERS AND SKIN FRICTION

This appendix presents the effects on the turbulent boundary-layer parameters produced by homogeneous injections of water and aqueous solutions of polyethylene oxide. Tables 10 through 14 list the Effects of Injections on the Boundary-Layer Thickness. The Effects on the Momentum Deficit in the Boundary Layer are given in Tables 15 through 19. Tables 20 through 24 present the Effects on Skin Friction. The Effect of Injection on the Shear-Stress Distributions at Station 6 are shown in Tables 25 through 29. Table 30 lists values of the Non-Dimensional Skin Friction as a Function of the Injection Parameter. Finally, Table 31 presents the Concentration of Polyethylene Oxide in the Transpired Boundary Layer.

Table 10. Effect of Injections on the Velocity Boundary-Layer Thickness
Injected Fluid: None
Injection Rate: -- mls/min
Concentration: -- ppm

Station	Run No.	Experimental Boundary-Layer Thickness (inches)	Average Boundary-Layer Thickness (inches)	Deviation (inches)	Deviation (percent)
1	101	1.000	0.800	+0.200	+25.0
1	102	0.907	0.800	+0.107	+13.4
1	*	0.865	0.800	+0.065	+8.1
1	*	0.844	0.800	+0.044	+5.5
1	*	0.740	0.800	-0.060	-7.5
2	101	0.855	0.875	-0.020	-2.3
2	102	0.906	0.875	+0.031	+3.5
2	103	0.872	0.875	-0.003	-0.3
3	101	0.968	0.950	+0.018	+1.9
3	*	0.836	0.950	-0.114	-12.0
5	101	1.096	1.085	+0.011	+1.0
5	*	0.989	1.085	-0.096	-8.8
6	101	1.128	1.155	-0.027	-2.3
6	102	1.057	1.155	-0.098	-8.5
6	103	1.128	1.155	-0.027	-2.3
6	*	1.064	1.155	-0.091	-7.9
8	101	1.093	1.265	-0.172	-13.6
8	102	1.124	1.265	-0.141	-11.1
8	*	1.141	1.265	-0.124	-9.8

* Partial velocity profile which is not listed in Appendix B.

Table 11. Effect of Injections on the Velocity Boundary-Layer Thickness
Injected Fluid: Water
Injection Rate: 537.0 mls/min
Concentration: -- ppm

Station	Run No.	Experimental Boundary-Layer Thickness (inches)	Average Boundary-Layer Thickness (inches)	Deviation (inches)	Deviation (percent)
2	104	0.779	0.875	-0.096	-11.0
6	104	1.092	1.092	+0.000	+0.0
8	104	1.056	1.124	-0.068	-6.0
8	105	1.124	1.124	+0.000	+0.0
8	106	1.124	1.124	+0.000	+0.0

Table 12. Effect of Injections on the Velocity Boundary-Layer Thickness
Injected Fluid: Aqueous Solution of Polyethylene Oxide
Injection Rate: 60.0 mls/min
Concentration: 50.0 ppm

Station	Run No.	Experimental Boundary-Layer Thickness (inches)	Average Boundary-Layer Thickness (inches)	Deviation (inches)	Deviation (percent)
2	107	0.972	0.887	+0.085	+9.6
2	108	0.959	0.887	+0.072	+8.1
6	107	0.960	1.043	-0.083	-8.0
6	108	1.045	1.043	+0.002	+0.2
8	107	1.068	1.070	-0.002	-0.2

Table 13. Effect of Injections on the Velocity Boundary-Layer Thickness
Injected Fluid: Aqueous Solution of Polyethylene Oxide
Injection Rate: 134.0 mls/min
Concentration: 50.0 ppm

Station	Run No.	Experimental Boundary-Layer Thickness (inches)	Average Boundary-Layer Thickness (inches)	Deviation (inches)	Deviation (percent)
2	109	0.840	0.860	-0.020	-2.3
2	110	0.879	0.860	+0.019	+2.2
3	109	0.852	0.910	-0.058	-6.4
3	110	0.852	0.910	-0.058	-6.4
5	109	0.822	0.972	-0.150	-15.4
5	110	0.932	0.972	-0.040	-4.1
6	109	1.036	0.990	+0.046	+4.6
6	110	1.128	0.990	+0.138	+13.9
6	111	1.128	0.990	+0.138	+13.9
6	112	1.021	0.990	+0.031	+3.1
8	109	1.134	1.017	+0.117	+11.5
8	110	0.978	1.017	-0.039	-3.8
8	111	0.974	1.017	-0.043	-4.2
8	112	0.894	1.017	-0.123	-12.1
8	*	0.968	1.017	-0.049	-4.8
8	*	1.024	1.017	+0.007	+0.7

* Partial velocity profile which is not listed in Appendix B.

Table 14. Effect of Injections on the Velocity Boundary-Layer Thickness
Injected Fluid: Aqueous Solution of Polyethylene Oxide
Injection Rate: 537.0 mls/min
Concentration: 50.0 ppm

Station	Run No.	Experimental Boundary-Layer Thickness (inches)	Average Boundary-Layer Thickness (inches)	Deviation (inches)	Deviation (percent)
2	116	0.940	0.872	+0.068	+7.8
2	117	0.906	0.872	+0.034	+3.9
2	118	0.906	0.872	+0.034	+3.9
2	*	0.840	0.872	-0.032	-3.7
2	*	0.906	0.872	+0.034	+3.9
3	116	1.053	0.922	+0.131	+14.2
3	117	1.053	0.922	+0.131	+14.2
5	116	1.047	0.990	+0.051	+5.1
5	117	1.184	0.990	+0.194	+19.6
5	*	1.048	0.990	+0.058	+5.9
6	116	1.028	1.010	+0.018	+1.8
6	117	1.060	1.010	+0.050	+4.9
6	118	1.060	1.010	+0.050	+4.9
6	*	0.938	1.010	-0.072	-7.1
6	*	0.938	1.010	-0.072	-7.1
8	116	1.035	1.035	+0.000	+0.0
8	117	1.082	1.035	+0.047	+4.5
8	118	0.956	1.035	-0.079	-7.6
8	119	1.082	1.035	+0.047	+4.5
8	120	1.083	1.035	+0.048	+4.6
8	*	0.942	1.035	-0.093	-9.0

* Partial velocity profile which is not listed in Appendix B.

Table 15. Effect of Injections on the Momentum Deficit* in the Boundary Layer
Injected Fluid: None
Injection Rate: -- mls/min
Concentration: -- ppm

Station	Run No.	Experimental Momentum Deficit (lbf/ft)	Average Momentum Deficit (lbf/ft)	Deviation (lbf/ft)	(percent)
1	101	0.03230	0.03000	+0.00230	+7.7
1	102	0.02996	0.03000	-0.00004	-0.1
2	101	0.03104	0.03250	-0.00146	-4.5
2	102	0.03168	0.03250	-0.00082	-2.5
2	103	0.03200	0.03250	-0.00050	-1.5
3	101	0.03244	0.03510	-0.00266	-7.6
5	101	0.03634	0.04020	-0.00386	-9.6
6	101	0.04410	0.04280	+0.00130	+3.0
6	102	0.04282	0.04280	+0.00002	+0.0
6	103	0.04370	0.04280	+0.00090	+2.1
8	101	0.04700	0.04800	-0.00100	-2.1
8	102	0.04690	0.04800	-0.00110	-2.3

* The momentum deficit is $\int_0^{\delta} \frac{\rho u(u_\infty - u)}{g_c}\, dy$.

Table 16. Effect of* Injections on the Momentum Deficit in the Boundary Layer
Injected Fluid: Water
Injection Rate: 537.0 mls/min
Concentration: -- ppm

Station	Run No.	Experimental Momentum Deficit (lbf/ft)	Average Momentum Deficit (lbf/ft)	Deviation (lbf/ft)	(percent)
2	104	0.02720	0.02820	-0.00100	-3.5
6	104	0.03950	0.03860	+0.00090	+2.3
8	104	0.04217	0.04363	-0.00146	-3.3
8	105	0.04355	0.04363	-0.00008	-0.2
8	106	0.04348	0.04363	-0.00015	-0.3

* The momentum deficit is $\int_0^{\delta} \frac{\rho u(u_\infty - u)}{g_c}\, dy$.

Table 17. Effect of* Injections on the Momentum Deficit in the Boundary Layer
Injected Fluid: Aqueous Solution of Polyethylene Oxide
Injection Rate: 60.0 mls/min
Concentration: 50.0 ppm

Station	Run No.	Experimental Momentum Deficit (lbf/ft)	Average Momentum Deficit (lbf/ft)	Deviation (lbf/ft)	(percent)
2	107	0.03410	0.03200	+0.00210	+6.6
2	108	0.03206	0.03200	+0.00006	+0.2
6	107	0.03740	0.03980	-0.00240	-6.0
6	108	0.03966	0.03980	-0.00014	-0.4
8	107	0.04380	0.04380	+0.00000	+0.0

* The momentum deficit is $\int_0^{\delta} \frac{\rho u(u_\infty - u)}{g_c}\, dy$.

Table 18. Effect of* Injections on the Momentum Deficit in the Boundary Layer
Injected Fluid: Aqueous Solution of Polyethylene Oxide
Injection Rate: 134.0 mls/min
Concentration: 50.0 ppm

Station	Run No.	Experimental Momentum Deficit (lbf/ft)	Average Momentum Deficit (lbf/ft)	Deviation (lbf/ft)	(percent)
2	109	0.02918	0.03160	-0.00242	-7.7
2	110	0.02980	0.03160	-0.00180	-5.7
3	109	0.02814	0.03320	-0.00506	-15.2
3	110	0.02789	0.03320	-0.00531	-16.0
5	109	0.03480	0.03620	-0.00140	-3.9
5	110	0.03446	0.03620	-0.00174	-4.8
6	109	0.04010	0.03780	+0.00230	+6.1
6	110	0.03740	0.03780	-0.00040	-1.1
6	111	0.04000	0.03780	+0.00220	+5.8
6	112	0.03740	0.03780	-0.00040	-1.1
8	109	0.04206	0.04100	+0.00106	+2.6
8	110	0.03996	0.04100	-0.00104	-2.5
8	111	0.04098	0.04100	-0.00002	-0.0
8	112	0.03980	0.04100	-0.00120	-2.9

* The momentum deficit is $\int_0^{\delta} \frac{\rho u(u_\infty - u)}{g_c}\, dy$.

Table 19. Effect of* Injections on the Momentum Deficit in the Boundary Layer
Injected Fluid: Aqueous Solution of Polyethylene Oxide
Injection Rate: 537.0 mls/min
Concentration: 50.0 ppm

Station	Run No.	Experimental Momentum Deficit (lbf/ft)	Average Momentum Deficit (lbf/ft)	Deviation (lbf/ft)	(percent)
2	116	0.03180	0.03180	+0.00000	+0.0
2	117	0.03210	0.03180	+0.00030	+0.9
2	118	0.03352	0.03180	+0.00172	+5.4
3	116	0.03336	0.03380	-0.00044	-1.3
3	117	0.03328	0.03380	-0.00052	-1.5
5	116	0.03470	0.03740	-0.00270	-7.2
5	117	0.03880	0.03740	+0.00140	+3.7
6	116	0.04046	0.03940	+0.00106	+2.7
6	117	0.03974	0.03940	+0.00034	+0.9
6	118	0.04032	0.03940	+0.00092	+2.3
8	116	0.04390	0.04300	+0.00090	+2.1
8	117	0.04256	0.04300	-0.00044	-1.0
8	118	0.04120	0.04300	-0.00180	-4.2
8	119	0.04340	0.04300	+0.00040	+0.9
8	120	0.04388	0.04300	+0.00088	+2.0

* The momentum deficit is $\int_0^{\delta} \frac{\rho u(u_\infty - u)}{g_c}\, dy$.

Table 20. Effect of Injections on Skin Friction
Injected Fluid: None
Injection Rate: -- mls/min
Concentration: -- ppm

Station	Run No.	$\frac{d}{dx}\left[\int_0^\delta \frac{\rho u(u_\infty - u)}{g_c}\,dy\right]$ (lbf/ft^2)	$\frac{\rho_w v_w u_\infty}{g_c}$ (lbf/ft^2)	$\frac{\delta \rho_\infty u_\infty}{g_c}$ (lbf.sec/ft^2)	$\int_0^\delta \frac{\rho u}{g_c}\,dy$ (lbf.sec/ft^2)	$\frac{du_\infty}{dx}\left[\frac{\delta \rho_\infty u_\infty}{g_c} - \int_0^\delta \frac{\rho u}{g_c}\,dy\right]$ (lbf/ft^2)	τ_w (lbf/ft^2)
1	101	0.005143	0	0.2044	0.1935	0.000318	0.005461
1	102	0.005143	0	0.2044	0.1870	0.000507	0.005650
2	101	0.005143	0	0.2257	0.1941	0.000921	0.006064
2	102	0.005143	0	0.2257	0.2008	0.000726	0.005869
2	103	0.005143	0	0.2257	0.2004	0.000737	0.005880
3	101	0.005143	0	0.2473	0.2230	0.000680	0.005823
5	101	0.005143	0	0.2870	0.2551	0.000793	0.005936
6	101	0.005143	0	0.3078	0.2724	0.000799	0.005942
6	102	0.005143	0	0.3078	0.2740	0.000763	0.005906
6	103	0.005143	0	0.3078	0.2731	0.000783	0.005926
8	101	0.005143	0	0.3412	0.3048	0.000687	0.005830
8	102	0.005143	0	0.3412	0.3093	0.000602	0.005745

Table 21. *Effect of Injections on Skin Friction*
Injected Fluid: Water
Injection Rate: 537.0 mls/min
Concentration: -- ppm

Station	Run No.	$\frac{d}{dx}\left[\int_0^\delta \frac{\rho u(u_\infty - u)}{g_c}\, dy\right]$ (lbf/ft^2)	$\frac{\rho_w v_w u_\infty}{g_c}$ (lbf/ft^2)	$\frac{\delta \rho_\infty u_\infty}{g_c}$ (lbf.sec/ft^2)	$\int_0^\delta \frac{\rho u}{g_c}\, dy$ (lbf.sec/ft^2)	$\frac{du_\infty}{dx}\left[\frac{\delta \rho_\infty u_\infty}{g_c} - \int_0^\delta \frac{\rho u}{g_c}\, dy\right]$ (lbf/ft^2)	τ_w (lbf/ft^2)
2	104	0.05143	0.000279	0.2257	0.1990	0.000778	0.005642
6	104	0.05143	0.000289	0.2910	0.2622	0.000650	0.005504
8	104	0.05143	0.000292	0.3032	0.2681	0.000662	0.005513
8	105	0.05143	0.000292	0.3032	0.2696	0.000634	0.005485
8	106	0.05143	0.000292	0.3032	0.2698	0.000630	0.005481

Table 22. Effect of Injections on Skin Friction
Injected Fluid: Aqueous Solution of Polyethylene Oxide
Injection Rate: 60.0 mls/min
Concentration: 50.0 ppm

Station	Run No.	$\frac{d}{dx}\left[\int_0^\delta \frac{\rho u(u_\infty - u)}{g_c}\, dy\right]$ (lbf/ft^2)	$\frac{\rho_w v_w u_\infty}{g_c}$ (lbf/ft^2)	$\frac{\delta \rho_\infty u_\infty}{g_c}$ (lbf.sec/ft^2)	$\int_0^\delta \frac{\rho u}{g_c}\, dy$ (lbf.sec/ft^2)	$\frac{du_\infty}{dx}\left[\frac{\delta \rho_\infty u_\infty}{g_c} - \int_0^\delta \frac{\rho u}{g_c}\, dy\right]$ (lbf/ft^2)	τ_w (lbf/ft^2)
2	107	0.003914	0.000031	0.2288	0.2045	0.000708	0.004591
2	108	0.003914	0.000031	0.2288	0.2007	0.000819	0.004702
6	107	0.003914	0.000032	0.2779	0.2507	0.000614	0.004496
6	108	0.003914	0.000032	0.2779	0.2479	0.000677	0.004559
8	107	0.003914	0.000033	0.2886	0.2560	0.000615	0.004496

Table 23. Effect of Injections on Skin Friction
Injected Fluid: Aqueous Solution of Polyethylene Oxide
Injection Rate: 134.0 mls/min
Concentration: 50.0 ppm

Station	Run No.	$\frac{d}{dx}\left[\int_0^\delta \frac{\rho u(u_\infty - u)}{g_c}\, dy\right]$ (lbf/ft^2)	$\frac{\rho_w v_w u_\infty}{g_c}$ (lbf/ft^2)	$\frac{\delta \rho_\infty u_\infty}{g_c}$ (lbf.sec/ft^2)	$\int_0^\delta \frac{\rho u}{g_c}\, dy$ (lbf.sec/ft^2)	$\frac{du_\infty}{dx}\left[\frac{\delta \rho_\infty u_\infty}{g_c} - \int_0^\delta \frac{\rho u}{g_c}\, dy\right]$ (lbf/ft^2)	τ_w (lbf/ft^2)
2	109	0.003143	0.000070	0.2218	0.1994	0.000653	0.003726
2	110	0.003143	0.000070	0.2218	0.1900	0.000927	0.004000
3	109	0.003143	0.000070	0.2369	0.2212	0.000440	0.003513
3	110	0.003143	0.000070	0.2369	0.2205	0.000459	0.003532
5	109	0.003143	0.000072	0.2571	0.2370	0.000500	0.003571
5	110	0.003143	0.000072	0.2571	0.2311	0.000646	0.003717
6	109	0.003143	0.000072	0.2638	0.2391	0.000557	0.003628
6	110	0.003143	0.000072	0.2638	0.2336	0.000682	0.003753
6	111	0.003143	0.000072	0.2638	0.2337	0.000679	0.003750
6	112	0.003143	0.000072	0.2638	0.2370	0.000605	0.003676
8	109	0.003143	0.000073	0.2743	0.2385	0.000675	0.003745
8	110	0.003143	0.000073	0.2743	0.2430	0.000590	0.003660
8	111	0.003143	0.000073	0.2743	0.2414	0.000620	0.003690
8	112	0.003143	0.000073	0.2743	0.2457	0.000539	0.003609

Table 24. Effect of Injections on Skin Friction
Injected Fluid: Aqueous Solution of Polyethylene Oxide
Injection Rate: 537.0 mls/min
Concentration: 50.0 ppm

Station	Run No.	$\frac{d}{dx}\left[\int_0^\delta \frac{\rho u(u_\infty - u)}{g_c}\,dy\right]$ (lbf/ft^2)	$\frac{\rho_w v_w u_\infty}{g_c}$ (lbf/ft^2)	$\frac{\delta \rho_\infty u_\infty}{g_c}$ (lbf.sec/ft^2)	$\int_0^\delta \frac{\rho u}{g_c}\,dy$ (lbf.sec/ft^2)	$\frac{du_\infty}{dx}\left[\frac{\delta \rho_\infty u_\infty}{g_c} - \int_0^\delta \frac{\rho u}{g_c}\,dy\right]$ (lbf/ft^2)	τ_w (lbf/ft^2)
2	116	0.003714	0.000279	0.2249	0.1960	0.000842	0.004277
2	117	0.003714	0.000279	0.2249	0.2017	0.000676	0.004111
2	118	0.003714	0.000279	0.2249	0.2062	0.000545	0.003980
3	116	0.003714	0.000282	0.2415	0.2204	0.000591	0.004023
3	117	0.003714	0.000282	0.2415	0.2177	0.000666	0.004098
5	116	0.003714	0.000287	0.2619	0.2414	0.000510	0.003937
5	117	0.003714	0.000287	0.2619	0.2404	0.000534	0.003961
6	116	0.003714	0.000289	0.2691	0.2415	0.000623	0.004048
6	117	0.003714	0.000289	0.2691	0.2374	0.000715	0.004140
6	118	0.003714	0.000289	0.2691	0.2371	0.000722	0.004147
8	116	0.003714	0.000292	0.2793	0.2474	0.000602	0.004024
8	117	0.003714	0.000292	0.2793	0.2482	0.000587	0.004009
8	118	0.003714	0.000292	0.2793	0.2491	0.000570	0.003992
8	119	0.003714	0.000292	0.2793	0.2482	0.000587	0.004009
8	120	0.003714	0.000292	0.2793	0.2465	0.000619	0.004041

Table 25. Effect of Injection on the Shear-Stress Distribution
Injected Fluid: None
Injection Rate: -- mls/min
Concentration: -- ppm
Station: 6

y (inches)	τ_w	$\frac{y\rho_\infty u_\infty}{g_c}\frac{du_\infty}{dx}$	$\frac{\rho_w v_w u}{g_c}$	$u\frac{d}{dx}\int_0^y \frac{\rho u}{g_c}\,dy$	$\frac{d}{dx}\int_0^y \frac{\rho u^2}{g_c}\,dy$	τ^* (lbf/ft^2)
0	5840×10^{-6}	0×10^{-6}	0×10^{-6}	0×10^{-6}	0×10^{-6}	0.005840
0.01	5840	60	0	0	0	0.005780
0.02	5840	120	0	0	0	0.005720
0.03	5840	180	0	0	0	0.005660
0.05	5840	301	0	0	0	0.005539
0.10	5840	601	0	0	0	0.005239
0.20	5840	1200	0	0	0	0.004640
0.30	5840	1800	0	0	0	0.004040
0.40	5840	2400	0	0	0	0.003440
0.50	5840	3010	0	0	0	0.002830
0.60	5840	3600	0	0	252	0.002492
0.70	5840	4210	0	355	510	0.001785
0.80	5840	4800	0	634	737	0.001143
0.90	5840	5413	0	835	1106	0.000698
1.00	5840	6000	0	1190	1540	0.000190
1.10	5840	6600	0	1586	2247	0
1.15	5840	----	-	----	----	0

* $$\tau = \tau_w - \frac{y\rho_\infty u_\infty}{g_c}\frac{du_\infty}{dx} + \frac{\rho_w v_w u}{g_c} - u\frac{d}{dx}\int_0^y \frac{\rho u}{g_c}\,dy + \frac{d}{dx}\int_0^y \frac{\rho u^2}{g_c}\,dy.$$

Table 26. Effect of Injection on the Shear-Stress Distribution
Injected Fluid: Water
Injection Rate: 537.0 mls/min
Concentration: -- ppm
Station: 6

y (inches)	τ_w	$\frac{y\rho_\infty u_\infty}{g_c}\frac{du_\infty}{dx}$	$\frac{\rho_w v_w u}{g_c}$	$u\frac{d}{dx}\int_0^y \frac{\rho u}{g_c}dy$	$\frac{d}{dx}\int_0^y \frac{\rho u^2}{g_c}dy$	τ^* (lbf/ft^2)
0	5504 x 10^{-6}	0 x 10^{-6}	0 x 10^{-6}	0 x 10^{-6}	0 x 10^{-6}	0.005504
0.01	5504	60	55	0	0	0.005499
0.02	5504	120	157	0	0	0.005541
0.03	5504	180	174	0	0	0.005498
0.05	5504	301	193	0	0	0.005396
0.10	5504	601	217	0	0	0.005120
0.20	5504	1200	240	0	0	0.004544
0.30	5504	1800	253	0	0	0.003957
0.40	5504	2400	262	0	0	0.003366
0.50	5504	3010	270	0	0	0.002764
0.60	5504	3600	276	0	0	0.002180
0.70	5504	4210	280	0	0	0.001574
0.80	5504	4800	283	0	0	0.000987
0.90	5504	5413	286	0	0	0.000377
1.00	5504	6000	288	0	0	0.000000
1.09	5504	----	---	-	-	0.000000

$$\tau^* = \tau_w - \frac{y\rho_\infty u_\infty}{g_c}\frac{du_\infty}{dx} + \frac{\rho_w v_w u}{g_c} - u\frac{d}{dx}\int_0^y \frac{\rho u}{g_c}dy + \frac{d}{dx}\int_0^y \frac{\rho u^2}{g_c}dy.$$

Table 27. Effect of Injection on the Shear-Stress Distribution
Injected Fluid: Aqueous Solution of Polyethylene Oxide
Injection Rate: 60.0 mls/min
Concentration: 50.0 ppm
Station: 6

y (inches)	τ_w	$\frac{y\rho_\infty u_\infty}{g_c}\frac{du_\infty}{dx}$	$\frac{\rho_w v_w u}{g_c}$	$u\frac{d}{dx}\int_0^y \frac{\rho u}{g_c}\,dy$	$\frac{d}{dx}\int_0^y \frac{\rho u^2}{g_c}\,dy$	τ^* (lbf/ft^2)
0	4550×10^{-6}	0×10^{-6}	0×10^{-6}	0×10^{-6}	0×10^{-6}	0.004550
0.01	4550	60	8	13	17	0.004502
0.02	4550	120	17	133	136	0.004450
0.03	4550	180	19	150	222	0.004461
0.05	4550	301	21	270	318	0.004318
0.10	4550	601	23	498	770	0.004244
0.20	4550	1200	26	730	1033	0.003679
0.30	4550	1800	28	713	1300	0.003365
0.40	4550	2400	29	998	1700	0.002881
0.50	4550	3010	30	590	1410	0.002390
0.60	4550	3600	30	1140	2080	0.001920
0.70	4550	4210	31	1130	2517	0.001558
0.80	4550	4800	31	2030	3266	0.001017
0.90	4550	5413	32	3400	4800	0.000569
1.04	4550	----	--	----	----	0

*
$$\tau = \tau_w - \frac{y\rho_\infty u_\infty}{g_c}\frac{du_\infty}{dx} + \frac{\rho_w v_w u}{g_c} - u\frac{d}{dx}\int_0^y \frac{\rho u}{g_c}\,dy + \frac{d}{dx}\int_0^y \frac{\rho u^2}{g_c}\,dy.$$

Table 28. Effect of Injection on the Shear-Stress Distribution
Injected Fluid: Aqueous Solution of Polyethylene Oxide
Injection Rate: 134.0 mls/min
Concentration: 50.0 ppm
Station: 6

y (inches)	τ_w	$\frac{y\rho_\infty u_\infty}{g_c}\frac{du_\infty}{dx}$	$\frac{\rho_w v_w u}{g_c}$	$u\frac{d}{dx}\int_0^y \frac{\rho u}{g_c}dy$	$\frac{d}{dx}\int_0^y \frac{\rho u^2}{g_c}dy$	τ^* (lbf/ft^2)
0	3680 x 10^{-6}	0 x 10^{-6}	0 x 10^{-6}	0 x 10^{-6}	0 x 10^{-6}	0.003680
0.01	3680	60	19	21	41	0.003659
0.02	3680	120	36	82	179	0.003693
0.03	3680	180	43	154	220	0.003609
0.05	3680	300	47	218	333	0.003541
0.10	3680	600	53	243	380	0.003269
0.20	3680	1200	58	641	963	0.002860
0.30	3680	1800	62	907	1433	0.002468
0.40	3680	2400	64	1190	1983	0.002137
0.50	3680	3010	67	1524	2633	0.001846
0.60	3680	3600	68	1940	3300	0.001508
0.70	3680	4210	69	2370	4000	0.001169
0.80	3680	4800	69	2920	4900	0.000929
0.90	3680	5410	70	3490	5400	0.000250
0.99	3680	----	--	----	----	0.000000

*
$$\tau = \tau_w - \frac{y\rho_\infty u_\infty}{g_c}\frac{du_\infty}{dx} + \frac{\rho_w v_w u}{g_c} - u\frac{d}{dx}\int_0^y \frac{\rho u}{g_c}dy + \frac{d}{dx}\int_0^y \frac{\rho u^2}{g_c}dy.$$

Table 29. Effect of Injection on the Shear-Stress Distribution
Injected Fluid: Aqueous Solution of Polyethylene Oxide
Injection Rate: 537.0 mls/min
Concentration: 50.0 ppm
Station: 6

y (inches)	τ_w	$\frac{y\rho_\infty u_\infty}{g_c}\frac{du_\infty}{dx}$	$\frac{\rho_w v_w u}{g_c}$	$u\frac{d}{dx}\int_0^y \frac{\rho u}{g_c}\,dy$	$\frac{d}{dx}\int_0^y \frac{\rho u^2}{g_c}\,dy$	τ^* (lbf/ft^2)
0	4030×10^{-6}	0×10^{-6}	0×10^{-6}	0×10^{-6}	0×10^{-6}	0.004030
0.01	4030	60	126	29	34	0.004101
0.02	4030	120	154	121	250	0.004193
0.03	4030	180	173	227	435	0.004231
0.05	4030	301	192	429	765	0.004257
0.10	4030	601	211	763	1305	0.004182
0.20	4030	1200	234	1319	2103	0.003848
0.30	4030	1800	250	1792	2803	0.003491
0.40	4030	2400	260	2281	3433	0.003042
0.50	4030	3010	268	2910	4100	0.002478
0.60	4030	3600	274	3272	4767	0.002199
0.70	4030	4210	279	4080	5501	0.001520
0.80	4030	4800	283	4676	6400	0.001237
0.90	4030	5413	285	5655	7467	0.000714
1.01	4030	----	---	----	----	0.000000

* $$\tau = \tau_w - \frac{y\rho_\infty u_\infty}{g_c}\frac{du_\infty}{dx} + \frac{\rho_w v_w u}{g_c} - u\frac{d}{dx}\int_0^y \frac{\rho u}{g_c}\,dy + \frac{d}{dx}\int_0^y \frac{\rho u^2}{g_c}\,dy.$$

Table 30. Non-Dimensional Skin Friction as a Function of the Injection Parameter

Station	Injection Rate (mls/min)	Concentration (ppm)	τ_w (lbf/ft^2)	$c_{f_o} = \frac{2\tau_{w_o} g_c}{\rho u_\infty^2}$	$\frac{\tau_w}{\tau_{w_o}}$	$\frac{\rho_w v_w}{\rho_\infty u_\infty}$	$\frac{2\rho_w v_w}{\rho_\infty u_\infty c_{f_o}}$
2	0	0	0.005890	0.002384	1.000	0	0
2	60.0	0	0.005859	--------	0.995	0.00000632	0.00530
2	134.0	0	0.005820	--------	0.988	0.00001411	0.01184
2	268.0	0	0.005750	--------	0.976	0.00002822	0.02367
2	537.0	0	0.005642	--------	0.958	0.00005654	0.04743
2	60.0	50.0	0.004650	--------	0.789	0.00000632	0.00530
2	134.0	50.0	0.003740	--------	0.635	0.00001411	0.01184
2	268.0	50.0	0.003899	--------	0.662	0.00002822	0.02367
2	537.0	50.0	0.004110	--------	0.698	0.00005654	0.04743
6	0	0	0.005840	0.002214	1.000	0	0
6	60.0	0	0.005808	--------	0.995	0.00000612	0.00553
6	134.0	0	0.005768	--------	0.988	0.00001366	0.01234
6	268.0	0	0.005696	--------	0.975	0.00002732	0.02468
6	537.0	0	0.005504	--------	0.942	0.00005472	0.04943
6	60.0	50.0	0.004550	--------	0.779	0.00000612	0.00553
6	134.0	50.0	0.003680	--------	0.630	0.00001366	0.01234
6	537.0	50.0	0.004030	--------	0.690	0.00005472	0.04943
8	0	0	0.005820	0.002154	1.000	0	0
8	60.0	0	0.005787	--------	0.995	0.00000604	0.00561
8	134.0	0	0.005747	--------	0.987	0.00001350	0.01253
8	268.0	0	0.005674	--------	0.975	0.00002700	0.02507
8	537.0	0	0.005485	--------	0.942	0.00005408	0.05021
8	60.0	50.0	0.004500	--------	0.773	0.00000604	0.00561
8	134.0	50.0	0.003650	--------	0.627	0.00001350	0.01253
8	268.0	50.0	0.003753	--------	0.645	0.00002700	0.02507
8	537.0	50.0	0.004000	--------	0.687	0.00005408	0.05021

Table 31. Concentrations of Polyethylene Oxide in the Transpired Turbulent Boundary Layer
Injected Fluid: Aqueous Solutions of Polyethylene Oxide
Injection Rate: Indicated
Concentration: 50.0 ppm

Injection Rate (mls/min)	y (inches)	Concentration, C (ppm)
60.0	0.001	2.3
	0.001	2.3
	0.005	1.0
	0.005	0.9
	0.020	0.1
	0.020	0.2
134.0	0.001	3.6
	0.001	3.8
	0.001	3.7
	0.001	3.7
	0.005	1.5
	0.005	1.4
	0.020	0.5
	0.020	0.4
537.0	0.002	6.0
	0.002	5.9
	0.005	2.7
	0.005	2.2
	0.005	1.7
	0.005	1.7
	0.005	2.4
	0.010	1.5
	0.010	1.1
	0.020	1.8
	0.020	1.7
	0.020	0.5

(continued)

Table 31. (Continued)

Injection Rate (mls/min)	y (inches)	Concentration, C (ppm)
537.0 (continued)	0.020	0.5
	0.020	1.4
	0.100	1.6
	0.200	1.3
	0.300	1.1
	0.400	1.3
	0.600	1.4
	0.800	1.2
	1.000	1.5

BIBLIOGRAPHY

1. Sproull, W. T., "Viscosity of Dusty Gases," Nature 190, 976-978 (June, 1961).

2. Elata, C. and A. T. Ippen, The Dynamics of Open Channel Flow with Suspensions of Neutrally Buoyant Particles, Technical Report No. 45, Hydrodynamics Laboratory, Massachusetts Institute of Technology (1961).

3. Daily, J. W. and T. K. Chu, Rigid Particle Suspensions in Turbulent Shear Flow, Technical Report No. 48, Hydrodynamics Laboratory, Massachusetts Institute of Technology (1961).

4. Daily, J. W. and G. Bugliarello, "Basic Data for Dilute Fiber Suspensions in Uniform Flow with Shear," TAPPI 44, No. 7, 497-512 (July, 1961).

5. Bobkowicz, A. G. and W. H. Gauvin, Paper presented at the December Meeting of the American Institute of Chemical Engineers, 1964.

6. Toms, B. A., "Some Observations on the Flow of Linear Polymer Solutions Through Straight Tubes at Large Reynolds Numbers," Proceedings of the First International Congress on Rheology Vol. II, North Holland Publishing Company, 135-141 (1948).

7. Thurston, S. and R. D. Jones, "Experimental Model Studies of Non-Newtonian Soluble Coatings for Drag Reduction," Journal of Aircraft 2, No. 2, 122-126 (March-April, 1965).

8. Love, R. H., The Effect of Ejected Polymer Solutions on the Resistance and Wake of a Flat Plate in a Water Flow, Report to the Office of Naval Research, Contract No. Nonr-4181(00), NR 062-325, Hydronautics, Inc. (June, 1965).

9. Forester, R. E. and P. S. Francis, Development of a Fluid Concentrated Dispersion of a Water-Soluble Polymer Capable of Reducing the Friction of Water Under Turbulent Conditions, North Star Research and Development Institute, Minneapolis, Minnesota (July, 1966).

10. Wells, Jr., C. S. and J. G. Spangler, Injection of a Drag-Reducing Fluid Into Turbulent Pipe Flow of a Newtonian Fluid, NASA CR-852, Contract No. NASw-729, LTV Research Center, Dallas, Texas (July, 1967).

11. Pruitt, G. T., C. M. Simmons, G. H. Neill, and H. R. Crawford, "A Method of Minimizing the Cost of Pumping Fluids Containing Friction-Reducing Additives," Journal of Petroleum Technology 17, 641-646 (June, 1965).

12. Ousterhout, R. S. and C. B. Hall, "Reduction of Friction Loss in Fracturing Operations," Journal of Petroleum Technology 13, 217-222 (March, 1961).

13. Kowalski, T., "Reduction of Frictional Drag by Non-Newtonian Additives," Naval Engineers Journal 78, 293-297 (April, 1966).

14. Prandtl, L., "Ueber Fluessigkeitsbewegung bei sehr kleiner Reibung," Proceedings Third International Mathematical Congress, Heidelberg, 1904, Reprinted in Vier Abhandlungen zur Hydrodynamik und Aerodynamik, Goettingen, 1927.

15. Runstadler, P. W., S. J. Kline, and W. C. Reynolds, An Experimental Investigation of the Flow Structure of the Turbulent Boundary Layer, Report MD-8, Thermoscience Division, Department of Mechanical Engineering, Stanford University, Stanford, California (1963).

16. Schraub, F. A. and S. J. Kline, A Study of the Structure of the Turbulent Boundary Layer With and Without Longitudinal Pressure Gradients, Report MD-12, Thermoscience Division, Department of Mechanical Engineering, Stanford University, Stanford, California (March, 1965).

17. Hinze, J. O., Turbulence, McGraw-Hill Book Company, Inc., New York (1959).

18. Coles, D., "The Law of the Wake in the Turbulent Boundary Layer," Journal of Fluid Mechanics 1, 191-226 (1956).

19. Lumley, J. L., "The Reduction of Skin Friction Drag," Proceedings of the Fifth Symposium on Naval Hydrodynamics, Bergen, Norway, September 12, 1964, Office of Naval Research, Washington, D. C., 915-929 (1966).

20. Fabula, A. G., The Toms Phenomenon in the Turbulent Flow of Very Dilute Polymer Solutions, Paper presented at the Fourth International Congress on Rheology, Brown University, Providence, Rhode Island, 26-30 (August, 1963).

21. Hoyt, J. W. and A. G. Fabula, The Effect of Additives on Fluid Friction, AD 612056, NAVWEPS Report 8636, U.S. Naval Ordnance Test Station, China Lake, California (December, 1964).

22. Shaver, R. G. and E. W. Merrill, "Turbulent Flow of Pseudoplastic Polymer Solutions in Straight Cylindrical Tubes," Journal of the American Institute of Chemical Engineers 5, No. 2, 181-188 (June, 1959).

23. Elata, C., J. Lehrer, and A. Kahanovitz, "Turbulent Shear Flow of Polymer Solutions," Israel Journal of Technology 4, No. 1, 87-95 (1966).

24. Pruitt, G. T. and H. R. Crawford, Investigation for the Use of Additives for the Reduction of Pressure Losses, AD 613345, The Western Electric Company, Dallas, Texas (January 30, 1965).

25. Elata, C. and J. Tirosh, "Frictional Drag Reduction," Israel Journal of Technology 3, No. 1, 1-6 (February, 1965).

26. Wells, Jr., C. S., "Anomalous Turbulent Flow of Non-Newtonian Fluids," Journal of the American Institute of Aeronautics and Astronautics 3, No. 10, 1800-1805 (October, 1965).

27. Ernst, W. D., Investigation of the Turbulent Shear Flow of Dilute Aqueous CMC Solutions, NASA CR-395, Contract No. NASw-729, LTV Research Center, Dallas, Texas (1966).

28. Lindgren, E. R., Friction Reduction Effects on Turbulent Flows of Water in Rough Pipes by Dilute Additive of High Molecular Weight Polymer, Technical Report No. 1, Contract NONr-2595(05), School of Civil Engineering, Oklahoma State University (June, 1965).

29. Shin, H., Reduction of Drag in Turbulence by Dilute Polymer Solutions, Sc.D. Thesis, Massachusetts Institute of Technology, Cambridge, Massachusetts (1965).

30. Lee, T. S., Turbulent Flow of Dilute Polymer Solutions - Studies in Couette Flow, Sc.D. Thesis, Massachusetts Institute of Technology, Cambridge, Massachusetts (1966).

31. Rouse, P. E., "A Theory of the Linear Viscoelastic Properties of Dilute Solutions of Coiling Polymers," Journal of Chemical Physics 21, No. 7, 1272-1280 (July, 1953).

32. Rubin, H. and C. Elata, "Stability of Couette Flow of Dilute Polymer Solutions," Physics of Fluids 9, No. 10, 1929-1933 (October, 1966).

33. Wells, Jr., C. S., J. Harkness, and W. A. Meyer, Turbulence Measurements in Pipe Flow of a Drag-Reducing Non-Newtonian Fluid, Report No. 0-71000/6R-22, LTV Research Center, Dallas, Texas (December, 1966).

34. Pruitt, G. T., B. Rosen, and H. R. Crawford, Effect of Polymer Coiling on Drag Reduction, AD 642441, Contract NONr-4306(00), The Western Electric Company, Dallas, Texas (August, 1966).

35. Hoyt, J. W. and A. G. Fabula, "The Effect of Additives on Fluid Friction," Proceedings of the Fifth Symposium on Naval Hydrodynamics, Bergen, Norway, September 12, 1964, Office of Naval Research, Washington, D. C., 947-973 (1966).

36. Little, R. C., Drag Reduction by Dilute Polymer Solutions in Turbulent Flow, AD 654160, NRL Report 6542, Naval Research Laboratory, Washington, D. C. (May, 1967).

37. Virk, P. S., The Toms Phenomenon - Turbulent Pipe Flow of Dilute Polymer Solutions, Sc.D. Thesis, Massachusetts Institute of Technology, Cambridge, Massachusetts (1966).

38. Goren, Y. and J. F. Norbury, Turbulent Flow of Dilute Aqueous Polymer Solutions, Paper presented at the Winter Annual Meeting of the American Society of Mechanical Engineers, November 12-17, 1967, Pittsburgh, Pennsylvania.

39. Merrill, E. W., K. A. Smith, and R. Y. C. Chung, "Drag Augmentation by Polymer Addition," Journal of the American Institute of Chemical Engineers 12, No. 4, 809-810 (July, 1966).

40. Lang, T. G. and H. V. L. Patrick, Drag of Blunt Bodies in Polymer Solutions, Paper presented at the Winter Annual Meeting and Energy System Exposition of the American Society of Mechanical Engineers, New York, N. Y., November 27-December 1, 1966.

41. Ruszczycky, M. A., "Sphere Drop Tests in High-Polymer Solutions," Nature 206, 614-615 (May, 1965).

42. Vogel, W. M. and A. M. Patterson, "An Experimental Investigation of the Effect of Additives Injected Into the Boundary Layer of an Underwater Body," Proceedings of the Fifth Symposium on Naval Hydrodynamics, Bergen, Norway, September 12, 1964, Office of Naval Research, Washington, D. C., 975-997 (1966).

43. Baronet, C. N. and W. H. Hoppmann II, Drag Reduction Caused by High Polymer Solutions Injected Into Water Flowing Around Cylindrical Bodies, AD 636158, Rensselaer Polytechnic Institute, Troy, New York (July, 1966).

44. Oldroyd, J. G., "A Suggested Method of Detecting Wall Effects in Turbulent Flow Through Tubes," Proceedings of the First International Congress on Rheology Vol. II, North Holland Publishing Company, 130-134 (1948).

45. Ward, A. G. and E. B. Atkinson, Proceedings of the First International Congress on Rheology Vol. III, North Holland Publishing Company, 44-45 (1948).

46. Lumley, J. L., "Turbulence in Non-Newtonian Fluids," Physics of Fluids 7, No. 3, 335-337 (March, 1964).

47. Gadd, G. E., "Turbulence Damping and Drag Reduction Produced by Certain Additives in Water," Nature 206, 463-467 (May, 1965).

48. Black, T. J., A New Approach to Wall Turbulence 1. The Shear Stress Mechanism, Mechanical Technology, Incorporated, Latham, New York (July, 1967).

49. Black, T. J., "Some Practical Applications of a New Theory of Wall Turbulence," Proceedings of the 1966 Heat Transfer and Fluid Mechanics Institute, Stanford University Press, Stanford, California, 366-386 (1966).

50. Nikuradse, J., "Gesetzmässigkeit der Turbulenten Strömung in Glatten Rohren," VDI-Forschungsheft 356 (1932).

51. Von Kármán, Th., National Advisory Committee for Aeronautics Technical Memorandum 611 (1931).

52. Meyer, W. A., "A Correlation of the Frictional Characteristics for Turbulent Flow of Dilute Viscoelastic Non-Newtonian Fluids in Pipes," Journal of the American Institute of Chemical Engineers 12, No. 3, 522-525 (May, 1966).

53. Virk, P. S., E. W. Merrill, H. S. Mickley, and K. A. Smith, "The Critical Shear Stress for Reduction of Turbulent Drag in Pipe Flow," Modern Developments in the Mechanics of Continua, Edited by Salamon Eskinazi, Academic Press, New York, 37-52 (1966).

54. Ram, A., E. Finkelstein, and C. Elata, "Reduction of Friction in Oil Pipelines by Polymer Additives," Industrial and Engineering Chemistry 6, No. 3, 309-313 (July, 1967).

55. Fabula, A. G., J. L. Lumley, and W. D. Taylor, "Some Interpretations of the Toms' Effect," Modern Developments in the Mechanics of Continua, Edited by Salamon Eskinazi, Academic Press, New York, 145-164 (1966).

56. Giles, W. B., Pipe Experiments with Friction-Reducing Additive in Water, General Electric Report 64GL210 (1964).

57. Goren, Y., P. O. Kane, and J. F. Norbury, "A Method of Measuring the Concentration of Certain Polymers in Dilute Aqueous Solutions," Journal of the Royal Aeronautical Society 71, 381-383 (May, 1967).

58. Baily, Jr., F. E., J. L. Kucera, and L. G. Imhof, "Molecular Weight Relations of Polyethylene Oxide," Journal of Polymer Science 32, 517 (1958).

59. Encyclopedia of Chemical Technology, Edited by R. E. Kirk and D. F. Othmer, Second Supplement Volume, Editor A. Standen, The Interscience Encyclopedia, Inc., New York, 606 (1960).

60. Eckert, E. R. G. and R. M. Drake, Jr., Heat and Mass Transfer, McGraw-Hill Book Company, Inc., New York, Second Edition, 464 (1959).

61. Bird, R. B., W. E. Stewart, and E. N. Lightfoot, Transport Phenomena, John Wiley & Sons, Inc., New York, First Edition, Third Printing, (1963).

62. MacMillan, F. A., "Viscous Effects on Flattened Pitot Tubes at Low Speeds," Journal of the Royal Aeronautical Society, London 58, 837-839 (December, 1954).

63. Young, A. D. and J. N. Haas, The Behavior of a Pitot Tube in a Transverse Total-Pressure Gradient, Aeronautical Research Committee Reports and Memoranda, R. & M. No. 1770, London (1937).

64. Goldstein, S., "A Note on the Measurement of Total Head and Static Pressure in a Turbulent Stream," Proceedings of the Royal Society, Series A, Mathematical and Physical Sciences 155, 570-575 (1936).

65. Shaw, R., "The Influence of Hole Dimensions on Static Pressure Measurements," Journal of Fluid Mechanics 7, 550-564 (1960).

66. Schlichting, H., Boundary Layer Theory, McGraw-Hill Book Company, Inc., New York, p. 537 (1955).

67. Virk, P. S., E. W. Merrill, H. S. Mickley, K. A. Smith, and E. L. Mollo-Christensen, "The Toms Phenomenon: Turbulent Pipe Flow of Dilute Polymer Solutions," Journal of Fluid Mechanics 30, Part II, 305-328 (1967).

68. Wooldridge, C. E. and R. J. Muzzy, "Boundary Layer Turbulence Measurements with Mass Addition and Combustion," Journal of the American Institute of Aeronautics and Astronautics 4, No. 11, 2009-2016 (1966).

69. Chin, Y. T., J. Hulsebos, and G. H. Hunnicutt, "Investigation of Helium Addition into a Turbulent Boundary Layer on a Cylinder in Axisymmetric Flow," Report No. ER-8681, Lockheed-Georgia Company, Marietta, Georgia, (December, 1966).

VITA

Jan Hulsebos was born in Amsterdam, the Netherlands on November 7, 1934. He attended the local public schools and graduated from the Gereformeerd Gymnasium in June, 1953. He entered the Georgia Institute of Technology in January, 1955, after having attended the Vrije Universiteit in Amsterdam for two years of studies in chemistry, mathematics, and physics. In December, 1957, he received the Bachelor of Chemical Engineering degree.

Mr. Hulsebos was employed as a chemical engineer with Tennessee Corporation from January, 1958 to January, 1963. Here, he conducted and directed research projects in the general area of transport phenomena. He was also engaged in process development and improvement, pilot plant design and studies, and plant start-up. Studying on a part-time basis, he received the Master of Science in Chemical Engineering degree in June, 1961.

In January, 1963, Mr. Hulsebos accepted employment as a Senior Engineer with the Lockheed-Georgia Company in Marietta, Georgia. Here, he conducted advanced research projects in the areas of drag reduction in air and water, and in the field of gas diffusion. In January, 1966, he re-entered the Graduate Division of the Georgia Institute of Technology to complete the requirements for the Doctor of Philosophy degree.

In addition to several company reports, Mr. Hulsebos has authored or co-authored the following manuscripts and articles:

A Review and Evaluation of the Utilization of Solar Energy, Master's Thesis, Georgia Institute of Technology, Atlanta, Georgia (1961).

Hydrogen Permeation Measurements on Vapor-Barrier Materials for Cryogenic Insulations, Paper presented at the National Aeronautic and Space Engineering and Manufacturing Meeting, Los Angeles, California (September 23-27, 1963).

"Leak Detector Measures Hydrogen Permeation of Vapor-Barrier Materials," Journal of the Society of Automotive Engineers 71, No. 11, 99-101 (1963).

"Effect of Lateral Curvature on the Characteristics and Skin Friction of a Turbulent Air Boundary Layer with and without Helium Addition," Proceedings of the 1967 Heat Transfer and Fluid Mechanics Institute, Stanford University Press, 394-409 (1967).

Mr. Hulsebos is co-inventor of patent no. 3,392,693: "Method of and Means for Reducing Drag," dated July 16, 1968.